DEVELOPMENT OF A SEGREGATED MUNICIPAL SOLID WASTE GASIFICATION SYSTEM FOR ELECTRICAL POWER GENERATION

A Dissertation

by

AMADO LATAYAN MAGLINAO JR

Submitted to the Office of Graduate Studies of
Texas A&M University
in partial fulfillment of the requirements for the degree of

DOCTOR OF PHILOSOPHY

Approved by:

Chair of Committee,	Sergio C. Capareda
Committee Members,	Calvin B. Parnell Jr.
	Wei Zhan
	Mahmoud M. El-Halwagi
Head of Department,	Stephen W. Searcy

May 2013

Major Subject: Biological and Agricultural Engineering

ABSTRACT

Gasification technologies are expected to play a key role in the future of solid waste management since the conversion of municipal and industrial solid wastes to a gaseous fuel significantly increases its value. Municipal solid waste (MSW) gasification for electrical power generation was conducted in a fluidized bed gasifier and the feasibility of using a control system was evaluated to facilitate its management and operation. The performance of an engine using the gas produced was evaluated. A procedure was also tested to upgrade the quality of the gas and optimize its production. The devices installed and automated control system developed was able to achieve and maintain the set conditions for optimum gasification. The most important parameters of reaction temperature and equivalence ratio were fully controlled. Gas production went at a rate of 4.00 kg min^{-1} with a yield of 2.78 m^3 kg^{-1} of fuel and a heating value (HV) of 7.94 MJ Nm^{-3}. Within the set limits of the tests, the highest production of synthesis gas and the net heating value of 8.97 MJ Nm^{-3} resulted from gasification at 725°C and ER of 0.25 which was very close to the predicted value of 7.47 MJ Nm^{-3}. This was not affected by temperature but significantly affected by the equivalence ratio. The overall engine-generator efficiency at 7.5 kW electrical power load was lower at 19.81% for gasoline fueled engine compared to 35.27% for synthesis gas. The pressure swing adsorption (PSA) system increased the net heating value of the product gas by an average of 38% gas over that of inlet gas. There were no traces of carbon dioxide in the product gas indicating that it had been completely adsorbed by the system. MSW showed relatively

lower fouling and slagging tendencies than cotton gin trash (CGT) and dairy manure (DM). This was further supported by the compressive strength measurements of the ash of MSW, CGT and DM and the EDS elemental analysis of the MSW ash.

DEDICATION

To my fiancée, Joan Hernandez, who supported and encouraged me in every step of the way. To my baby, Jillian Maglinao, for giving me the inspiration to succeed. To my family, my father, Amado R. Maglinao, my mother, Erlinda L. Maglinao, and my two brothers, Ryan and Randy Maglinao and also to my soon to be official family Jose Hernandez, Julie Hernandez and Jonalyn Hernandez who have always been supportive to me since the beginning of my studies.

ACKNOWLEDGEMENTS

I would like to express my gratitude to all those who gave me the possibility to complete my dissertation. First of all, I would like to thank God for all the blessings He has given to me and to my family and friends.

Special thanks to the distinguished faculty members who served as my committee: Dr. Sergio C. Capareda (chair), Dr. Calvin B. Parnell, Jr., Dr. Wei Zhan and Dr. Mahmoud M. El-Halwagi. As the chair of my advisory committee, Dr. Capareda provided full support and encouragement throughout the dissertation. Thanks to all my committee members for their guidance, patience, support, and helpful suggestions and comments throughout the course of this dissertation.

To the BAEN department faculty and staff, co-majors and colleagues. To *mylabs* Joan Hernandez, *kabatch* Bjorn Santos, Froilan Aquino, Jewel Capunitan and Monet Maguyon with all your help provided throughout the research. To David Carney for providing the guidance and the *yelling.* To all the students who helped me with the laboratory work especially to David Lacey, Clint Sternadel, Tyler Haas and Zachary Skrabanek. Thank you very much. Thanks to all for your help and support. My stay at BAEN, Texas A&M University has become a fun and learning experience.

I also would like to extend my gratitude to the SDL Citadel, LLC and Texas Agricultural Experiment Station (TAES), for generously providing financial support during my studies and research. The FEI-SEM acquisition was supported by the NSF grant DBI0116835, the VP for Research Office, and the TX Eng. Exp. Station.

Thanks also to the Filipino *bagets* in College Station (Sam, JC, Kat, Aldrin, Jess, Alnald, Gally, Kristian and Paul) and to the entire Filipino community (Kuya Roy & Ate Faye, Kuya Ricky & Ate Ime Tita, Kuya Cesar & Ate Mel, Tita Nora & Tito Rey, Tita Lou & Tito John, and a lot more) that I have met here in Bryan-College Station and all over the United States, for making my stay worthwhile. I really enjoy and appreciate all your company and help. May God bless you always.

Finally, thanks to my family, both the Maglinao and Hernandez families, for their love, encouragement, support and guidance. My angel Baby Jillian. I am so honored and grateful to have you all in my life. Thank you and I love you very much!

NOMENCLATURE

Φ_s – Sphericity

ϵ_{mf} – Voidage

μ – Viscosity

ρ_b – Bulk Density

ρ_s – Particle Density

AI – Alkali Index

ANOVA – Analysis of Variance

ASTM – American Society for Testing and Materials

BAI – Bed Agglomeration Index

BTU – British Thermal Unit

CCD – Central Composite experimental Design

CGT – Cotton Gin Trash

daf.b – Dry Ash Free Basis

DAQ – Data Acquisition

d.b – Dry Basis

DM – Dairy Manure

DP – Differential Pressure

d_p – Mean particle diameter

e – error

EDS – Electron Dispersive X-ray Spectroscopy

ER- Equivalence Ratio

FBG – Fluidized Bed Gasifier

FC – Fixed Carbon

GUI – Graphical User Interface

h – Hour

HC – Hydrocarbons

HHV – High Heating Value

HID – Helium Ionization Detector

hp – Horsepower

LabVIEW – Laboratory Virtual Instrumentation Engineering Workbench

LHV – Low Heating Value

LFE – Laminar Flow Element

MSW – Municipal Solid Waste

mol – Moles

MV – Manipulated Variable

MW_e – Megawatts (electrical energy)

η_G – Gasification Efficiency

NI – National Instruments

PID – Proportional-Integral-Derivative

PLC – Programmable Logic Controller

PSA – Pressure Swing Adsorption

PV – Process Variable

$R_{b/a}$ – Base to acid ratio

R_f – Fouling ratio

R_s – Slagging ratio

RSM – Response Surface Methodology

SCFM – Standard Cubic Feet per Minute

SEM – Scanning Electron Microscopy

SP – Setpoint

TCD – Thermal Conductivity Detector

u – Controller output

u_I – Integral action

u_{mf} – Minimum fluidization velocity

u_P – Proportional action

u_t – Terminal velocity

VI – Virtual instruments (LabVIEW)

VM – Volatile Matter

vol% – Volume percent

TABLE OF CONTENTS

Page

LIST OF FIGURES

Page

LIST OF TABLES

Page

CHAPTER I

INTRODUCTION

BACKGROUND

Waste Management

As societies develop, the amount of waste materials generated increases to a level that makes them excessive and a tremendous waste management problem. The disposal and utilization of these waste materials pose a big challenge not only to our policymakers and researchers but also to many relevant industries. One strategy that can potentially address the waste management issues is the development and application of a waste to energy program that will identify and use processes that will ensure provision of greater recovery value from the wastes while maintaining the sustainability of the process (Mastellone and Arena, 2008). This development strategy should be able to address the issue of cleaner energy generation and enhanced environmental quality. Wastes, especially coming from different industries, can be used as fuel for waste-to-energy facilities. Waste-to-energy plants can convert waste streams into biofuels or steam using direct combustion, anaerobic digestion, or gasification technologies.

Management of Municipal Solid Wastes (MSW)

Municipal Solid Waste (MSW) consists of items used and then thrown away, such as product packaging, grass clippings, food scraps and newspapers. In 2010, the US generated about 250 million tons of MSW with organic materials constituting the largest component (Figure 1). Paper and paperboard account for 29 percent and yard trimmings

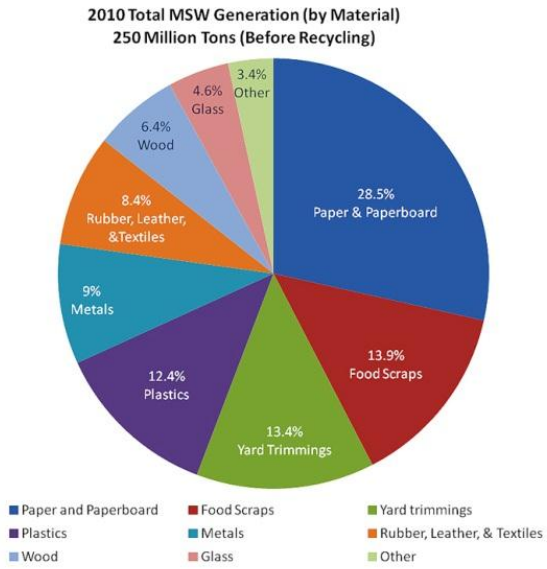

Figure 1. US total MSW generation (by material) in year 2010 (EPA, 2010)

and food scraps account for another 27 percent. Plastics comprise 12 percent; metals make up 9 percent; and rubber, leather, and textiles account for 8 percent. Wood follows at 5 percent. Other miscellaneous wastes make up approximately 3 percent of the MSW generated.

Waste management hierarchy includes source reduction and reuse, recycling or composting, energy recovery and treatment and disposal (Figure 2). The concept of source reduction is focused mainly on the product manufacturing sector. In most cases, the drive to avoid producing waste is provided by government or industry policies, with the major aim focused on avoiding the costs associated with handling or managing wastes. The reuse of materials or products is another option which avoids the generation of waste.

Recycling is another waste management strategy which deals with recovery and use of useful materials from the waste as a raw material for the manufacture of a new or similar type of product. The concept has been promoted as a means to conserve resources and prevent materials from entering the waste stream, thus reducing the environmental impacts associated with extracting raw materials and at the same time managing the wastes. Many recycling schemes have had difficulty sustaining themselves due to widely fluctuating markets for waste materials.

Figure 2. Waste management hierarchy (EPA, 2010).

Biological treatment technologies like composting are now reemerging as commercially viable means to permanently remove the organic material fraction from the waste stream. Composting involves collecting organic waste, such as food scraps and

yard trimmings, and storing it under conditions designed to help it break down naturally. The resulting compost can then be used as a natural fertilizer.

Municipal solid waste landfills receive household waste and non-hazardous sludge, industrial solid waste, and construction and demolition debris. Modern landfills are well-engineered facilities that are located, designed, operated, and monitored to ensure compliance with federal regulations. Solid waste landfills are designed to protect the environment from contaminants which may be present in the solid waste stream.

Waste to Energy Conversion

Energy recovery from wastes is the conversion of non-recyclable waste materials into usable heat, electricity, or fuel through a variety of processes. Often called waste-to-energy processes, these include combustion, gasification, pyrolization, anaerobic digestion, and landfill gas recovery. Converting non-recyclable waste materials into electricity and heat generates a renewable source of energy for various industries. It likewise reduces carbon emissions from too much dependence on energy from fossil fuels and reduces methane generation from landfills. Combustion of municipal solid waste aims to sterilize the wastes and reduce the volume of materials requiring final disposal. Combustion facilities have also been designed for energy recovery. Over the past decade, the concern over air emissions from these facilities has resulted in most countries adopting very stringent air emission control regulations which increased the cost of constructing and operating incinerators (Sakai et al., 1996).

Gasification

The biodegradable components of municipal solid waste and commercial and industrial wastes are significant bio-energy resources, although they may require extensive processing before conversion, particularly in the case of MSW. Biomass and other organic residues can be converted to energy through thermal, biological or mechanical and physical processes (Bridgwater and Maniatis, 2004). Biological conversion processes like anaerobic fermentation and landfill gas by digestion gives single or specific products such as ethanol or biogas. However, they are a slow process that takes time for reactions to be completed. Thermal conversion usually takes place in shorter reaction time but gives multiple and often complex products. It often employs the use of catalysts to improve the product quality or spectrum (Bridgwater, 2006).

Conversion processes available for the thermal treatment of solid wastes are combustion, gasification and pyrolysis. As shown in Figure 3, different products are obtained from the application of these processes and different energy and matter recovery systems can be used to treat them. Four stages occur during gasification of carbonaceous material: drying, volatilization, combustion, and reduction (Knoef, 2005). The drying stage heats and removes the moisture within the material. Continued heating volatilizes the material where volatile matter exits the particle and comes in contact with the oxygen. The very exothermic combustion process then provides the heat for the reduction reactions to occur. The reduction reactions include water gas reaction, Boudouard reaction, water-gas-shift reaction, and methanation reaction (Swanson et al., 2010).

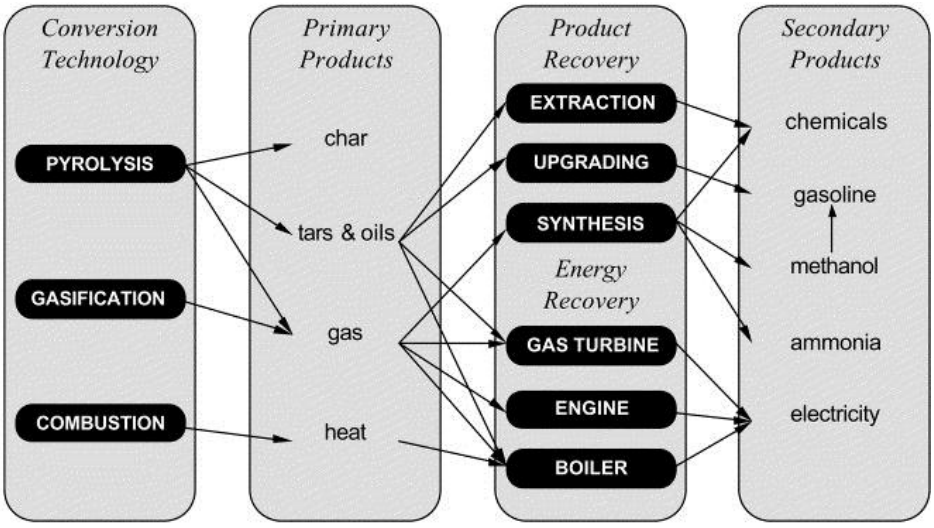

Figure 3. Thermal conversion processes and their products (Bridgewater 1994)

Gasification is regarded the main and effective technology for the thermochemical conversion of biomass to energy or synthesis gas (Xiao et al., 2011). The number of different uses of gas shows the flexibility of gasification allowing it to be integrated with several industrial processes, including power generation systems (Mastellone and Arena, 2008). Gasification technologies are expected to play a key role in the future of solid waste management since the conversion of municipal and industrial solid wastes to a gaseous fuel significantly increases its value (Klein et al., 2004)

Several studies have focused their efforts on the development of the biomass gasification processes carried out in gasifiers with fluidized bed reactors (Arena and Mastellone, 2006; Basu, 2006; McMillian and Lawson, 2006). Among the different reactor configurations, fluidized bed reactors show promise as they are the most suitable for continuous process and scalable over a large range of sizes. The flexibility of

fluidized bed reactor operation makes it possible to be utilized with different fluidizing agents, at various reactor temperatures and gas residence times. In addition, it allows adding reagents along the reactor height and to be operated with or without a specific catalyst (Ahtikoski et al., 2008).

The production of a useful fuel gas, commonly known as producer gas or synthesis gas (syngas) is one of the objectives of gasification. Its efficiency (η_G) can be defined as the ratio of the heat content of the fuel gas generated by the gasification of the biomass and the heat content of that biomass when it is totally burned (Mathieu and Dubuisson, 2002).

$$\eta_G = \frac{M_g LHV_b}{M_g LHV_b} \quad [1]$$

where M = mass flow rate
LHV = lower heating value
g,b = subscripts for synthesis gas and biomass, respectively

The net or lower heating value (LHV) of the product gas is defined as

$$LHV(MJ\ Nm^{-3}) = \frac{1}{100}\left(\begin{matrix}12.63\times CO + H_2\times 10.78 + CH_4\times 35.88 + C_2H_2\times 56.07 \\ + C_2H_4\times 59.45 + C_2H_6\times 64.34 + C_3H_6\times 87.57\end{matrix}\right) \quad [2]$$

where, H_2, CO, CH_4, C_2H_4 and C_2H_6 were the molar percentages of the components of product gas.

Carbon conversion efficiency is measured in terms of the carbon in gaseous phase as a fraction of carbon originally present in the biomass (Al-Mansour and Zuwala, 2010). The carbon conversion efficiency can be calculated as

$$\text{Carbon Conversion Efficiency (\%)} = \frac{12(\text{GP})}{M_b C\%_b}(CO\% + CH_4\% + CO_2\% + 2(C_2H_2\% + C_2H_4\% + C_2H_6\%) + 3C_3H_6\%) \times 100 \quad [3]$$

where GP - product gas production ($Nm^3\ min^{-1}$),
C% - the mass percentage of carbon in ultimate analysis of biomass fuel
CO_x% and C_yH_z% - molar percentages of components of the product gas (Wang et al., 2012).

Gasification has several advantages over traditional combustion of solid wastes, mainly due to the possibility of combining the type of starting wastes, operating conditions and features of the specific reactor to obtain a syngas suited for use in different applications as a chemical feedstock, or a fuel gas that can be burned in gas reciprocating engines or gas turbines to generate electricity (Vamvuka and Zografos, 2004). However, waste gasification must cope with problems specific to the waste feedstock such as large variability of composition, high concentrations of contaminants, unfavorable chemical properties (high moisture, low LHV, high ash content), and unfavorable physical properties (variable particle size, low density). Moreover, the varying characteristics of MSW tend to make gasification much more challenging in producing a major impact on the design, performance, maintenance and cost of gasification (Consonni and Viganò, 2012).

Biomass gasification has trailed coal gasification due to technical differences in the characteristics of the feedstock and the typical scale of operation. However, technological advances in biomass gasification have been successfully demonstrated and commercial-scale projects are proceeding. Around the world, more than 100 biomass gasifier projects are operating or ordered. In the U.S., construction began in 2009 on a 42 MW_e commercial-scale project in Tallahassee, Florida, and another 28 MW_e gasifier is planned for Forsythe, Georgia. Small-scale gasification is moving ahead as well with a 300 kW farm-scale demonstration using straw as a feedstock and a 320 kW project at a sawmill constructed and now beginning operation (Roos, 2009).

Recent MSW Gasification Studies

A number of technologies where MSW is partially oxidized in a gasifier as an alternative to conventional waste to energy technologies, where MSW is fully oxidized in a single-step combustion process have been proposed and studied (Heermann et al., 2001). In principle, most of the concepts and the process schemes applicable to fossil fuels or biomass are also applicable to MSW (Arena, 2011; Malkow, 2004). However, unsorted MSW is not suitable for gasification because of its varying composition and size of some of the constituent materials. Furthermore, an increase of the dry/wet ratio to values higher than those normally available from MSW is required (Paolucci et al., 2010).

Pinto et al. (2002) utilized fluidized bed steam gasification to convert biomass, plastic and other undesirable wastes into fuel gases. The addition of plastics to pine

wastes gasification decreased CO content of synthesis gas, but increased H_2 released reaching up to 50% (v/v). The highest gas yield was 1.96 Nm^3 kg^{-1} of dry ash free of pines-plastic wastes mixture for 98% energy conversion (Pinto et al., 2002). Chiemchaisri et al. (2010) used solid wastes from landfills in a gasifier. The wastes contained high plastic content, majority in polyethylene plastic bag form. The produced gas contained an average energy content of 1.76 MJ Nm^{-3} and yielded a cold gas efficiency of 66% (Chiemchaisri et al., 2010). Wang et al. (2012) conducted MSW gasification at different temperatures. The highest synthesis gas yield of 1.85 Nm^3 kg^{-1} of MSW was obtained during gasification at 850°C while the highest gas heating value of 13.15 MJ Nm^{-3} was obtained at 700°C (Figure 4.) Elbaba et al. (2011) utilized waste tires for hydrogen production using pyrolysis-gasification with nickel/cerium catalyst. The experiments produced 56% by volume of hydrogen and 9% of hydrocarbons (Elbaba et al., 2011). Pyrolysis and gasification behavior were evaluated in terms of syngas flow rate, hydrogen flow rate, output power, total syngas yield, total hydrogen yield, total energy yield, and apparent thermal efficiency (Ahmed and Gupta, 2010). Gasification was more beneficial than pyrolysis based on the criteria, but longer time was needed to finish the gasification process. Longer time of gasification was attributed to the slow reactions between the residual char and gasifying agent.

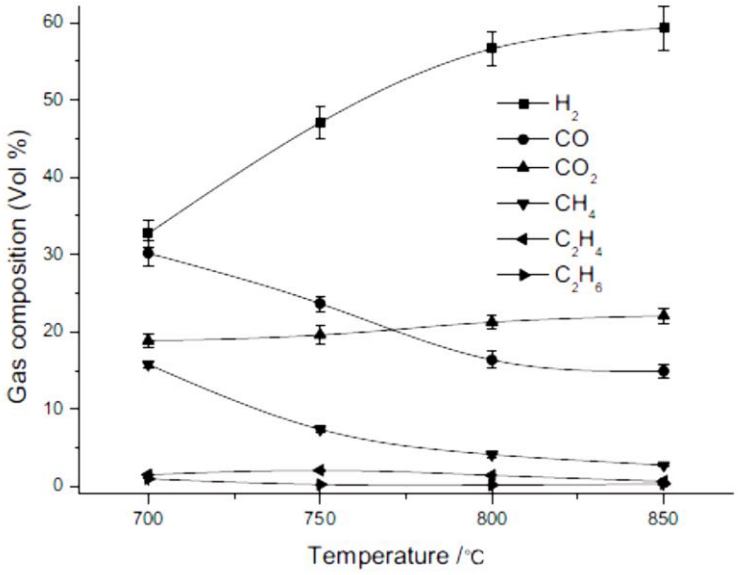

Figure 4. Effect of temperature on gas composition in MSW gasification (Wang et al., 2012)

Power Production from Gasification

Developing an economy that involves renewable resources as energy source, especially biofuels, has many benefits. According to Greene et al. (2004), biofuel production has the potential to provide a new source of revenue for farmers by generating $5 billion per year. Additionally, toxic and greenhouse gas emissions can be reduced by the use of biofuels. In the same study, they reported that 22% of the total greenhouse gas emissions of the United States could be reduced if biofuels were developed to replace half of the petroleum consumption (Greene et al., 2004).

One of the most promising alternatives for generating power from coal and other fuels, while capturing the carbon dioxide generated during the energy conversion process at a minimum efficiency penalty is based on gasification (Cormos, 2012). It also

represents an attractive alternative to the well-established thermal treatment systems for the recovery of energy from solid wastes. Gasification of solid wastes produces electricity at an efficiency of about 34% compared to 20% for incineration. This suggests that gasification of the residual component of solid wastes is more advantageous than incineration where a market for thermal product does not exist. Gasification produces more electricity than incineration and when thermal product is not utilized generates less greenhouse gas per kWh than incineration (Murphy and McKeogh, 2004).

Biomass/waste gasification has always been struggling with delivery/scale dilemma in its operation. Single-site gasifiers built at an economic scale can overcome the high delivery costs of the feedstock. A gasification system module fitted into a single animal farm or gin or waste industry can make significant headway as it takes advantage of on-site collection and processing of biomass wastes. Biofuels produced in this way can be used in reciprocating engines, or in steam or gas turbines to generate electricity and thermal energy needed by energy consumers (Bullock et al., 2008).

The greatest technical challenge to overcome for the successful development of commercial advanced waste gasification technologies is the improvement in the quality of the produced gas. This will make it suitable for different final applications, mainly energy generation in gas engines or turbines, and in the production of hydrogen or chemical feedstock (Arena et al., 2010). Tar formation associated with the process also prevents its immediate utilization (Zhao et al., 2009). Tar causes problems in the process equipment and the engines and turbines used in the application of the producer

gas (Devi et al., 2005). The preferable tar and dust loads in gases for engines must be lower than 10 mg m_0^{-3} (Bui et al., 1994). Its control aims to avoid various problems associated with condensation of tars which may damage process equipment as well as devices for end-use applications. Tar removal can be done by downstream cleaning (secondary methods) or primary measures during the gasification process itself. Secondary methods include physical removal, thermal conversion and catalytic destruction. Removing tar can well be performed with the help of a catalyst.

Utilization of synthesis gas for electrical power production can be done in different ways. Earlier studies (McMillian and Lawson, 2006; Mustafi et al., 2006; Shah et al., 2010; Shudo et al., 2003; Sobyanin et al., 2005) explored the potential of syngas as an alternative engine fuel. The acceptable synthesis gas quality for engine use requires a lower heating value of 4.2 MJ Nm^{-3}, and tar and particulates composition of less than 50 mg Nm^{-3}. The common ways are pressurized gasification with a gas turbine in a combined cycle mode and atmospheric gasification with a gas turbine or engine.

The use of synthesis gas for diesel engines is suitable for large applications such as generators. The power loss is less in diesel engine compared to spark ignition engine when both are converted to operate with synthesis gas. The synthesis gas is mixed with intake air stream in a diesel engine and usually called diesel dual-fuel mode. In Shah et al. (2010), experiments, the overall efficiency of the generator at maximum electrical power is the same for both synthesis gas and gasoline as fuel. The CO and NO_x emissions were lower but higher CO_2 emissions during the synthesis gas operation. Mustafi et al. (2006) had contradicting results of the synthesis gas fuel engine having

higher NO_x emissions compared to gasoline operation. Personal power systems, such as domestic commercial generators, could be a way of decentralized energy production and hence, could play a significant role in energy independence (Shah et al., 2010). Implementation of the smaller power systems run by synthesis gas relies on the exhaust emission levels and the performance parameters.

OBJECTIVES

The proposed study developed a modular municipal solid waste gasification system for electrical power generation. Segregated municipal solid waste (MSW) gasification experiments were carried out for an in-depth study on the effects of gasification parameters on the synthesis gas production and net heating value. Instrumentation and control system were developed to facilitate the management and operation of the gasification processes. The synthesis gas produced was used as a fuel to run a spark ignition engine generator and its performance evaluated based on engine efficiency and exhaust gas emissions.

CHAPTER II

FEASIBILITY OF A CONTROL SYSTEM FOR GASIFICATION

INTRODUCTION

Conversion of biomass through gasification into an alternative source of energy is an accepted potential solution to the problem of the dwindling supply of fossil fuels and their contribution to a diminishing environmental quality. There are several types of gasification system that are available and can be utilized for biomass conversion, the most common of which use the fixed bed or the fluidized bed types of reactor. One significant advantage of the fluidized bed over the fixed bed reactor is the use of a broad size particle distribution in the fluidized bed reactor (Warnecke, 2000). The fluidized bed reactors also provide good mass and heat transfer rate between the fluid and the particles (Fu and Liu, 2007). The turbulent, fluidized state of inert particles in the bed creates a near isothermal zone and enables accurate control of reaction temperature. Thermal energy stored in large mass of inert particles is rapidly transferred to solid fuel at stable temperatures. Violent agitation of solids provides efficient conversion reactions and allows introduction of fuels with wide variations in composition and particle size (LePori and Soltes, 1985).

Instrumentation and development of advanced control systems on a biomass gasifier are considered key areas to further improve and facilitate its operation. However, the development of a control system for biomass gasification to facilitate its operation is not an easy task since it is multivariable and highly nonlinear. The control

system involves subsystems and processes assembled for the purpose of controlling the outputs of the processes (Nise, 2000). Usually, closing a conventional PID (Proportional-Integral-Derivative) controllers around feed actuators is utilized to provide automatic control in existing biomass gasification systems (Sagues et al., 2007). Currently, the PID algorithm is the most common control algorithm used in industry.

The use of programmable logic controllers which normally use PID algorithms is often referred to as automation. In their study on the development of a low-density biomass gasification system for thermal applications using sugarcane leaves and bagasse, Jorapur and Rajvanshi (1997) employed a Programmable Logic Controller (PLC)-based control system designed to take automatic corrective actions under certain critical conditions. The biomass feeding and ash removal rates were fully controlled by this system. It also helped the operator in trouble-shooting by monitoring the temperatures at various critical points in the gasification process. Ignition of the producer gas was provided by automatic burner sequence controllers. However, the use of the classical PID control with its parameters tuned for specific conditions of the biomass results in poor performance once those conditions change. Conventional PI controllers have also been used in more advanced ideas related to multi-objective optimization on coal gasifiers (Liu et al., 2000).

The ability to reliably measure a variety of gasification input parameters including compositional analysis of the feedstock to control the gasifier would be most useful. A number of parameters can be controlled to differentiate the various feedstock conversion processes and obtain the desired end product. These include heating rate,

final temperature, residence time at certain temperature, presence or absence of air or oxygen, fuel particle size, and fuel moisture content. The most basic feedback system measures the controlled variables, compares the actual measurements with the desired values and uses the difference between them (error) to identify the appropriate corrective action. It is therefore necessary to first measure the variables that are to be maintained at the desired standard values (Anderson, 1997). According to LePori and Soltes (1985), the fuel to air ratio and operating temperature are probably the two most critical parameters to control during the biomass conversion.

This particular study explored the feasibility of an appropriate instrumentation and control system for a pilot scale fluidized bed biomass gasification unit to facilitate measurement, operation and control. The specific objectives were to: (a) identify the important operational parameters to be monitored and controlled (b) install measuring and control devices for the operation of the gasification unit (c) develop a control system to provide automatic control of the gasification operation, and (d) evaluate the feasibility of the automatic control system in facilitating the operation of the gasifier.

METHODOLOGY

Biomass Gasifier Used in the Study

The pilot scale gasification system used was a fluidized bed gasifier developed by the Texas A&M University at College Station, Texas and protected under intellectual property disclosures TAMUS 2814 serial No. 61/302,001 (Figure 5). It has a 305 mm

square reactor with an average throughput of 100 kg h^{-1} and designed to convert a variety of biomass residues.

Figure 5. Fluidized bed gasification system

The operation of the fluidized bed gasification system which utilizes air as the gasifying agent is described in Figure 6. The fuel feedstock is placed in the fuel bin and fed in the fluidized bed reactor through a 10 cm diameter screw conveyor system (auger). Mulgrain 47- 10 x 18 (C E Minerals, Andersonville, GA) was used as the bed material inside the reactor. The proper adjustment and control of the fuel feed rate and air flow rate result in the partial oxidation of the biomass inside the reactor. This process

produces combustible gases and solid particulates which are separated using two-stage TAMU designed cyclones.

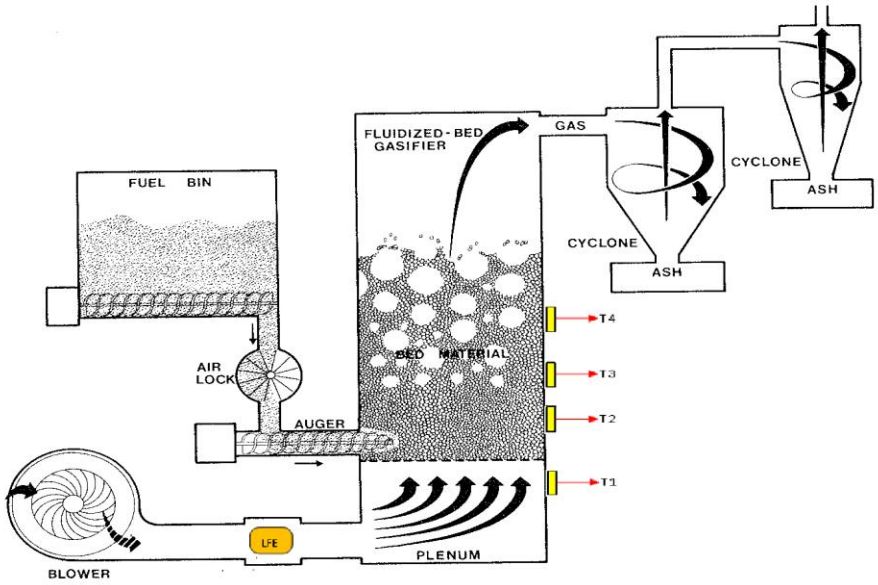

Figure 6. Operation of the fluidized bed gasifier (LePori and Soltes, 1985)

Instrumentation for Measurement and Control of the Gasification System

The gasification system was instrumented to conveniently monitor and control the important parameters that may affect its operation. Proper identification and evaluation of these parameters would surely make the control of the gasification system much easier and facilitated. The important parameters that have significant influence on the measurement and control of the gasification process include the gasification temperature, pressure, the air flow rate and the fuel feed rate. In this study, the reaction temperature was limited to only as high as 850°C which is based on the materials used in

the construction of the particular gasification system. Typically, the gasification operation is maintained at an average reaction temperature of 730°C to produce the desired quality of the synthesis gas.

Monitoring the pressure across the bed in the reactor provided indication that the bed material inside the reactor is in fluidized state. The differential pressure across the laminar flow element determines the amount of air being supplied to the system. The air flow rate values are needed to set up the air to fuel ratio during the operation of the gasifier while the biomass feeding rate regulates the amount of feedstock fed into the gasifier. The current air temperature, pressure and relative humidity are also necessary factors to calculate the standard flow rate. Calibration of the fuel screw conveyor determined the amount of the feedstock material to be used.

Installation of the Control Devices

To measure and monitor the temperature in the gasifier, KQXL-14U-12-DUAL K-type thermocouples (Omega, Stamford, CT) were installed at different locations. Omega PX274 current output differential pressure transducers with field selectable ranges (Omega, Stamford, CT) were used to record the pressure readings taken at different points in the gasifier and displayed using Magnehelic differential pressure gauges. An AF-300 Mini AC motor controller (Grainger, Bryan, TX) was used to regulate the air flow rate for the 5 hp motor blower air system. The screw conveyor system driven by a 2 hp DC motor, a Washguard 174102 SCR motor controller, was used to regulate the biomass feeding rate. The speed of the motor was measured using a

PU-2E magnetic pickup which produces a square wave with a frequency proportional to the speed. Dwyer Series RH-R Humidity/Temperature transmitter was used to measure the relative humidity and temperature of the fluidizing air. All of the devices used were properly calibrated during the whole study to ensure accuracy.

Gasification Control System Development

The gasification control system employed a closed PID flow loop to control the key input variables to the gasification system. Fuel (biomass) flow and air flow were set as the key input variables to the gasification system. The control system should be able to adjust these input variables to regulate the gasification reactor temperature. Synthesis gas calorific value, fluidization velocity and equivalence ratio were also maintained within its acceptable range during operation. In addition, safety indicators in reactor temperature and pressure, feeder malfunction and oxygen concentration were determined by the control system.

In PID control, a process variable (PV) and a setpoint (SP) must be specified. The process variable is the system parameter, such as temperature, pressure, or flow rate that needs to be controlled, while the setpoint is the desired value of the parameter being controlled. A PID controller determines a controller output value. The controller applies the output value to the manipulated variable (MV) of the system, which in turn drives the process variable toward the setpoint value. In this gasification system, the reaction temperature was set as the process variable while the fuel feed rate as the manipulated

variable. Fuel and air properties were some of the disturbance variables (D) which also exist but cannot be adjusted by the controller (Svrcek et al., 2000).

A program was developed for the NI CompactDAQ with the NI software, LabVIEW (short for Laboratory Virtual Instrumentation Engineering Workbench), to process all the electrical signals into readable values and monitor the sensor measurements in the gasification unit and for modular instrumentation. LabVIEW uses graphical programming to develop the measurement, test and control of the operation. In LabVIEW, the PID controller compares the SP to the PV to obtain the error (e). The NI CompactDAQ provides the plug-and-play simplicity of USB to sensor and electrical measurements on the benchtop, in the field, and on the production line. It provides fast and accurate measurements in a small and simple system. A cDAQ-9178 8 slot USB CompactDAQ chassis was selected and used in the development of the control system.

The proportional action (u_P) is the controller gain times the error. The integral action (u_I) was done by using trapezoidal integration to avoid sharp changes in its action when there is a big change in error. The controller output (u) would be the sum of the proportional and integral action (National Instruments, 2001).

$$e(\mathrm{k}) = \mathrm{SP} - \mathrm{PV} \quad [4]$$

$$\mathrm{u_P(k)} = \mathrm{K_c} \times \mathrm{e(k)} \quad [5]$$

$$\mathrm{u_I(k)} = \frac{\mathrm{K_c}}{\mathrm{T_i}} \sum_{\mathrm{i=1}}^{\mathrm{k}} \left[\frac{e(\mathrm{i}) + e(\mathrm{i}-1)}{2} \right] \Delta \mathrm{t} \quad [6]$$

$$\mathrm{u(k)} = \mathrm{u_P(k)} + \mathrm{u_I(k)} \quad [7]$$

where $e(k)$ = current error
K_c = controller gain
T_i = integral time

The graphical user interface (GUI) was first developed for quick control of the gasification process and displaying all important information and indicating faulty operation. This interface is appropriately designed to work with the measurement and control of the gasification process. The control system was also organized by developing different virtual instruments (VIs) to perform specific tasks.

The minimum fluidization velocity was obtained for the bed material, Mulgrain 47-10x18, by using empirical formulas and conducting cold fluidization experiments. Fluidization is the process by which fine solids are transformed to behave like fluid through contact with gas or liquid. Granular materials are converted from a static solid-like state to a dynamic fluid-like state and occur when a fluid, like a liquid or a gas is passed through the material. Utilizing enough fluid velocity to just suspend the particles in upward flowing air is referred to as minimum fluidization (Kunii and Levenspiel, 1969). For non-spherical particles, a variety of measures of nonsphericity can be used. Sphericity (Φ_s) is the measure of how round the particle is or as defined by Kunii and Levenspiel (1977) in the following equation,

$$\Phi_s = \left(\frac{\text{surface of sphere}}{\text{surface of particle}}\right)_{\text{both of same volume}} \quad [8]$$

Leva et.al. (1959) reported that sand has a sphericity of 0.6 while Shirai (1954) calculated a value of 0.628 for the same material. Fraction voids, ε_m in the bed particles represents the volume of voids over the total volume. Kunii and Levenspiel (1977) suggested that voidage at fluidization, ε_{mf} is a little larger than a packed bed and should be measured experimentally.

In addition to the use of the above empirical formula, fluidization was also determined by conducting experiments in a 15.2 cm diameter fluidization set up utilizing bubble caps as air distributors (Figure 7). Air was slowly introduced at a constant rate into the bed material while measuring the flow using a Z50MC2-2 Meriam laminar flow element. Air flow and pressure drop across the bed were measured throughout the whole test using a developed NI LabVIEW program (Appendix A). Kunii and Levenspiel (1969) indicated that the air velocity and pressure drop plot can determine the fixed bed and fluidized bed region (Figure 8). The transition point from fixed bed to fluidized bed signifies the minimum fluidization velocity.

Figure 7. Cold fluidization setup

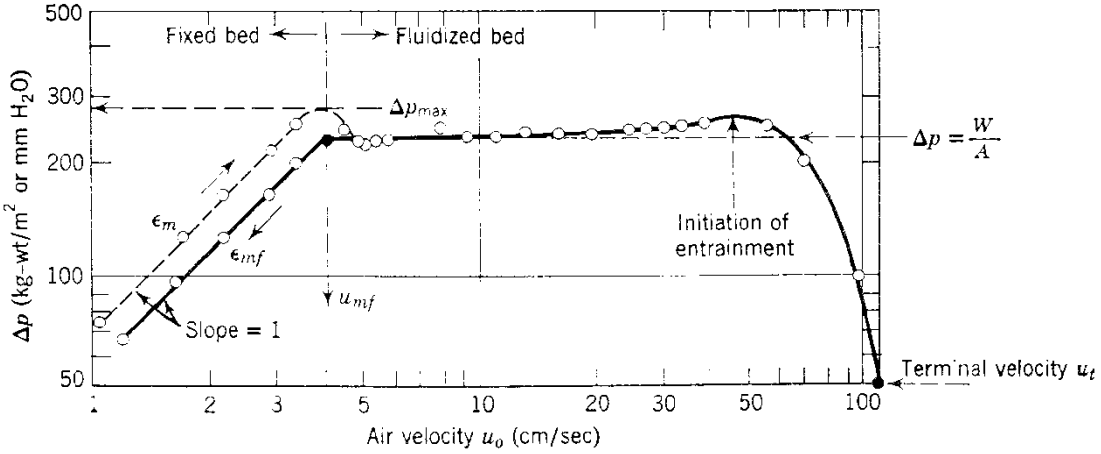

Figure 8. Pressure drop versus gas velocity for a bed of uniformly sized sand particles (Shirai, 1958).

Feasibility of the Instrumentation and Control System for the Gasifier Operation

The feasibility of the developed process control program was evaluated based on its ability to facilitate measurement, operation and control of the fluidized bed gasification system. A good control of the gasification reaction temperature and its stability would indicate good performance of the devices installed in and the control system for the gasifier. The gasification reaction temperature was controlled by the proper adjustments in the fuel feed flow and air flow. The minimum fluidizing velocity of the bed material was determined using existing formula and conducting fluidization experiments.

Gasification tests were done using segregated municipal solid waste (MSW) pellets as fuel feedstock. Preliminary characterization of the MSW was conducted before gasification and the char produced was used for further analysis. Determining the bulk density and stoichiometric air to fuel combustion ratio of the MSW pellets is important in the development of the control system program to properly operate the gasification system.

RESULTS AND DISCUSSION

Graphical User Interface Development

The graphical user interface (GUI) was designed to provide quick control of the process, display all important information and indicate faulty operation. Figure 9 shows the schematic diagram of the main GUI developed for the overall gasification system

indicating the important parameters such as air flow, fuel flow and reaction temperature. The other GUIs developed are shown in Appendix B. The gasifier tabs indicate the

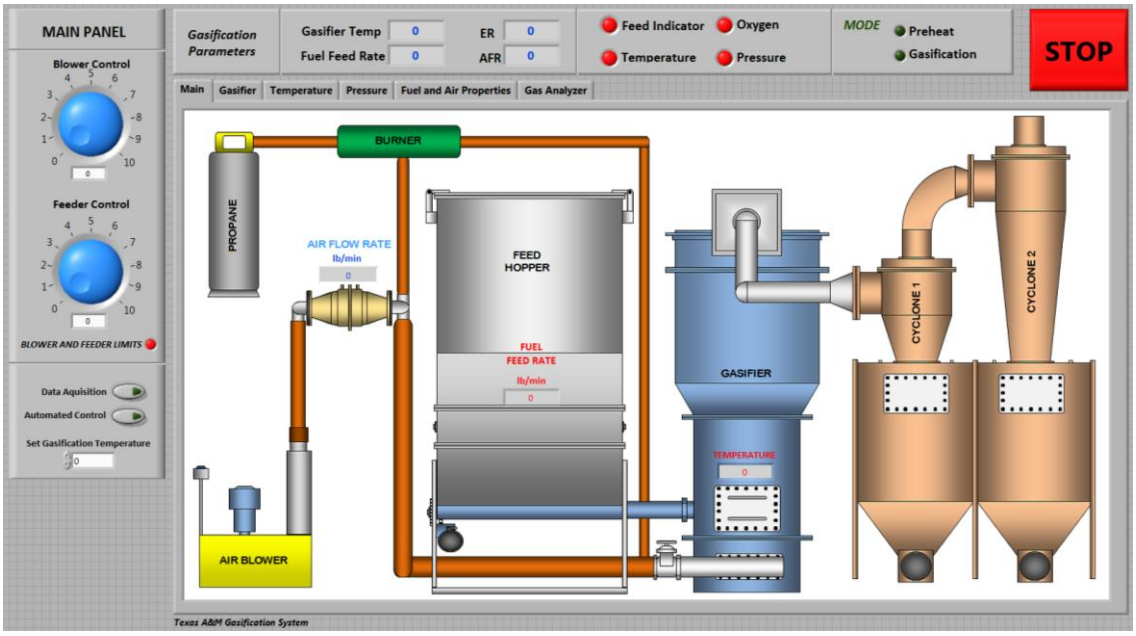

Figure 9. Main interface of the gasification control

current temperature at the different locations in the reactor: plenum, gas distributor plate, middle bed, upper bed and freeboard (Figure 10). These temperature points were displayed in real time and provided valuable information in the gasification operation. The temperature and pressure tabs create a time-based chart of the said parameters during the operation. The chart provides the important temperature and pressure profile of the gasification operation that the operator can make use of. Temperature profile presents the gasification reaction while the pressure profile provides the fluidization state

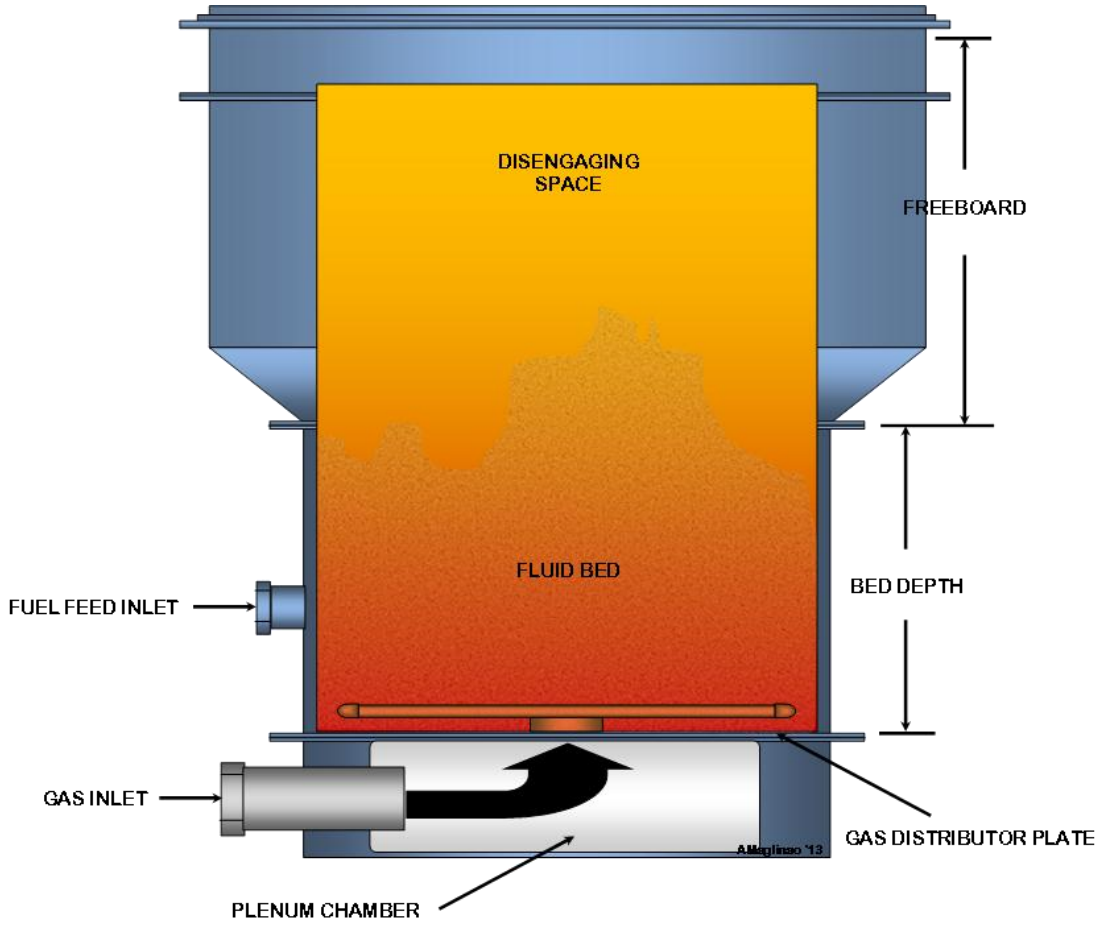

Figure 10. Gasification in a fluidized bed reactor

and the need for additional bed particles. The remaining tabs indicate the fuel and air properties and also the synthesis gas composition throughout the operation. The air and fuel properties were used to calculate the current equivalence ratio which is essential during operation. These tabs were specifically designed to provide detailed information of the gasification system. The other parts of the GUI provide control and monitoring of the major parameters of the gasification system. These provide the control of the air

flow and fuel flow and also different safety indicators to warn the operator of the unexpected problems that may be encountered.

Modules Used in the Control System

Seven different modules for the NI CompactDAQ were used in the development of the control system (Figure 11 and Table 1). These modules correspond to the instrument being measured or controlled. Common gasification parameters were easily monitored by using the proper modules and settings.

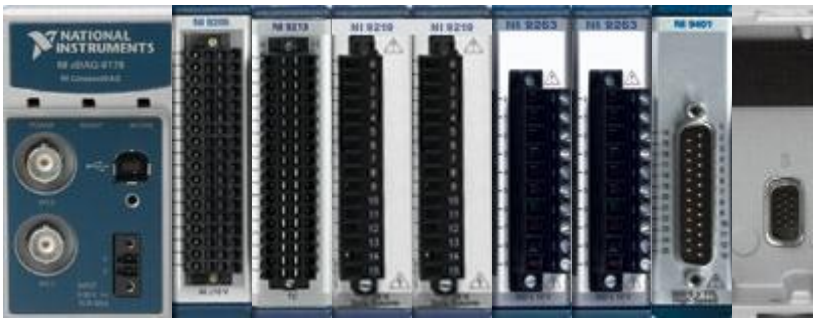

Figure 11. NI CompactDAQ system

Table 1. Modules used for CompactDAQ and the instruments being measured/controlled

CompactDAQ Module	Instruments being measured/controlled
NI 9213 16-ch TC, 24-bit C Series module	K-type thermocouples
NI 9203 8-Ch ±20 mA, 200 kS/s, 16-Bit AI Module	Differential pressure transducers NDIR gas analyzer
NI 9401 8-Channel, 100 ns, TTL Digital Input/Output Module	Magnetic pickup tachometer
NI 9263 4 ch,16-bit, +/-10 V, 100 kS/s/Ch, AO Module	AC motor controller DC motor controller
NI 9205 32-Channel ±10 V, 250 kS/s, 16-Bit Analog Input Module	Relative humidity and temperature transmitter

Gasification temperatures were measured by utilizing the thermocouple module and selecting a type K setting. Current output of differential transducers was converted into mm of water (mmW) by obtaining the proper calibration curve. The speed of the driving motor of the feed screw conveyor was measured with the use of the magnetic pickup tachometer. The driving motor and screw conveyor were connected with gears having a reduction ratio of 129. The actual speed of the screw conveyor was obtained via transistor-transistor logic (TTL) digital input readings with the gear ratio and related to the biomass fuel feed rate through calibration.

Organization of the Gasification Control System

The control system was likewise organized into seven LabVIEW Virtual Instruments (VIs) to do specific functions (Table 2). Temperature and pressure VIs set to gather 50 samples in 3 seconds were used to monitor these parameters and obtain their average during operation. The feeder calibration VI was used to determine the fuel feed rate based on the motor RPM. A regular helicoid flighting screw conveyor was utilized

Table 2. Different VIs developed and their specific function

LabVIEW VI	Function
TAMUFBGCS	Serve as the Main Control System
Temp module	Take the average temperature profile
Pressure module	Take the averaged pressure profile
Feeder Calibration	Convert motor RPM to fuel feed rate
CFM Calculation	Convert laminar flow element differential to air flow with correction factors
Indicators	Provide operation and safety indicators
PID module	Provide control of reaction temperature

to measure the mass flow rate of solids in the feeding system by using its dimension in the equation proposed by Woodcock and Mason (1987) as shown below.

$$\dot{m}_s = \rho_b \frac{1}{4} \pi \left(D_{sc}^2 - D_{sh}^2 \right) k \lambda N \quad [9]$$

where ρ_b, bulk density
D_{sc}, trough of flight diameter
D_{sc}, shaft diameter

Figure 12 describes the measurements of the screw conveyor that was used in the equation. The loading factor values for different fuels where obtained by conducting several experiments (Table 3).

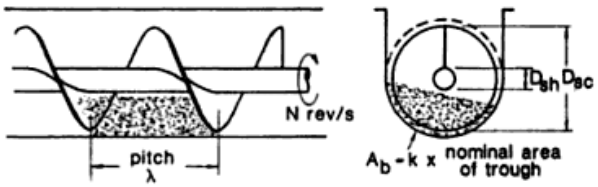

Figure 12. Screw conveyor measurements (Woodcock and Mason, 1987)

For accuracy, the loading factor values were obtained by calibration experiments to obtain the relationship between the motor RPM and fuel feed rate (Appendix C). For other solid fuels, the developed control system has the option to estimate the feed rate by using the bulk density of the particular fuel and a safe loading factor assumption.

Table 3. Bulk density and loading factor

Fuel	Bulk Density $kg\ m^{-3}$	Loading Factor
MSW Pellets	421	0.65
Sorghum[a]	163	0.10
Manure[a]	264	0.49
CGT[a]	189	0.16

[a](Maglinao, 2009)

The CFM calculation VI enabled the conversion of the laminar flow differential pressure to air flow. For an accurate actual and standard air flow, the static pressure, temperature and relative humidity were obtained to have the appropriate correction factors. The standard volumetric flow rate (SCFM) of air was calculated using the equation:

$$\mathrm{SCFM} = (\mathrm{B} \times \mathrm{DP} + \mathrm{C} \times \mathrm{DP}^2)\left(\frac{\mu_{std}}{\mu_f}\right)\left(\frac{P_f}{P_{std}}\right)\left(\frac{T_{std}}{T_f}\right)\left(\frac{\rho_{wet}}{\rho_{dry}}\right) \quad [10]$$

where DP = differential pressure
μ = viscosity
P = pressure
T= temperature
B, C = laminar flow element constants
ρ = density
std = standard conditions
f = actual conditions

The actual constants and correction factors for the actual laminar flow element used are summarized in Appendix D. Safety indicator VI was developed to provide warnings of faulty operation. Part of the main VI provides control for the blower and feeding systems. The motor controllers for both the blower and feeding systems have the capability of regulating the speed of the motor by an external 10V analog voltage. The voltage supplied to the motor controllers was varied based on the tasks created.

The control system developed had the ability to reliably measure a variety of gasification input parameters including compositional analysis of the fuel and relate this to the control of the gasifier. A number of parameters can be controlled to differentiate the various feedstock conversion processes and obtain the desired end product. These include heating rate, final temperature, residence time at certain temperature, presence or absence of air or oxygen, fuel particle size, and fuel moisture content. A good control system is also able to take automatic corrective actions under certain critical conditions. The most basic feedback system measures the controlled variables, compares the actual measurements with the desired values and uses the difference between them (error) to identify the appropriate corrective action. It is therefore necessary to first measure the variables that are to be maintained at the desired standard values (Anderson, 1997). According to LePori and Soltes (1985), the fuel to air ratio and operating temperature are probably the two most critical parameters to control during the biomass conversion. The air flow rate and fuel feed rate were the main parameters used for the proper control of the gasification process. Fluidization, stoichiometric conditions and other safety conditions were also monitored in real-time.

Fluidization of the Bed Material

The minimum fluidization velocity was obtained for the bed material, Mulgrain 47-10x18, by using the quadratic equation shown below and inputting the properties of the bed material used and also by conducting cold fluidization experiments. The properties of the bed material used are given in Table 4.

$$\frac{1.75}{\phi_s {\epsilon_{mf}}^3}\left(\frac{d_p u_{mf}\rho_g}{\mu}\right)^2 + \frac{150(1-\epsilon_{mf})}{{\phi_s}^2 {\epsilon_{mf}}^3}\left(\frac{d_p u_{mf}\rho_g}{\mu}\right) = \frac{{d_p}^3 \rho_g(\rho_s - \rho_g)g}{\mu^2} \qquad [11]$$

Table 4. Properties of the bed material used

Properties	Values for Mulgrain 47
Mean particle diameter (mm), d_p	1.06
Particle Density (g cm^{-3}), ρ_s	2.45
Voidage, ϵ_{mf}	0.40
Sphericity, ϕ_s	0.63

By using the equation, the superficial velocity at minimum fluidizing conditions, u_{mf}, was calculated. Having the air at 25°C and considering the related properties of the bed material, the minimum fluidization velocity was estimated at 33.71 cm s^{-1}. Since the gas flow rate through a fluidized bed is not just limited by the minimum fluidization velocity but also the entrainment of solids by gas, the u_{mf} provides the lower limit of the gas flow rate. The upper limit of the gas flow rate was estimated at 823 cm s^{-1} which corresponds to the terminal velocity of the particles using the equation,

$$u_t = \left[\frac{4}{225}\frac{(\rho_s - \rho_g)^2 g^2}{\rho_g \mu}\right]^{1/3} d_p \qquad [12]$$

The resulting gas velocity limits were used in the process control program.

The results of the cold fluidization experiments wherein the gas flow and pressure drop across the bed were measured while increasing the air flow at constant rate

are shown in Figure 13. The figure shows that the minimum fluidization velocity, u_{mf} of 37 cm s^{-1} was observed. This signifies that an air flow rate lower than 37 cm s^{-1} would result in a fixed bed and in a fluidized bed at higher values. To effect fluidization in a 305 mm reactor, a volumetric air flow rate of 2 Nm^3 min^{-1} would be required. The minimum fluidization value calculated from empirical formulas and that obtained from actual experimentation did not differ significantly with a difference of just 9%.

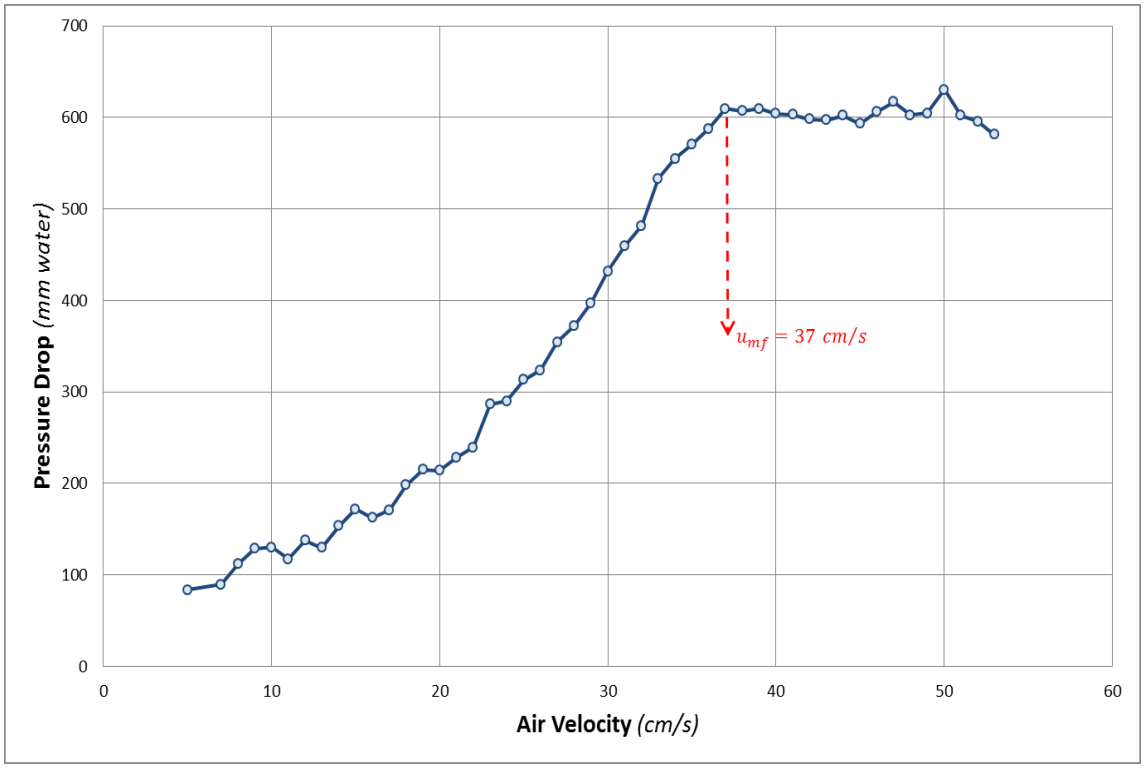

Figure 13. Plot of pressure drop against air velocity from fluidization experiments

Control of Gasification Processes

With the variables defined, gasification control system was developed and presented in Figure 14. The program monitored the operation of the gasifier during the startup process of heating the reactor, while the propane burner was in use. It has the option of enabling the automated control once the reactor temperature reached 425°C and above. The default setpoint reaction temperature was set at 700°C. The appropriate equivalence ratio (ER) was set at different temperature ranges (Table 5). The ER was varied by altering the fuel feed flow based on fuel elemental composition and the current air flow being used. The ER values were obtained from previous experiments and this method eliminated the need for having a big alteration on the fuel feed flow. It was necessary to have uniform fuel size to provide consistent flow

Table 5. Equivalence ratio used at different gasification temperature ranges for MSW

Gasification Temperature Range (°C)	Equivalence Ratio
425 - 535	1.5
535 - 595	0.8
595 - 650	0.5
650 - 700	0.4
700 - 760	0.3
760 - 815	0.2

through the screw conveyor. Once at the desired temperature, minimal variation in the feed was made using the PID control of LabVIEW. Proportion and integral constants were set based on experimental runs while the derivative constant was set at zero. PI control was used since the speed of the response was not necessary to have the results

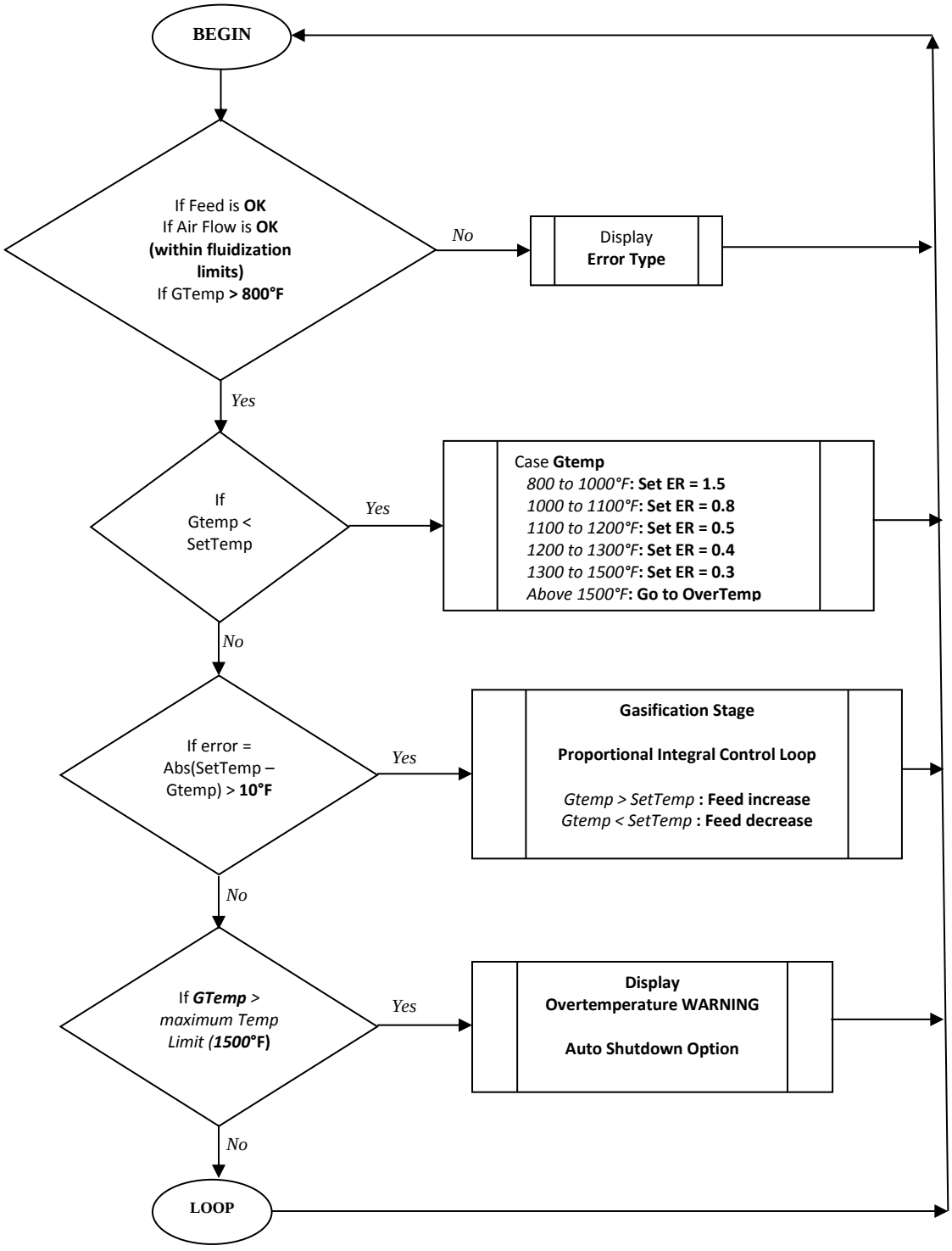

Figure 14. Gasification control system flowchart and PI control loop VI

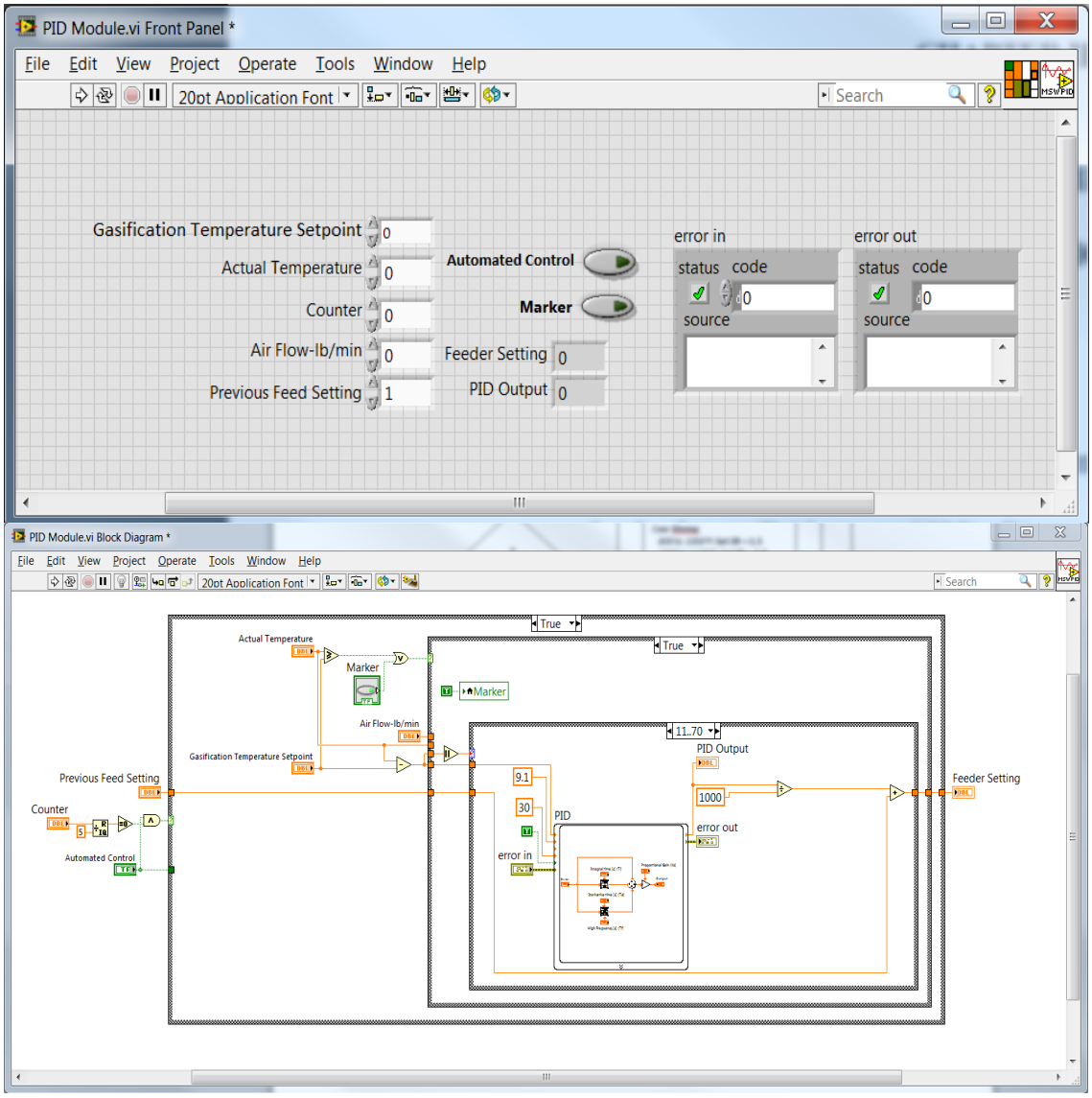

Figure 14 Continued

reach the setpoint in a slower time. The lack of derivative action made the control system steady within a noisy background. The PI control compared the setpoint temperature with the current reaction temperature to obtain the error (e) and calculate

the appropriate fuel feed controller action. Based from previous experiments, proportional gain of 9.1 and integral time of 30 were used for the PI control for MSW.

Feasibility of the Instrumentation and Process Control System

After the reactor temperature reached 450°C and the propane burner was turned off, the automated control system was switched on. It was observed that the process control program adjusted the fuel flow based on the current reaction temperature and setpoint temperature of 700°C. Once the setpoint temperature was reached, the PI loop was activated and the reaction temperature was maintained. The control system was also able to check the fluidization and other safety indicators. The appropriate equivalence ratio was controlled during gasification by the adjustment in the fuel feed rate. A change in the fuel feed was necessary once the absolute error, $|e|$ reached more than 10. During the test, the feed rate was increased as the error reached more than 10. Continuous adjustment in the fuel feed was experienced to compensate for the decrease in fuel in the bin that caused the change of the flow in the screw conveyor.

The operation of the gasification system lasted for 1 h at the desired reaction temperature (Figure 15). As shown on the figure, the control loop made the appropriate changes in the fuel feed rate thereby maintaining the desired reaction temperature. In about 55 min reaction time, the automated control system had full control of the operation of the gasifier. It was also able to perform corrective actions with the disturbances associated with the system. As shown in Figure 16, the gasification control system kept the fluidizing air velocity at an average of 48 cm s^{-1}. This was 30% higher

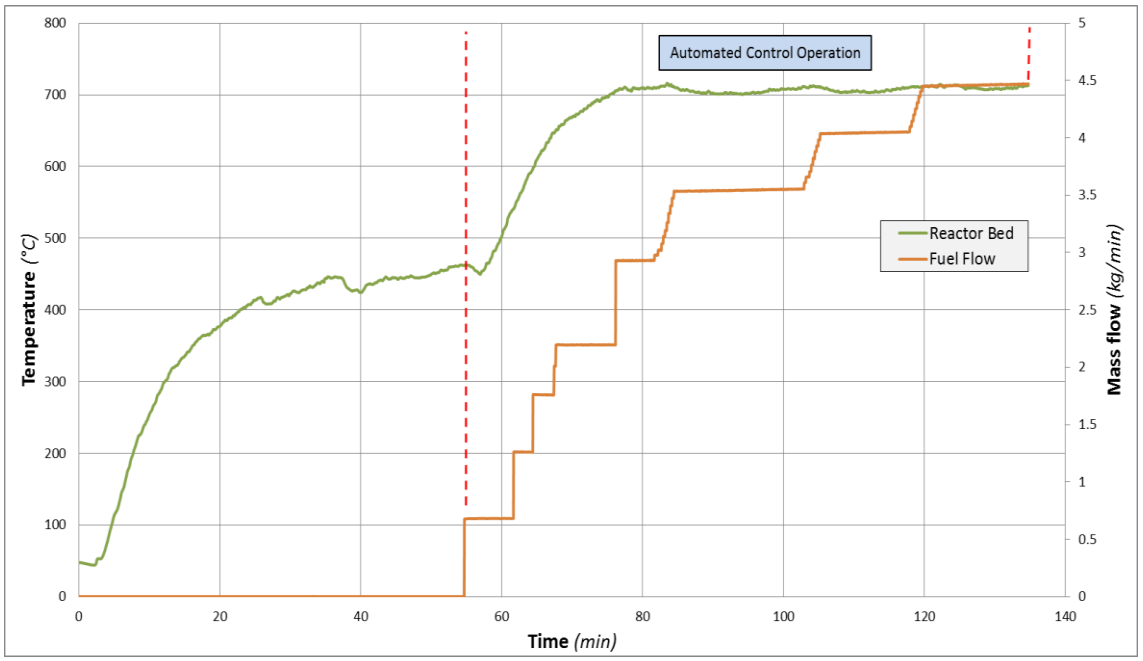

Figure 15. Automated gasification temperature control

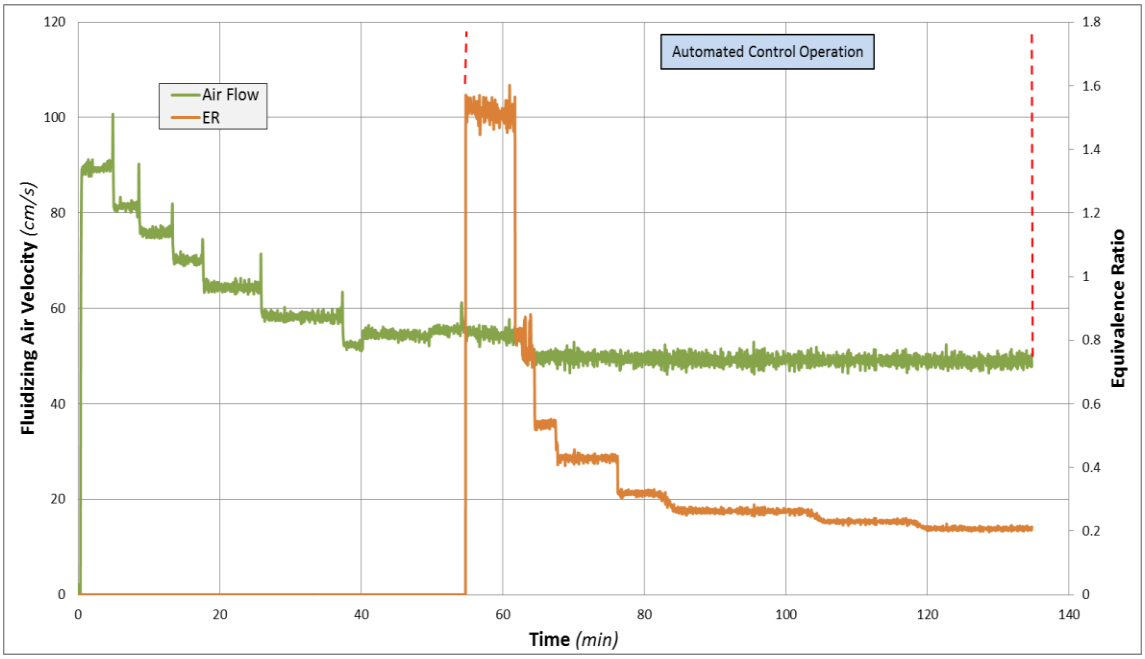

Figure 16. Fluidizing air and equivalence ratio plot during operation

than the minimum fluidization velocity indicating good fluidization of the bed inside the reactor. The desired equivalence ratio at different temperature ranges was also achieved throughout the whole test.

The temperature and pressure profiles observed during gasification further support the feasibility of the instrumentation and the process control program that was developed (Figure 17). The gasification temperature profile showed that the reaction temperature was well maintained at the desired value of 700°C during the operation of the gasifier. The expected start-up time was achieved without any trouble. Near isothermal condition within the reactor was also observed during the experiments. As indicated by the pressure profile, good fluidization also occurred during gasification. The stable pressure profile within the reactor likewise indicated that the bed material loss was minimal because of the optimized gasification operation. These results were comparable with the observations from similar tests conducted by highly trained operator of controlled gasification system (Maglinao and Capareda, 2010a).

Another indication of the feasibility of the instrumentation and the use of the control program was the good production of the synthesis gas from the gasification of MSW. Analysis of the gas produced indicated a heating value (HV) of 7.94 MJ Nm^{-3} (Table 6). The gasification system operated at 94% carbon conversion efficiency and 59% cold gasification efficiency. Gas production went at a rate of 4.71 kg min^{-1} and a yield of 2.37 m^3 kg^{-1} of fuel. The net heating value of the synthesis gas produced was higher than minimum requirement of 4.2 MJ Nm^{-3} suggesting its acceptability for

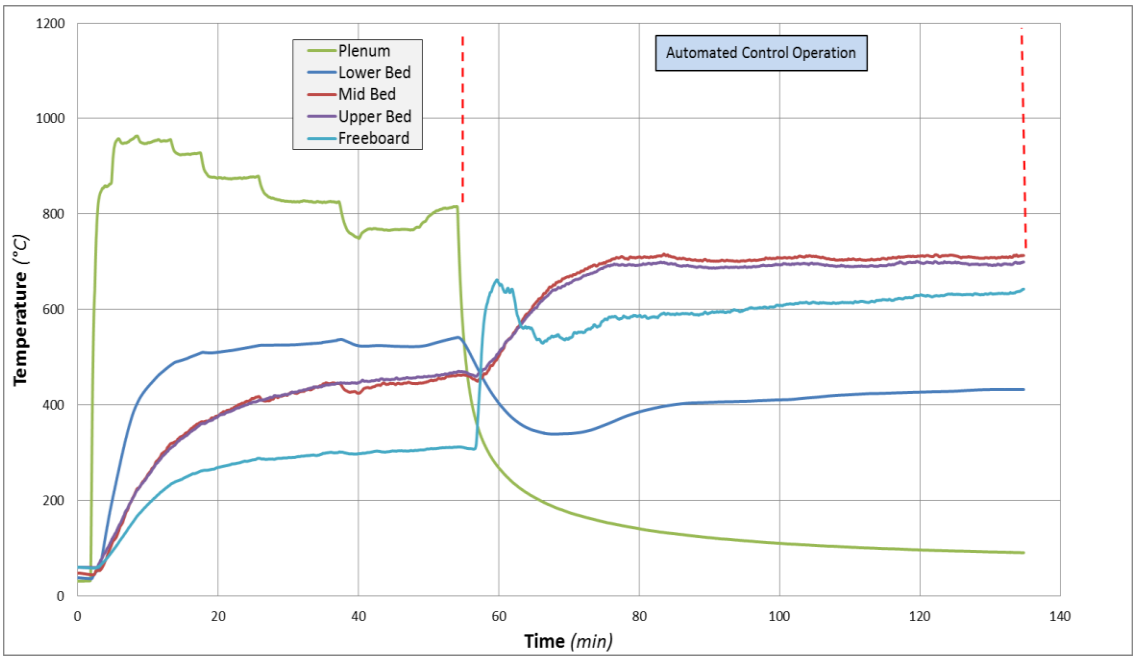

(a)

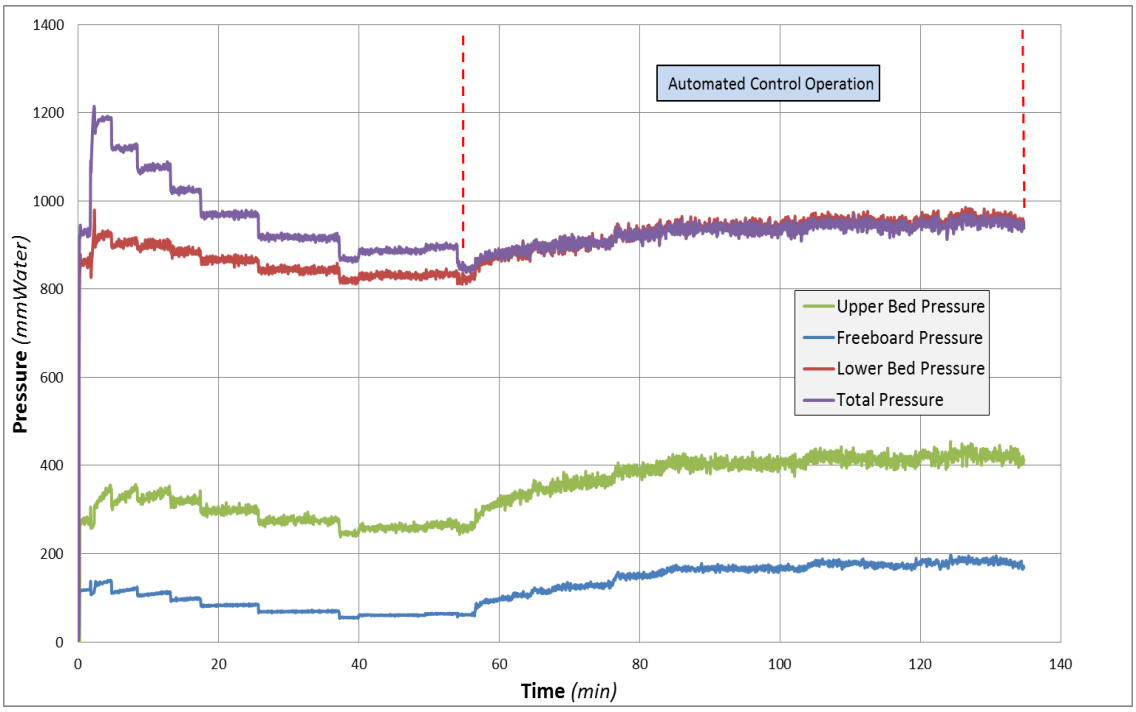

(b)

Figure 17. Gasification (a) temperature and (b) pressure profile.

engine use (Shah et al., 2010). Moreover, consistent flare from the stack was observed that signifies a continuous high quality synthesis gas production. The control system adjusted with the varying conditions of the MSW in the feeding system. These observations indicate a good performance of the TAMU fluidized bed gasifier and the control process developed appeared to work well.

Table 6. Gasification results using MSW

Components and Properties	Resulting Values	
Component Gas (mole %)		
Hydrogen	4.91 ± 0.29	%
Nitrogen	61.70 ± 3.08	%
Carbon Monoxide	8.43 ± 1.11	%
Methane	3.51 ± 0.34	%
Carbon Dioxide	13.58 ± 1.20	%
Acetylene	0.28 ± 0.01	%
Ethylene	4.31 ± 0.25	%
Ethane	0.49 ± 0.01	%
Propylene	2.35 ± 0.06	%
Net HV	7.94 ± 0.19	$MJ\ Nm^{-3}$
Gas Yield	2.78 ± 0.54	$Nm^3\ kg_{MSW}^{-1}$
Gas Production	4.00 ± 0.34	$kg\ min^{-1}$
Carbon Conversion Efficiency	93.75 ± 0.04	*%*
Cold Gasification Efficiency	59.01 ± 0.11	*%*

CONCLUSION

This particular study explored the feasibility of an appropriate instrumentation and control system for a pilot scale atmospheric fluidized bed biomass gasification unit to facilitate its operation. The most important parameters were properly identified and evaluated to make the control of the gasification system much easier and facilitated.

These parameters include the gasification temperature, pressure, the air flow rate and the fuel feed rate. The necessary devices were installed in the gasification system and calibrated to conveniently monitor and control these identified parameters. A control system program was developed to process all the electrical signals into readable values and monitor the sensor measurements in the gasification unit. The feasibility of the developed process control program was evaluated based on its ability to facilitate measurement, operation and control of the fluidized bed gasification system using segregated municipal solid waste (MSW) pellets as fuel feedstock.

In about 55 min reaction time, the automated control system had full control of the operation of the gasifier. The desired gasification reaction temperature of 700°C was maintained for about 1 h during the test. The control system was also able to check the fluidization conditions and other safety indicators. The appropriate equivalence ratio was controlled during gasification by the adjustment in the fuel feed rate. During the test, the feed rate was increased as the error reached more than 10. Continuous adjustment in the fuel feed was experienced to compensate for the decrease in fuel in the bin that caused the change of the flow in the screw conveyor. It was also able to perform corrective actions with the disturbances associated with the system.

The gasification control system kept the fluidizing air velocity at an average of 48 cm s^{-1}. This was 30% higher than the minimum fluidization velocity indicating good fluidization of the bed inside the reactor. The desired equivalence ratio at different temperature ranges was also achieved throughout the whole test.

The temperature and pressure profiles observed during gasification further support the feasibility of the instrumentation and the process control program that was developed. The gasification temperature profile showed that the reaction temperature was well maintained at the desired value of 700°C during the operation of the gasifier. The expected start-up time was achieved without any trouble. Near isothermal condition within the reactor was also observed during the experiments. As indicated by the pressure profile, good fluidization also occurred during gasification. The stable pressure profile within the reactor likewise indicated that the bed material loss was minimal because of the optimized gasification operation.

Another indication of the feasibility of the instrumentation and the use of the control program was the good production of the synthesis gas from the gasification of MSW. Analysis of the gas produced indicated a heating value (HV) of 7.94 MJ Nm^{-3}. The gasification system operated at 94% carbon conversion efficiency and 59% cold gasification efficiency. Gas production went at a rate of 4.00 kg min^{-1} and a yield of 2.78 $m^3 kg^{-1}$ of fuel.

CHAPTER III

OPTIMIZATION OF SEGREGATED MUNICIPAL SOLID WASTE GASIFICATION

INTRODUCTION

Biomass, which can be classified as plant, animal manure or municipal solid waste, is widely considered a major potential fuel and renewable energy resource for the future (Bridgwater, 1995). Biomass resources are abundant in most parts of the world and various commercially available conversion technologies could transform the current traditional technology into modern applications for energy source (Johansson et al., 2006). Like fossil fuels, biomass contain high percentages of carbon and hydrogen and can be a good alternative source of energy (LePori and Soltes, 1985). Biomass used as energy source can reduce CO_2 gas emission and SO_2 and NO_x pollution due to its neutral carbon contribution to the atmosphere (Cao et al., 2005).

The generation of excessive amounts of waste is a common occurrence in most developed countries. As societies develop, the amount of waste material generated increases to a level that its disposal becomes a problem. The development of processes in the disposal and utilization of industrial solid wastes has caught attention of policymakers and researchers to address the issue of cleaner energy generation for enhanced environmental quality. Techniques in waste management should be able to generate greater recovery value from the wastes and maintain the sustainability of the process (Mastellone and Arena, 2008).

Gasification is one of the thermochemical processes that can convert waste into a useful product known as synthesis gas and these conversion routes have an excellent future (Sipila, 1995). Without complete combustion of the fuel, conversion occurs in an oxygen deficient (partial oxidation) condition at high temperatures. The partial oxidation process of the biomass takes place at temperature of about 800°C and produces primarily combustible gases consisting of carbon monoxide (CO), hydrogen (H_2) and traces of methane and some other products like tar and char (Rajvanshi, 1986). Four stages occur during gasification of carbonaceous material: drying, volatilization, combustion, and reduction (Knoef, 2005). The moisture within the material is heated and removed during the drying process. Continued heating volatilizes the material where volatile matter separates from the particle and comes into contact with the oxygen. The very exothermic combustion process then occurs providing the heat for the last stage, the reduction reactions, to occur. The reduction reactions include water gas reaction, Boudouard reaction, water-gas-shift reaction, and methanation reaction (Swanson et al., 2010).

In order to effect the most efficient transformation of biomass to fuels and other forms at the desired scale of operation, an understanding of the physical and chemical characteristics of different biomass resources is needed (Goswami and Kreith, 2008). Large scale projects for gasification have been envisioned for alternative energy sources and yet many of these have remained in the proposal stage. Agricultural industries, such as the cotton gin, poultry and dairy industries, generate tons of wastes while consuming enormous amounts of heat and power in their operations. Thus, the on-site conversion of

the generated wastes into useful products is the most practical option as it will also minimize the transport cost of the biomass. Ultimately, this system will make these industries produce their heat and power requirement thereby indirectly contributing to reduced dependence on foreign oil and generating new businesses in the farm.

This part of the research looked at the optimization of the production of synthesis gas from the gasification of segregated municipal solid waste (MSW) as feedstock. The specific objectives of the study were to: (a) characterize the segregated municipal solid waste (b) evaluate the most appropriate preparation of the feedstock for gasification and (c) apply the response surface methodology to optimize synthesis gas production.

METHODOLOGY

Gasification Experiments

The gasification experiments were conducted using two different fluidized bed biomass gasifiers developed at Texas A&M University at College Station. Texas (Figure 18). The first fluidized bed gasification system (FBG1) has a circular reactor with a 305 mm diameter while the second one (FBG2) has a 305 mm square reactor. These reactors are protected under US Patent No. 4848249 and intellectual property disclosures TAMUS 2814 serial No. 61/302,001, respectively. Both gasification systems utilize air as the gasifying agent and a feeding system using a 5 cm and 10 cm diameter screw conveyor, respectively. Two stage TAMU design cyclones were installed on the units to capture the solid products (char) that are produced with the gas.

Mulgrain 47- 10 x 18 (C E Minerals, Andersonville, GA) was used as the bed material. For FBG1, the bed material was sieved using Tyler sieves 12 and 20 to obtain a particle size of -1.70 mm to + 0.85 mm. Approximately 30 kg of sieved bed material was placed inside the reactor. FBG2 used the standard particle distribution and about 80 kg

FBG1 FBG2

Figure 18. Gasification systems

of bed was used in the reactor. The gasification units were equipped with monitoring and control devices and a software program developed to facilitate the operation of the system.

Municipal Solid Waste Characterization

The inherent characteristics of the biomass resources determine both the choice of conversion and any subsequent processing difficulties that may arise (McKendry, 2002). Therefore, the utilization of biomass resources and other organic waste materials

need an extensive study of its physical, chemical, and thermodynamic properties (Nhuchhen and Abdul Salam, 2012). These properties, for example, determines the higher heating value which is defined as the quantity of energy released when a unit mass is combusted including the latent heat of vaporization of water.

The gasification test was conducted using segregated municipal solid waste (MSW) provided by the Balcones Resources (Dallas, TX). They are 2.5 cm x 5 cm fuel cubes made up of items that cannot be traditionally recycled such as food packaging wastes, waxed cardboard and software wastes. Before gasification, the MSW was characterized by conducting proximate and ultimate analyses of the biomass samples in three replicates. About 1 g sample of the biomass was used for proximate analysis. The ash and volatile matter (VM) contents were determined using the gravimetric method according to ASTM standards E 1755 (Standard Test Method for Ash in Biomass) for ash and D3175 (Standard Test Method for Volatile Matter in the Analysis Sample of Coal and Coke) for VM. The amount of fixed carbon (FC) was obtained by difference. In addition, the moisture content was determined by oven drying in air approximately 1 g of ground sample materials overnight at 105°C following the modified ASTM E871(Standard Method for Moisture Analysis of Particulate Wood Fuels). The higher heating value (HHV) was measured from the combustion of the biomass using a Parr 6200 bomb calorimeter (Parr Instrument, Moline, Illinois).

For ultimate analysis, 2 g samples of MSW were ground to nominally -200 mesh size particles using a Wiley Mill (Thomas Scientific, Swedesboro, NJ). The amounts of carbon, hydrogen, nitrogen and sulfur were determined using a Vario Micro Cube

elemental analyzer (Elementar Americas Inc, Mt. Laurel, NJ) and the amount of oxygen obtained by difference assuming no halogens were present. This analysis conforms to ASTM D 3176 which defines ultimate analysis as determining the amounts of the carbon and hydrogen in the material, as gaseous products in complete combustion, determining the amounts of sulfur, nitrogen and ash and the estimation of oxygen by difference. In this study, the amount of ash was obtained from proximate analysis. The resulting values from the analysis were reported in weight percent and dry basis (db).

MSW Feed Material Preparation and Gasification Tests

Feed processing and gasification testing were necessary as the provided MSW fuel cubes were not suitable for the feeding system of the gasification units. The MSW were processed into 3 forms: (a) fluff (b) shredded and (c) pellets (Figure 19). The fluff was obtained by processing the cubes using a hammer mill with 0.6 cm sieve. The shredded MSW was prepared using a Troy-Bilt CS 4265 chipper/shredder and the 6 mm diameter pellets were made using a GC-9PK-200 Fodder pellet press. The bulk density of each form was obtained using ASTM E-873-06 (Standard Test Method for Bulk Density of Densified Particulate Biomass Fuels) standard method. The friction angle of the different MSW forms was obtained by tilting a 50 cm x 25 cm general purpose low carbon steel sheet.

The fluff and shredded MSW forms were tested in FBG1 and their behavior was observed and noted. Due to FBG1 limitations in the feed hopper design, MSW pellet was not tested and instead the FBG2 was used. Shredded and pellet MSW forms were

tested in FBG2. Due to its friction angle, the MSW fluff was not tested in FBG2. The observations from the MSW gasification tests using the two systems were recorded and evaluated and the production of the synthesis gas analyzed.

Figure 19. Different MSW forms

Gasification Experiments

The FBG2 (with 305 mm square reactor) gasification unit was prepared for each test by first checking and calibrating instrument connections and readings. Mulgrain 47-10x18 with a mean particle diameter of 1.06 mm was the bed material used. A height of 610 mm of bed material was placed inside the reactor. The process control program was started to regulate the system and gather all instrument readings. At startup, the air blower system was turned on to attain fluidization inside the reactor and the desired operating temperature was achieved by heating the air using a propane burner. As soon as the desired temperature was obtained, the supply of the hot gas from the burner was discontinued and feeding of the biomass was started.

The desired equivalence ratio (ER) was obtained by setting the speed of the screw conveyor of the feeding system and the air flow used. Equivalence ratio is defined as the ratio between the actual air to fuel ratio used to the stoichiometric air to fuel ratio of the particular feedstock. Stoichiometric combustion is the ideal combustion process when the fuel is burned completely. The stoichiometric air to fuel ratio was calculated by using the chemical equation for fuel as shown by equation

$$C_vH_wO_x + \mathbf{a}O_2 \rightarrow \mathbf{b}H_2O + \mathbf{c}CO_2 \quad [13]$$

where a, b and c represent the number of moles of oxygen, water and carbon dioxide, respectively, to effect complete combustion and the subscripts correspond to the mole fraction values derived from the ultimate analysis of the feedstock. Gasification operation normally operates between 20% - 40% of stoichiometric air to fuel ratio.

Optimization of the Net Heating Value of the Synthesis Gas

The response surface methodology (RSM) and facilitated by the Central Composite Design (CCD). Design expert statistical software was applied to optimize the net HV of synthesis gas from the gasification of MSW. RSM is a collection of mathematical and statistical techniques that are useful for the modeling and analysis of problems which have been applied in research in complex variable processes (Chiang and Liu, 2009; Jeong et al., 2009). By careful design of experiments, the objective is to optimize a *response* (output variable) which is influenced by several *independent factors* (input variables). An experiment or a series of tests, called *runs*, were done to make changes in the different factors in order to identify the reasons for changes in the output

response. Typical RSM aims to maximize the yield (y) of a process by determining the levels of two factors (x_1) and (x_1) which is given by the equation

$$y = f(x_1, x_2) + \in \quad [14]$$

where $\in$ represents the noise or error observed in the response y. The response surface is represented by $\eta = f(x_1, x_2)$. Performing the statistically designed experiments, estimating the coefficients in the quadratic polynomial equation and predicting the response are the three major steps involved in surface response methodology (Annadurai and Sheeja, 1998). Response surface fitting and analysis are greatly facilitated by the proper choice of an experimental design. The CCD is the most popular design used for fitting second order models.

In this work, the reaction temperature (x_1) and equivalence ratio (x_1) were set as factors while the synthesis gas composition (H_2, CO, CH_4, C_2H_2, C_3H_6) and net heating value as response variables. The response variables were fitted to the independent variables by means of multiple regression analysis. In order to test the statistical significance of the fit of the quadratic model to the experimental data and the significance of the regression model, the individual model coefficients and lack-of-fit were performed. This statistical evaluation of the models for all of the response variables was given by the Analysis of Variance (ANOVA) using the Design Expert. The ANOVA tests would show which of the proposed models were statistically significant. The terms in the models were evaluated by the p-value at a confidence level of 95%. The lack-of-fit was also calculated but found not to be significant for all the response surface models at a 95% confidence level. Quadratic equations were formulated to predict the

responses to a given value of gasification temperature and ER if the proposed models were found significant. Response surfaces and their respective contour plots were generated to visualize the combined effects of the two factors on the responses.

The control system developed for the fluidized bed gasification system was utilized to control the operation at different reaction temperatures and equivalence ratio. Once the desired temperature and ER were achieved, four gas samples were collected into a 1 L Tedlar bags (Restek, Bellefonte, PA) from each test and analyzed using SRI gas chromatograph (SRI Instruments, Torrance, CA) with TCD and HID detector to validate the H_2, CO, CO_2 and hydrocarbon composition. Shincarbon ST, 100/120 mesh and Molecular sieve 13x packed columns were used to separate the gas components. The detailed gas chromatograph settings are further discussed in Appendix E. Each gas component was analyzed using three standard calibration methods. The analysis of variance (ANOVA) was perfomed at 95% confidence interval level to fit the gasification temperature and ER with the selected experimental responses using a quadratic second order equation. The char produced during gasification was collected from the first and second cyclones, weighed and elemental analysis conducted. The results of the analysis of the char were used to do carbon balance and obtain the rate of synthesis gas production.

RESULTS AND DISCUSSION

MSW Characteristics

The characteristics of the MSW are summarized in Table 7. The heating value and proximate analysis showed that MSW had a heating value of about 30 MJ kg^{-1}, ash content of 2.6% and volatile matter (VM) of 93%. In any solid fuels, the proximate analysis gives the amount of fixed carbon (FC), volatile matter and ash content as solid, gaseous, and non-combustible components, respectively (Lyons 1985). The ash content of MSW was relatively lower and the heating value higher than other biomass wastes. Compared with the cotton gin trash, the MSW showed 82% higher heating value and 80% lower ash content (Maglinao, 2009). These figures together with a low moisture content of MSW make it suitable for gasification.

Table 7. Characteristics of MSW

Heating Value and Proximate Analysis		
Moisture Content	1.66 ± 0.76	%
Higher Heating Value (db)	30.36 ± 0.47	MJ kg^{-1}
Proximate Analysis (db)		
Volatile Matter	92.93 ± 0.62	%
Ash Content	2.60 ± 0.52	%
Fixed Carbon *(by difference)*	4.47 ± 0.90	%
Ultimate Analysis (db)		
Carbon	60.79 ± 0.98	%
Hydrogen	9.75 ± 0.31	%
Nitrogen	0.01 ± 0.21	%
Sulfur	0.08 ± 0.02	%
Oxygen*(by difference)*	26.77 ± 1.11	%

Ultimate analysis indicated that MSW is mainly composed of carbon, hydrogen and oxygen and only traces of nitrogen and sulfur. With low sulfur content, SO_2 emissions would not pose a problem in the utilization of MSW in energy conversion. The higher carbon and hydrogen contents of the MSW provide another advantage when compared with other common biomass wastes. A kg of MSW would require 9.2 kg of air based from its elemental composition and the stoichiometric combustion as shown in the following equation.

$$C_{5.07}H_{9.75}O_{1.67} + 6.73O_2 \rightarrow 4.875H_2O + 5.07CO_2 \quad [15]$$

With this information, about 1.8 kg to 3.7 kg of air per kg of MSW would result in a good operation of the gasification system. This would result in an equivalence ratio in the range of 0.2 to 0.4. Gasification can be operated at the minimum ER of about 0.20 because the production of tar would not be a problem and the gas would have the maximum possible heating value (Narvaez et al., 1996).

MSW Feed Preparation and Characteristics

Three different forms of the MSW were prepared and processed to make it more suitable for the feeding system of the gasification units. Table 8 shows the physical characteristics of the shredded, fluff and pellet forms. The MSW pellets showed the highest bulk density while the fluff form had the highest friction angle. Bulk density of solids is basically determined by dividing its mass by the bulk volume it occupies. This volume includes the inter particle spaces between particles as well as the particle volume

(Stanley-Wood, 2008). On the other hand, wall friction angle is defined as the arc tangent of the coefficient of sliding friction between the bulk solid and hopper wall material. This value is often affected by pressure change and the two have an inverse relationship (Carson, 2008). Based on previous work on infinitely long wedge-shaped hoppers, the fluff and shredded MSW friction angle was expected to result in a funnel flow on a 40° planar hopper angle (Jenike, 1964).

Table 8. Bulk density and friction angle of MSW

MSW Form	Bulk Density *kg m^{-3}*	Friction Angle *degrees*
Shredded	62 ± 3.15	25.16 ± 1.06
Fluff	33 ± 1.10	33.39 ± 1.32
Pellets	421 ± 37.13	17.95 ± 0.53

Gasification Experiments

Gasification Tests of the Fluff and Shredded Forms of MSW Using FBG1 Unit

The fluff form of MSW was first tested using FBG1 and resulted in good gasification. The gasification test was operated at around 760°C and lasted for about 40 min. Gasification temperature and pressure profiles are illustrated in Figure 20. As shown in the figure, a good control of the gasification temperature was achieved throughout the test. Hydrogen, carbon monoxide and hydrocarbons were the combustible gases produced during the gasification.

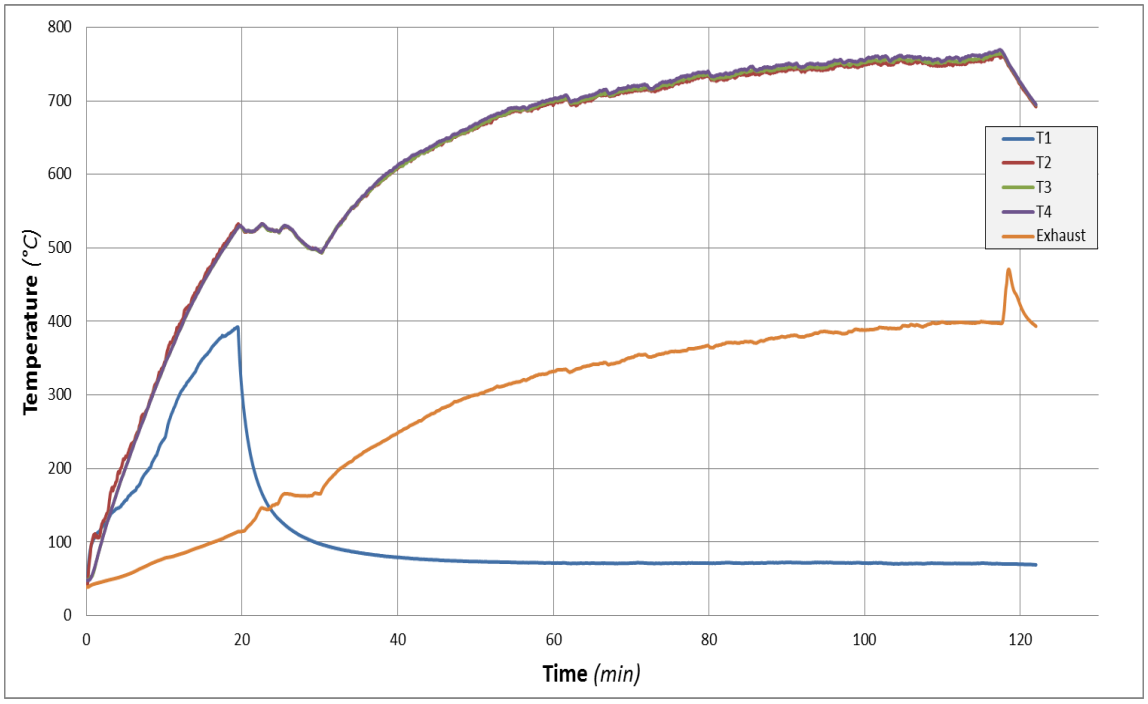

(a) Temperature profile

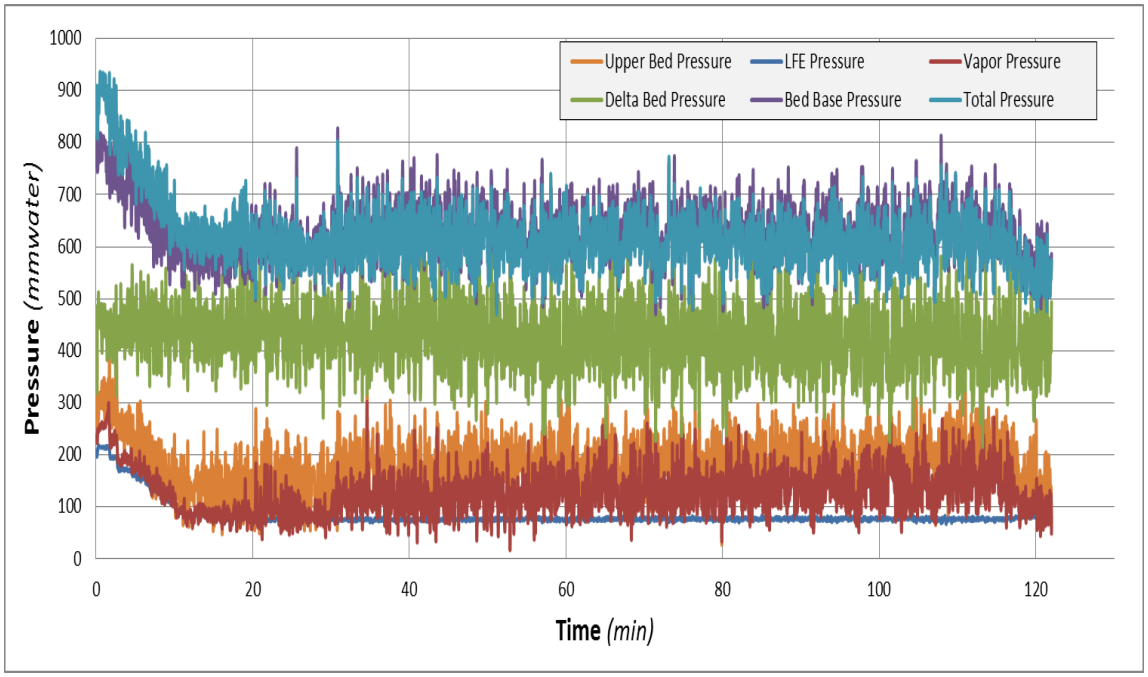

(b) Pressure profile

Figure 20. MSW fluff gasification using FBG1

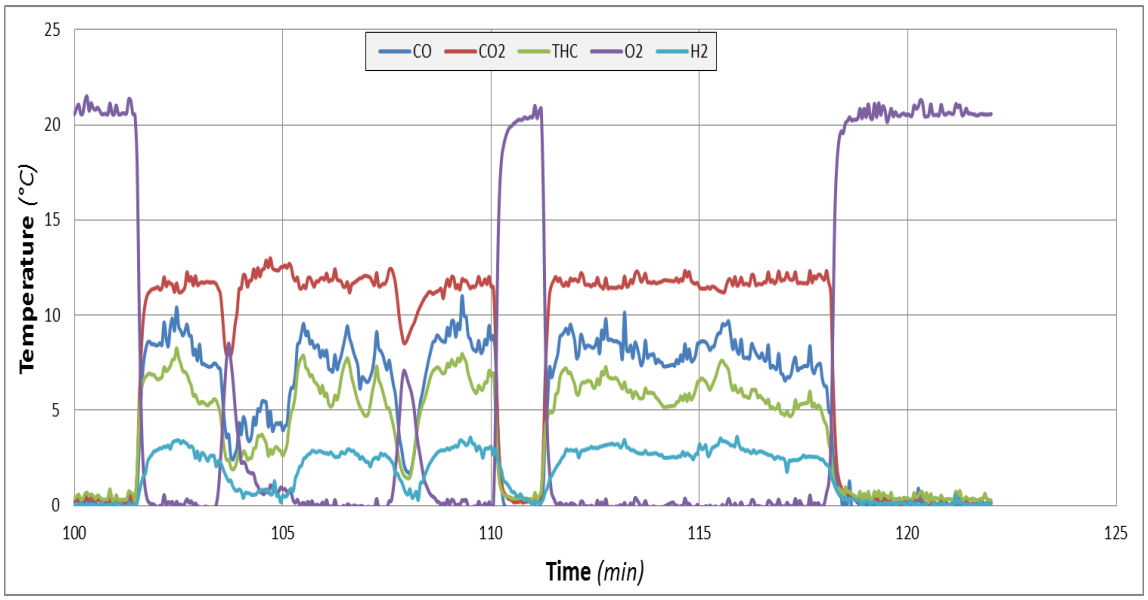

(c) Synthesis gas production

Figure 20. Continued

Gas samples obtained during the tests of fluff MSW and the synthesis gas produced using woodchips were compared and the results are summarized in Table 9. The synthesis gas produced from MSW had relatively higher heating value than that from woodchips. Since the woodchips gasification was operated at a lower ER of 0.35 compared to an ER value of 0.45 for MSW, the synthesis gas produced from MSW gasification could still be improved by lowering the ER. The ER can be lowered by either increasing the MSW feed rate or lowering the air flow rate. However, this was not possible as the gasification system was operating at the minimum fluidization and the fluff has a low bulk density for the feed rate to be increased through the screw auger.

Table 9. Synthesis gas production from woodchips and fluff MSW

Synthesis Gas Composition (mol %)	*Woodchips*	*Fluff MSW*
Hydrogen	4.28	3.28
Nitrogen	55.34	58.60
Carbon Monoxide	16.7	13.42
Methane	3.77	3.91
Carbon Dioxide	18.01	16.69
Ethylene	1.01	2.48
Ethane	0.32	0.40
Propylene	0.57	1.22
Heating Value of Gas (MJ Nm^{-3})	5.27	6.32

Expecting that the ER could further be lowered by using a material with higher bulk density, the shredded MSW was tested next. However, the tests resulted in clogging of the screw auger due to its small opening of 5 cm (Figure 21). Thus, no further tests were conducted using the first unit.

Tests of Shredded MSW Using FBG2 Unit

The shredded MSW was then tested with the FBG2 unit expecting that the bigger 10 cm feeding system would partially solve the clogging of the screw auger and lower the ER value. This was done with some additional work employed, particularly the agitation in the feed hopper for proper feeding of the MSW. However, problems were still encountered with feeding the shredded MSW even with agitators in place. A cohesive arch or bridge or a rathole were formed which caused flow obstruction (Figure 22, 23).

Figure 21. Shredded MSW clogging

Figure 22. Ratholing and arching of shredded MSW

Arching occurs when an obstruction in the shape of an arch or a bridge forms above the outlet of a silo and prevents any further discharge. It can be an interlocking arch or a cohesive arch. An interlocking arch where the particles mechanically lock to

form the obstruction occurs when the particles are large compared to the outlet size of the hopper. A cohesive arch occurs when particle-to-particle bonds form, allowing the material to pack together to form an obstruction. Ratholing or piping, is a phenomenon when more or less vertical flow channel develops above the hopper opening and remains stable once emptied. If the material being handled has sufficient cohesive strength, the stagnant material outside of this channel will not flow into it. Rathole can be strongly affected by the bulk solids temperature, time of storage at rest, moisture content and particle size distribution (Carson, 2008; Woodcock and Mason, 1987).

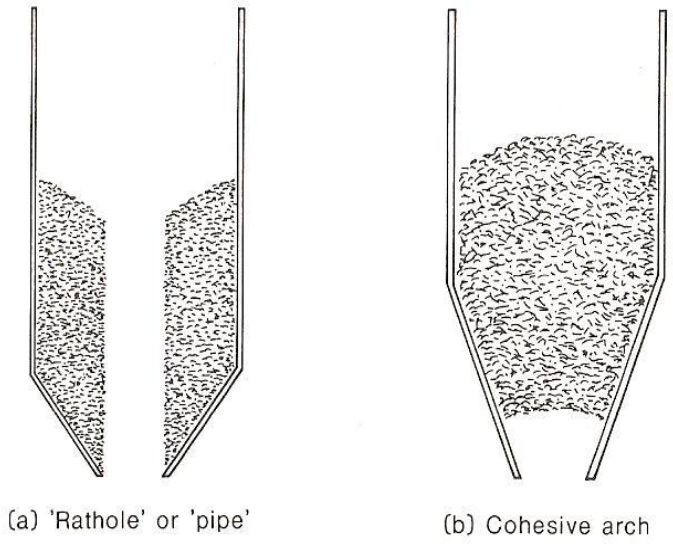

Figure 23. Obstructions to flow from hoppers (Woodcock and Mason, 1987)

Both rathole and cohesive arch are characteristics of cohesive materials like the shredded MSW. Cohesive materials allow gas flow to occur through channels rather than distributed throughout the interstitial voids. These obstructions occur when the bulk

solid has gained enough strength to support itself and therefore both are impossible in free flowing materials. Ratholing will occur if the non flowing material consolidates sufficiently to remain stable after the flow channel has emptied out.

Gasification Tests of MSW Pellets Using FBG2

With the problems still encountered with the shredded MSW, pellets were used to advance with the gasification experiments. The pellets were 6 mm in diameter with a bulk density of 421 kg m^{-3}. With a proper size and bulk density, the pellets moved through the screw conveyor uniformly without any problem. Its characteristics also eliminated the need for agitators in the feed hoppers. Calibration experiments were conducted as discussed in Chapter 2 and Appendix C. Gasification experiment was conducted at an average reaction temperature of 730°C. With the uniform feeding of MSW, a good control of the gasification temperature and fluidization was achieved during the tests (Figure 24). Compared to FBG1, the pressure profile in FBG2 was a lot stable due to the more uniform air distribution. Since FBG2 used larger mean particle size for bed material, the MSW gasification resulted in higher pressure and air flow providing flexibility in the gasification operation. With this, FBG2 produced a higher heating value synthesis gas compared with the gas produced by FBG1.

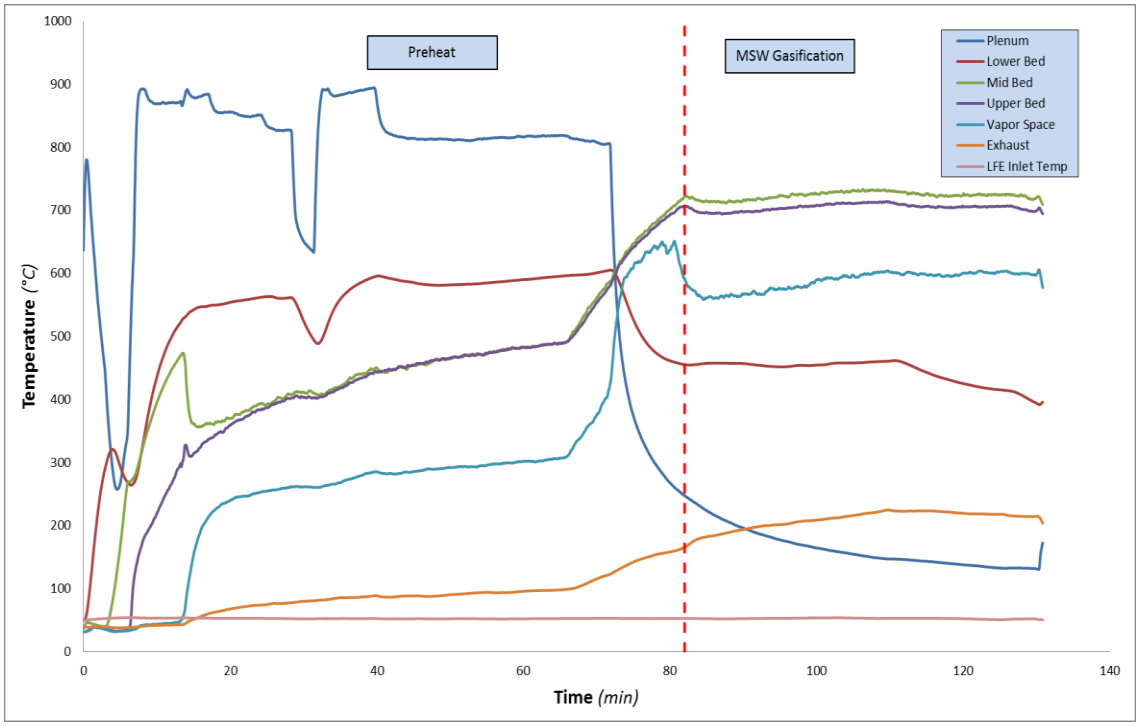

(a)

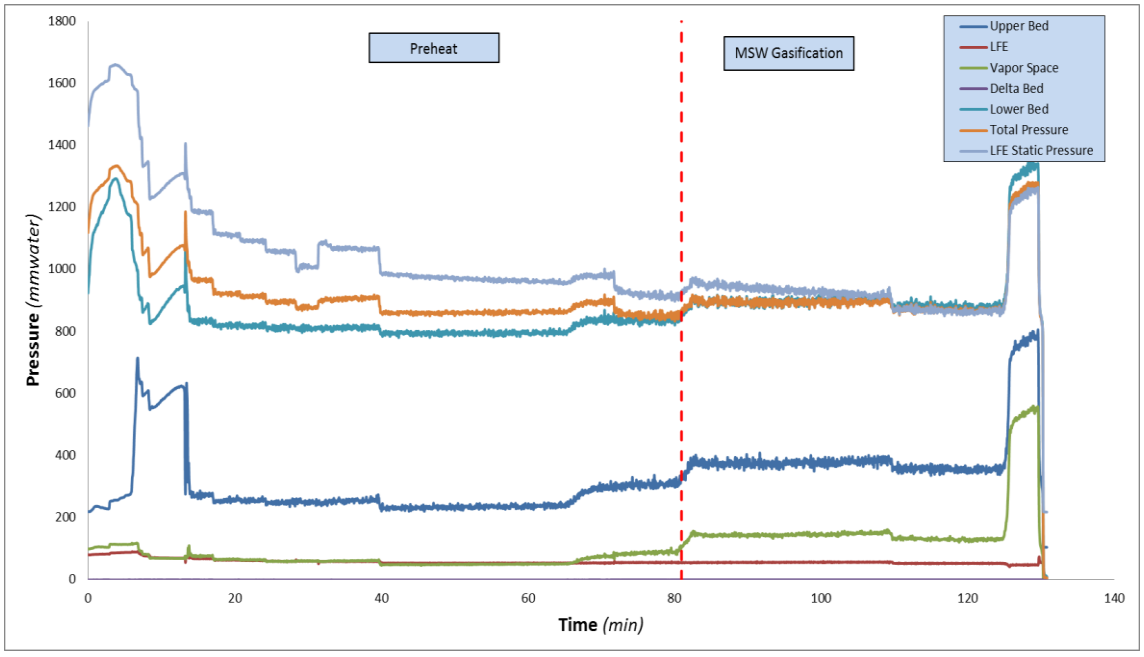

(b)

Figure 24. MSW pellet gasification profile using FBG2

Synthesis gas production and gasification are summarized in Table 10. Operating the gasification at a lower ER produced higher energy content of the synthesis gas with an average of 8.39 MJ Nm^{-3} compared to experiments using FBG1. The lower ER resulted in higher hydrocarbons concentrations (ethylene and propylene) in the synthesis gas produced. In addition, the gasification experiments produced an average of 2.5 Nm^3 of synthesis gas per kg of MSW used. The carbon conversion efficiency and cold gasification efficiency of the MSW gasification were 95% and 65%, respectively. The MSW gasification had relatively high conversion efficiency compared to regular agricultural biomass wastes.

Table 10. Synthesis gas production and gasification performance using MSW pellets

Components and Properties	Resulting Values	
Component Gas (mol %)		
Hydrogen	3.80 ± 0.18	%
Nitrogen	58.53 ± 0.91	%
Carbon Monoxide	12.77 ± 0.35	%
Methane	3.84 ± 0.11	%
Carbon Dioxide	14.23 ± 0.04	%
Acetylene	0.29 ± 0.01	%
Ethylene	4.35 ± 0.13	%
Ethane	0.53 ± 0.03	%
Propylene	1.66 ± 0.13	%
Net HV	8.39 ± 0.29	*MJ Nm^{-3}*
Gas Yield	2.50 ± 0.08	*Nm^3 kg_{MSW}^{-1}*
Gas Production	4.99 ± 0.15	*kg min^{-1}*
Carbon Conversion Efficiency	94.75 ± 0.07	*%*
Cold Gasification Efficiency	65.47 ± 0.02	*%*

Synthesis Gas Production Optimization

Within the set limits of 650°C to 800°C for reaction temperature and 0.30 to 0.55 for eqivalence ratio and using the CCD experimental design,twelve (12) randomized experiments or test runs were formulated (Table 11). These test runs were used in determining the relationships between the reaction temperature and equivalence ratio with the amount and heating value of the synthesis gas produced.

The highest synthesis gas heating value of 8.97 MJ Nm^{-3} resulted from the gasification of MSW at 725°C and ER of 0.25. It was also the condition that produced the highest yield of the synthesis gas, except for propylene which was highest at 650°C and ER of 0.30. The lowest production of hydrogen and carbon monoxide was observed at an ER of 0.60 and a temperature of 725°C. With these results, it can be suggested that

Table 11. Synthesis gas produced as affected by gasification temperature and equivalence ratio using the central composite experimental design

Experimental Factors			*Synthesis gas produced (Experimental Responses)*						
Test Run Order	Gasification Temperature °C	Equivalence Ratio	Hydrogen (mol %)	Carbon Monoxide (mol %)	Methane (mol %)	Ethylene (mol %)	Propylene (mol %)	Net HV (MJ Nm^{-3})	Energy Rate (kW)
1	725	0.25	4.87	10.33	5.19	5.22	1.81	8.97	548
2	725	0.43	3.77	8.58	3.61	3.37	0.81	5.99	272
3	725	0.43	3.95	8.85	3.82	3.47	0.77	6.14	276
4	650	0.55	3.23	7.26	2.87	2.49	0.36	4.48	182
5	725	0.43	4.15	8.96	3.89	3.54	0.72	6.21	280
6	650	0.3	2.99	8.61	2.86	3.63	2.54	7.28	225
7	830	0.43	3.68	8.58	3.46	2.79	0	4.78	246
8	620	0.43	2.53	7.42	2.50	2.69	1.17	5.09	248
9	725	0.43	4.14	9.31	4.07	3.80	0.80	6.56	283
10	725	0.6	2.71	6.53	2.56	1.89	0	3.53	147
11	800	0.3	3.59	9.24	4.23	4.08	0.58	6.43	398
12	800	0.55	3.44	7.37	2.97	2.12	0	4.04	176

operating at low equivalence ratio would result in higher heating value of synthesis gas as it increases its content of hydrocarbons. However, this would also result in generation of tar. Higher heating value of gas also resulted in higher energy production rate.

The ANOVA at 95% confidence level and the coded coefficients of the proposed quadratic models indicated that the gasification temperature and equivalence ratio had no significant effect on the hydrogen concentration of the synthesis gas (Table 12 and 13). The equivalence ratio affected all of the response variables except for hydrogen. As expected, the equivalence ratio is one of the important factors that affects the product gas in gasification. The quadratic model was only significant with carbon monoxide, ethylene, net heating value and energy production rate. However, the lack of fit test indicated that only ethylene and net heating value fits well with the surface plots generated. The empirical equation with actual factors for ethlylene and net heating value is summarized in Table 13.

Significant effects of temperature on the production of hydrogen gas might have been observed had the experiments been conducted at a higher temperature. As stated before, the type of reactor used limited the experiments to a maximum operating temperature of 830°C. According to Le Chatelier's principle, higher temperatures favor the reactants in exothermic reactions and favor the products in endothermic reactions. In gasification, hydrogen production involves endothermic reactions so the H_2 concentration would be expected to increase with temperature.

The response surface plot indicated that the net HHV increases as the ER decreases (Figure 20). At an ER of 0.30, and about 740°C, the predicted net HHV was

about 7.47 MJ Nm^{-3}. This figure was pretty close to the observed net HHV value of 8.97 MJ Nm^{-3} but run on a lower ER of 0.25. The surface plot developed was set to be within the gasification temperature and ER range. As also shown in the plot, the gasification temperature did not significantly affect the net HV. Table 12 further reconfirmed that the equivalence ratio was a significant factor in increasing the net heating value giving a p-value < 0.05. Lower equivalence ratio is predicted to result in higher net heating value. However, gasification at a lower equivalence ratio is predicted to produce less synthesis gas (by volume) per unit of feedstock used. The other response surface plots are shown in Appendix F.

Table 12. ANOVA for response surface quadratic model

	Hydrogen	Carbon Monoxide	Methane	Ethylene	Propylene	Net Heating Value	Syngas Production Rate
Source	p-value						
Model	0.2305	0.0064[$]	0.0837	0.0012[$]	0.0084	0.0005[$]	0.0236[$]
A-Gasification Temp	0.4644	0.4314	0.9568	0.4582	0.2446	0.9880	0.3168
B-Equivalence Ratio	0.1102	0.0006[$]	0.0186[$]	< 0.0001[$]	0.0017[$]	< 0.0001[$]	0.0026[$]
AB	0.4964	0.4609	0.2293	0.8992	0.0160[$]	0.1880	0.2032
A^2	0.0719	0.0311[$]	0.0680	0.0127[$]	0.1329	0.0076[$]	0.2713
B^2	0.5501	0.1516	0.8772	0.9242	0.3046	0.9879	0.3877
Lack of Fit	0.0198[$]	0.0580[$]	0.0245[$]	0.1266	0.0009[$]	0.1173	0.0003[$]
Std. Dev.	0.56	0.47	0.55	0.30	0.35	0.40	56.21
Mean	3.59	8.44	3.50	3.26	0.72	5.50	259.84
R-Squared	0.61	0.90	0.74	0.94	0.89	0.96	0.84
Adj R-Squared	0.29	0.81	0.52	0.89	0.79	0.92	0.70

[$] values of p-value less than 0.05 indicate model terms are significant

[$] The "Lack of Fit p-value" less than 0.05 implies the Lack of Fit is significant. Significant lack of fit is bad -- model doesn't fit.

Table 13. Coefficient Estimates and Quadratic Model Equation

	Coefficient Estimates	
Factor	Ethylene	Net Heating Value
Intercept	3.545	5.9225
A-Gasification Temp	-0.08482	-0.00221
B-Equivalence Ratio	-0.97617	-1.51915
AB	0.02	-0.2975
A^2	-0.41938	-0.625
B^2	-0.01188	-0.0025

Final Equation in Terms of Actual Factors*		
	Ethylene	Net Heating Value
x_0	-30.9843	-57.1005
x_1	0.106068	0.174568
x_2	-8.71	10.98947
x_3	0.002133	-0.03173
x_4	-7.5E-05	-0.00011
x_5	-0.76	-0.16

*Quadratic Model: $Response = x_0 + x_1A + x_2B + x_3AB + x_4A^2 + x_5B^2$

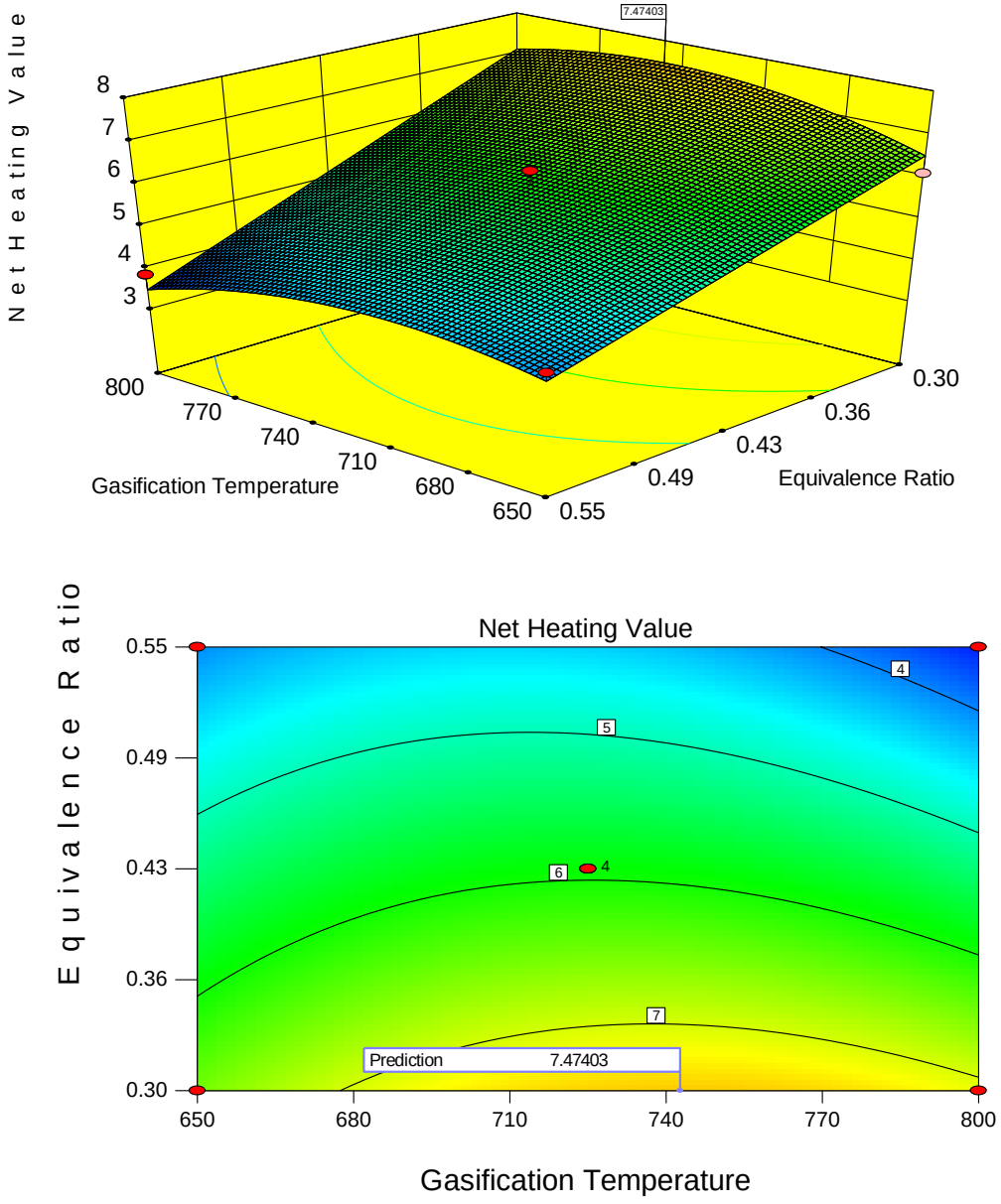

Figure 25. Synthesis gas heating value response surface

CONCLUSION

The production and net heating value of the synthesis gas from the gasification of segregated municipal solid waste (MSW) as feedstock was optimized based on the reaction temperature and equivalence ratio during gasification. The feedstock was characterized by conducting proximate and ultimate analyses and three different forms of preparation, fluff, shredded and pellets of the biomass samples tested. Gasification tests were conducted using two types of atmospheric fluidized bed gasifier, one with a 305 mm circular reactor (FBG1) and the other with a 305 mm square reactor (FBG2). Monitoring and control devices and a software program were utilized to facilitate the operation of the system. Optimization was done by applying the response surface methodology and facilitated by the Central Composite Design (CCD) expert statistical software.

Analysis of the samples showed a heating value of about 30 $MJ\ kg^{-1}$, ash content of 2.6% and volatile matter of 93%. The heating value was found to be 82% higher and the ash content 80% lower than that cotton gin trash. The ultimate analysis indicated that MSW is mainly composed of carbon, hydrogen and oxygen and only traces of nitrogen and sulfur. With low sulfur content, SO_2 emissions would not pose a problem in the utilization of MSW in energy conversion. Based on its elemental composition and stoichiometric combustion properties, it would require only about 1.8 kg to 3.7 kg of air per kg of MSW to achieve good operation of the gasification system with an equivalence ratio in the range of 0.2 to 0.4.

The MSW pellets showed the highest bulk density while the fluff form had the highest friction angle. The test conducted at around 760°C and for about 40 min using FBG1 and the fluff form of the biomass resulted in good gasification. A good control of the gasification temperature and fluidization of the bed material was achieved. Hydrogen, carbon monoxide and hydrocarbons were the combustible gases produced during the gasification. Compared with the gas produced from woodchips, the gas from MSW had comparable gas composition and concentrations but gave a relatively higher heating value even if the woodchips gasification was operated at a lower ER of 0.35. Lowering the ER either by increasing the feeding rate or lowering the air flow rate was not possible because of the low bulk density of the fluff preparation. Using the shredded form with a higher bulk density resulted in clogging of the screw auger because of its small opening of 5 cm.

The bigger opening of the feeding system of the FBG2 unit did not solve clogging problem with the shredded MSW even if agitation in the feed hopper was done. Formation of a cohesive arch or bridge or a rathole caused the flow obstruction. Thus, the tests were done using the pellet form in FBG2 which provided a uniform feeding of the sample and a good control of the gasification temperature and fluidization of the bed material. Compared with FBG1, the pressure profile in FBG2 was a lot stable due to the more uniform air distribution. Since FBG2 used larger mean particle size of the bed material, gasification resulted in higher pressure and air flow providing flexibility in the gasification operation. Moreover, FBG2 produced a higher energy content of the synthesis gas with an average of 8.39 MJ Nm^{-3}.

Within the set limits of the tests, the highest production of synthesis gas and the net heating value of 8.97 MJ Nm^{-3} resulted from gasification at 725°C and ER of 0.25. This is very close to the predicted value of 7.47 MJ Nm^{-3} based on the response surface plot which also indicated it was not affected by gasification temperature but significantly affected by the equivalence ratio. The ANOVA at 95% confidence level and the coded coefficients of the proposed quadratic models indicated that the gasification temperature and equivalence ratio had no significant effect on the hydrogen concentration of the synthesis gas. The equivalence ratio affected carbon monoxide and ethylene concentration while propylene and methane concentration was affected by both the gasification temperature and equivalence ratio. Significant effects of temperature on the production of hydrogen gas might have been observed had the experiments been conducted at a higher temperature because of the endothermic reactions in gasification. Lower equivalence ratio is predicted to result in higher net heating value. However, gasification at a lower equivalence ratio is predicted to produce less synthesis gas (by volume) per unit of feedstock used.

CHAPTER IV

UTILIZATION OF SYNTHESIS GAS TO OPERATE A SPARK IGNITION ENGINE GENERATOR

INTRODUCTION

Biomass resources such as woody biomass, energy crops, residues, and municipal waste (De Swaan Arons et al., 2004) can produce combustible gases through thermal conversion by gasification. These combustible gases commonly called synthesis gas can be used to generate electricity by means of internal combustion (IC) engines, gas turbines, and fuel cells. Industrial plant simplification and intensification could play an important role in biomass conversion applications in general, and in particular in increasing the feasibility of gasification technologies (Rapagnà et al., 2010).

The use of alternative fuels in engines has been the focus of much attention because of the imminent shortage of crude oil and the increasing concern for environmental protection. To confront these concerns, research in alternative fuels and low carbon technology has been on the rise (Lai et al., 2012). Recently published papers related to energy policy and sustainable energy indicated that several countries are promoting low carbon energy from biomass derived gas (Hao et al., 2008).

Hydrogen and biomass derived synthesis gas are two potential alternative fuels as source of energy. Hydrogen fueled engines have many attractive attributes, but they tend to suffer from premature ignition, especially under high load conditions (Gopal et al., 1982; Karim, 2003). Premature ignition is a much greater problem in hydrogen fueled

engines than in other IC engines, because of its lower ignition energy, wider flammability range and shorter quenching distance (Mohon Roy et al., 2009). The development of engines using producer gas has been explored since World War II. They were spark ignited engines, mostly in the lower compression ratio bracket operating either on charcoal or biomass derived gas (Sridhar et al., 2001). However, the development and subsequent availability of more economical gasoline and diesel engines caused the decline in syngas production and utilization.

A renewed interest in gasification technology and the use of syngas for power and electricity generation has again emerged because of the need for renewable energy. Gasification of solid wastes produces electricity at an efficiency of about 34% compared to 20% for incineration. This suggests that gasification of the residual component of solid wastes is more advantageous than incineration where a market for thermal product does not exist. Gasification produces more electricity than incineration and when thermal product is not utilized, it generates less greenhouse gas per kWh than incineration (Murphy and McKeogh, 2004).

Shashikantha (1994) developed a 15 kW_e spark ignition producer gas engine with an efficiency of 28–32%. Synthesis gas produced from wood gasification was used as engine fuel that has a calorific value of 6 to 7 MJ Nm^{-3} (Shashikantha et al., 1994). Shah (2010) determined the performance and exhaust emissions of a commercial 5.5 kW generator modified for operation with 100% synthesis gas at different flow rates. The 5.8 MJ Nm^{-3} synthesis gas used was produced from hardwood chips gasified in a fixed bed, downdraft atmospheric pressure gasifier. The maximum electrical power output for

syngas operation was 1392 W and that for gasoline operation was 2451 W. The overall efficiency of the generator at maximum electrical power output was the same for both the fuels. The concentrations of CO and NO_x in the generator exhaust were lower for the syngas operation, respectively by 30–96% and 54–84% compared to the gasoline operation. However, the concentrations of CO_2 in the generator exhaust were significantly higher by 33–167% for the syngas operation (Shah et al., 2010).

Currently, small scale electricity generation using biomass gasification is attracting increasing interest to provide remote districts with electrical power using local renewable fuels. An additional benefit in such a rural electrification mechanism is the possibility of the utilization of various organic wastes from the local industry and agriculture with a considerable CO_2 emission reduction (Martínez et al., 2012).

The objective of this study was to determine the overall performance of a spark ignition engine generator using synthesis gas from segregated municipal solid waste (MSW) gasification as fuel. The specific objectives were to: (a) determine the overall engine generator efficiency and its exhaust emissions (b) compare the performance of synthesis gas fueled engine with a standard gasoline engine, and (c) evaluate the feasibility of using the pressure swing adsorption for upgrading the synthesis gas.

METHODOLOGY

Gasification of MSW

The synthesis gas used in this study was produced using the atmospheric fluidized bed biomass gasifier with a 305 mm square reactor. It was developed at Texas

A&M University at College Station, Texas and protected under intellectual property disclosures TAMUS 2814 serial No. 61/302,001. The system used 80 kg of Mulgrain 47-10 x 18 (C E Minerals, Andersonville, GA) as the bed material inside the reactor. TAMU designed cyclones were used as gas cleanup system to separate the solid products from the gas. The gasification system was also equipped with monitoring and control devices and a software program was developed to facilitate its operation. The gasification was operated at a reaction temperature of 740°C, equivalence ratio of 0.25 and operating pressure of 1660 mm of water. Under these conditions, the optimum production of the synthesis gas and the net heating value had been observed (See Chapter 3).

The feedstock used for gasification was segregated municipal solid waste (MSW) provided by the Balcones Resources (Dallas, TX). Segregated MSW was processed into 6 mm diameter pellets using a GC-9PK-200 Fodder pellet press. Synthesis gas samples were collected into a 1 L Tedlar bags (Restek, Bellefonte, PA) throughout the study and analyzed using SRI gas chromatograph (SRI Instruments, Torrance, CA) with TCD and HID detector to validate the H_2, CO, CO_2 and hydrocarbon composition. Shincarbon ST, 100/120 mesh and Molecular sieve 13x packed columns were used to separate the gas components. The detailed gas chromatograph settings are further discussed in Appendix E.

Testing of the Synthesis Gas Fueled-Engine

Figure 27 shows the schematic diagram of the gasification system for power generation while Figure 26 shows the actual hook up of the gasification system to a 10 kW generator run by a 20 hp 614 cc Honda GX620 motor. To add the capability to use gaseous fuel in a standard gasoline engine, tri-fuel kit (US Carburation Kit Center, West Virginia) was utilized. The kit was designed such that the engine can use three different kinds of fuel - low pressure propane, natural gas and standard gasoline. The two main components of the tri-fuel kit are the adapter and the pressure regulator. The adapter

Figure 26. Gasification system connected to a 10 kW generator

was installed between the engine carburetor and air cleaner. It has a venturi at its center with an opening in the middle which resembles the shape of a doughnut. The center

opening has three small holes around its edge. As air passes through the center opening and the small holes, fuel from the pressure regulator is delivered to the air stream. The amount of fuel used depends on the amount of air that passes through the small holes which depends on how far the throttle is open.

To be able to use the kit for synthesis gas as fuel, the regulator was excluded and replaced with a 50 mm flexible steel pipe where the synthesis gas is introduced into the adapter. The venturi adapter remained installed between the air intake system and carburetor. The required synthesis gas flow was diverted to the engine with the use of a flow control valve while the excess gas was burned in a flare. The flow of synthesis gas through the engine was measured using a calibrated 50 mm orifice flow meter. The gasification system was operated at an additional pressure of 760 mm of water (normal operating pressure at 900 mm of water) to provide the necessary flow of the synthesis gas to run the engine. The additional pressure was achieved by restricting the flow of the synthesis gas to the flare tube. The synthesis gas temperature was cooled down to an average temperature of 95°C before being introduced to the engine.

A randomized complete block experimental design was used to determine the effects of the type of fuel and electrical load on the generator on the overall engine-generator efficiency, exhaust temperature and emissions, particularly the NO_x, hydrocarbons (HC), carbon monoxide (CO) and carbon dioxide (CO_2) concentrations. Standard gasoline and synthesis gas, at different electrical power loads – no load, ¼ load (2.5 kW), ½ load (5 kW) and ¾ load (7.5 kW), were used throughout the experiments. Electric heaters were utilized to provide the different electrical load to the generator.

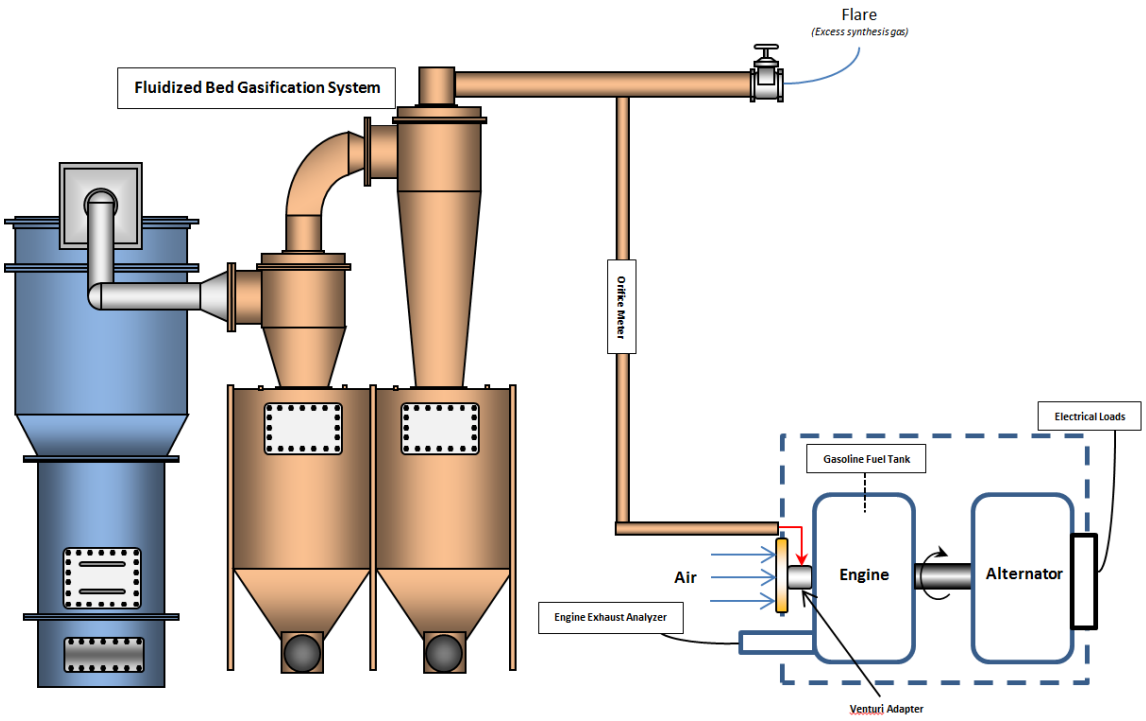

Figure 27. Schematic diagram of the MSW gasification power generation

The overall engine generator efficiency for each power rating for the two engine fuels was calculated as follows:

$$\text{Generator Efficiency, } \eta_{gen}(\%) = \frac{\text{Electrical Energy Output}}{\text{Fuel Energy Input}} \times 100 \qquad [16]$$

The fuel energy input to the generator for each electrical power load was quantified as the product of flow rate and the net heating value of the respective fuels.

Exhaust emissions were collected and analyzed using an ENERAC Model 3000E emissions analyzer (Enerac Inc., Holbrook, NY) during each test that lasted for 15 min. The emissions analyzer was designed to meet all the performance specifications of US

Environmental Protection Agency's Test Method for the Determination of Nitric Oxide, Nitrogen Dioxide and NO_x emissions from stationary combustion sources by electrochemical analyzer. Non-dispersive Infrared (NDIR) detectors were used to measure the hydrocarbons, carbon monoxide and carbon dioxide concentrations of the exhaust gas. Stack temperature was measured with a thermocouple placed at the inlet of the gas sample probe. The original exhaust pipe of the generator was extended using a 5 cm diameter and 60 cm long steel pipe where the gas sample probe with permeable filter was inserted. In addition, a visual inspection was done with the venturi adapter and engine carburetor and observations were made.

Upgrading of the Synthesis Gas

The pressure swing adsorption (PSA) system was used to upgrade the synthesis gas produced from MSW gasification. Before the conduct of the experiments, the system was first developed and instrumented for monitoring and control. An automated control system was also developed by LabVIEW programming.

The PSA System

The PSA system developed enabled the conduct of different gas separation experiments. It can be operated up to 10 bars pressure at ambient temperatures and gas flow rate from 0 to 15 L min^{-1}. It is composed of two main vessels made up of 316 stainless steel components with a flange for adsorbent replacement Figure 28. The vessels have 43 ft^3 of volume for the adsorbent bed such as zeolites, activated carbon

and carbon molecular sieves. For this study, SHIRASAGI MSC 3R-181 carbon molecular sieve (Japan EnviroChemicals, Ltd., Japan) was used as adsorbent. Its specifications are given in Table 14. This adsorbent is best suitable for nitrogen removal from nitrogen gas.

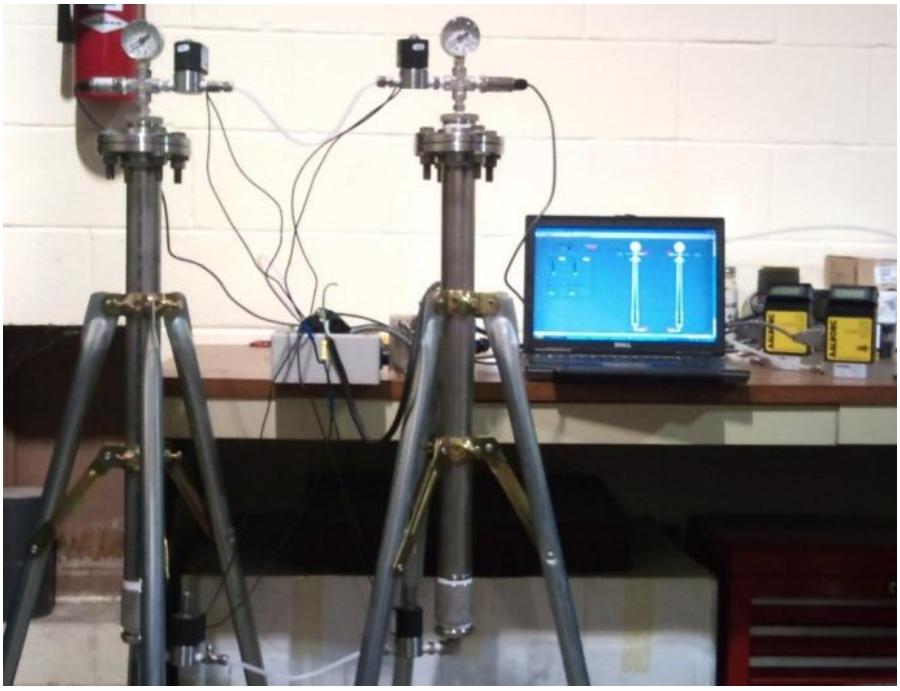

Figure 28. PSA system

Table 14. SHIRASAGI MSC-3R-181 specifications

Properties and Unit of Measure		Value
Loss on Drying	[%]	1.0 max.
Filling bulk density	[g/l]	680 - 730
Particle Size (2.360 – 1.000 mm) (8 - 16 mesh)	[%]	99.0 min.
Hardness	[%]	93.0 min.
PSA performance of 99 % Nitrogen at 30°C, 0.588MPaG		
Cycle time	[sec]	60
Recovery, Nitrogen / Air	[%]	37.0 min.
Productivity, Nitrogen	[Nm^3/hr.ton]	210 min
Exhaust	[NL/hr]	420 - 450

Particular instrumentation was installed for process monitoring and control. Pressure gauges and transmitters were placed on top of the vessels to monitor the bed pressure during operation. Solenoid valves and mass flow controllers were used to control the flow of the gas in the system.

Experiments Using the PSA System

The PSA experiments were conducted using a certified gas mixture standard prepared by Airgas (Airgas Southwest, Woodlands TX) with the components shown in Table 15. This gas mixture is a good representation of the synthesis gas produced from MSW gasification. The pressure was set at 400 kPa and the product gas outlet flow rate at 0.75 LPM. Product gas was collected into 1 L Tedlar bags (Restek, Bellefonte, PA) and analyzed using SRI gas chromatograph (SRI Instruments, Torrance, CA) with TCD and HID detector to validate the H_2, CO, CO_2 and hydrocarbons composition. The product gas was also analyzed in real time using the Horiba NDIR gas analyzer.

Table 15. Certified gas mixture standard components and concentration

Component	Actual Concentration (mol %)	Analytical Uncertainty
ACETYLENE	0.4997	± 2%
ETHANE	0.5	± 2%
PROPANE	0.4999	± 2%
PROPYLENE	1.998	± 2%
ETHYLENE	4.999	± 2%
HYDROGEN	4.998	± 2%
METHANE	5.002	± 2%
CARBON DIOXIDE	12.00	± 2%
CARBON MONOXIDE	12.00	± 2%
NITROGEN	Balance	± 2%

RESULTS AND DISCUSSION

Engine-Generator Overall Efficiency and Exhaust Temperature

The consumption of standard gasoline and synthesis gas at different electrical power loads are summarized in Table 16. The consumption of synthesis gas was observed to be the same for all power loads, but the consumption of gasoline increased with increasing power loads. During the experiments, the gasoline-fueled engine consumed an average of 636 g kW^{-1} h^{-1}. This is twice the rated value of 313 g kW^{-1} h^{-1} for a GX620 Honda engine (Appendix G).Using the measured lower heating value of the standard gasoline as 40 MJ kg^{-1} and 7.64 MJ Nm^{-3} (205 Btu scf^{-1}) for the synthesis gas, the overall engine-generator efficiency at 7.5 kW electrical power load of standard gasoline was calculated to be 19.81% and 35.27%, respectively. The overall engine-generator efficiency at 7.5 kW electrical power load was calculated as follows:

Gasoline Fuel:

$$\eta_{gen} = \frac{7.5\ \text{kW}}{\left(40{,}000\ \frac{\text{kJ}}{\text{kg}}\right)\left(0.0568\ \frac{\text{kg}}{\text{min}}\right)\left(\frac{\text{min}}{60\ \text{s}}\right)} \times 100 = 19.81\ \%$$

Synthesis Gas Fuel

$$\eta_{gen} = \frac{7.5\ \text{kW}}{\left(205\ \frac{\text{Btu}}{\text{scf}}\right)\left(5.9\ \frac{\text{ft}^3}{\text{min}}\right)\left(\frac{\text{min}}{60\ \text{s}}\right)\left(\frac{1.055\ \text{kJ}}{\text{Btu}}\right)} \times 100 = 35.27\ \%$$

Table 16. Gasoline and syngas consumption

Electrical Power Load *(kW)*	Gasoline *(g/min)*	Syngas *(Nm^3/min)*
No load	26.7	0.15
2.5	37.7	0.15
5	45.8	0.16
7.5	56.8	0.17

The synthesis gas fueled engine also showed higher efficiency at all electrical power loads tested (Figure 29a). The efficiency of the synthesis gas fueled engine-generator ranged from 12.61% to 35.27% while it was only from 9.95% to 19.81% for gasoline. It was also observed that the efficiency increased as the electrical power load was increased.

To run the engine smoothly throughout the test, the engine throttle should always be set at the wide open position. When the throttle was fully open, the air-fuel ratio was made richer and provided maximum torque. The richer mixture also served as coolant to prevent engine internal failure. Rich mixtures also inhibited NO_x emissions (Rajput, 2005). The efficiency was expected to be higher for gasoline at an electrical power load of 10 kW while it was maximized for synthesis gas by having the engine at full throttle. The engine fueled by synthesis gas was observed not to run smoothly especially at ¾ electrical power load. It is expected that the engine would stall at full 10kW electrical power load at the set synthesis gas flow. On gasoline engines, the use of lean air-fuel mixture results in higher combustion efficiency, however the engine becomes unreliable and frequent misfiring occur. Combustion at the lean limit is also very sensitive to the air to fuel ratio (Turner, 2009). Increasing gasification operating pressure would provide

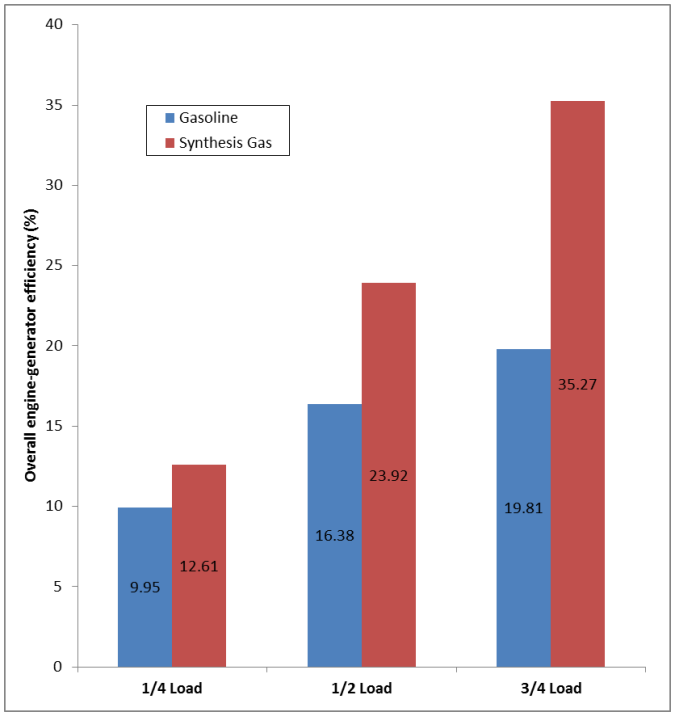

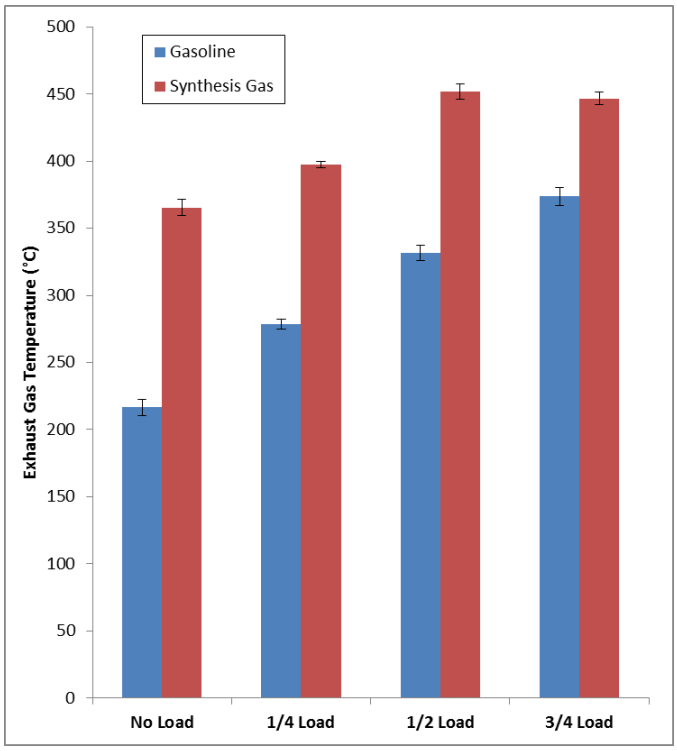

Figure 29. (a) Overall engine-generator efficiency at different electrical power loads and (b) exhaust gas temperature

a smooth engine run but the gasification system was not designed to be operated at elevated pressure.

The exhaust gas temperature of the synthesis gas fueled engine was relatively higher compared with the gasoline fueled engine (Figure 29b). Higher exhaust gas temperature was a consequence of using hot synthesis gas. With an average cold gasification efficiency of 59% (See Table 6, Chapter 2), the overall biomass to electricity conversion efficiency of MSW pellets was estimated to range from 7.44% to 20.6%. This is comparable to the 18% overall conversion efficiency found in the previous study of Dassapa (2011) on 100 kW_e biomass gasification power plant. Conversion of biomass to 500 kW electrical power would result to even higher conversion efficiency in the range of 25 to 30% (Dasappa et al., 2005; Sridhar et al., 2005).

Exhaust Emissions

The emission concentrations of NO_x, hydrocarbons, carbon monoxide and carbon dioxide are shown in Figures 30 to 33 and Table 17. The NO_x emissions for the synthesis gas fueled engine were relatively the same at different electrical loads. In the case of gasoline, NO_x emissions increased as the electrical power load increased. Both fuels had the highest NO_x emissions at the highest electrical power load. Exhaust emissions of the two fuels were found to be significantly different at the ½ and ¾ power loads. The lower NO_x emissions for syngas operation might be due to the lower temperatures in the engine cylinder because of the lower LHV of syngas and the less favorable condition for the reaction between nitrogen and oxygen to occur. NO_x are formed from the reaction

between oxygen and nitrogen at high temperatures in a reaction separate from combustion by Zeldovich mechanism (Sobyanin et al., 2005). This signifies the dependence of NO_x emissions on temperature. For gasoline operation, the higher NO_x emissions were expected as temperature is expected to increase as the electrical power load was increased. The temperature generated within the engine cylinder would be higher with higher electrical power output from the generator. The significantly lower

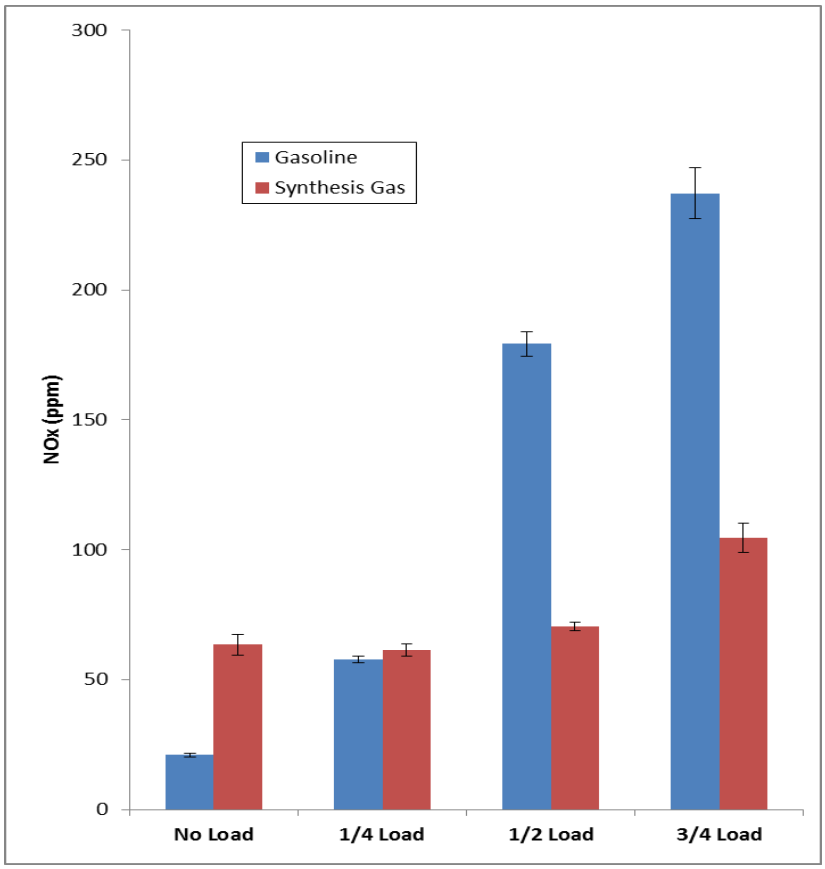

Figure 30. Exhaust emissions of NO_x concentrations.

NO_x emissions of syngas as engine fuel as compared to gasoline add to the potential use of synthesis gas to run engines. NO_x causes lung irritation, impairment of functions of the lungs, tissue damage and irritation of mucous membranes and increases the risk of nitric acid formation (Abdel-Rahman, 1998).

With an average of 108 ppm, the total hydrocarbon (HC) concentrations of the exhaust gas from the gasoline operation did not show any significant difference at different

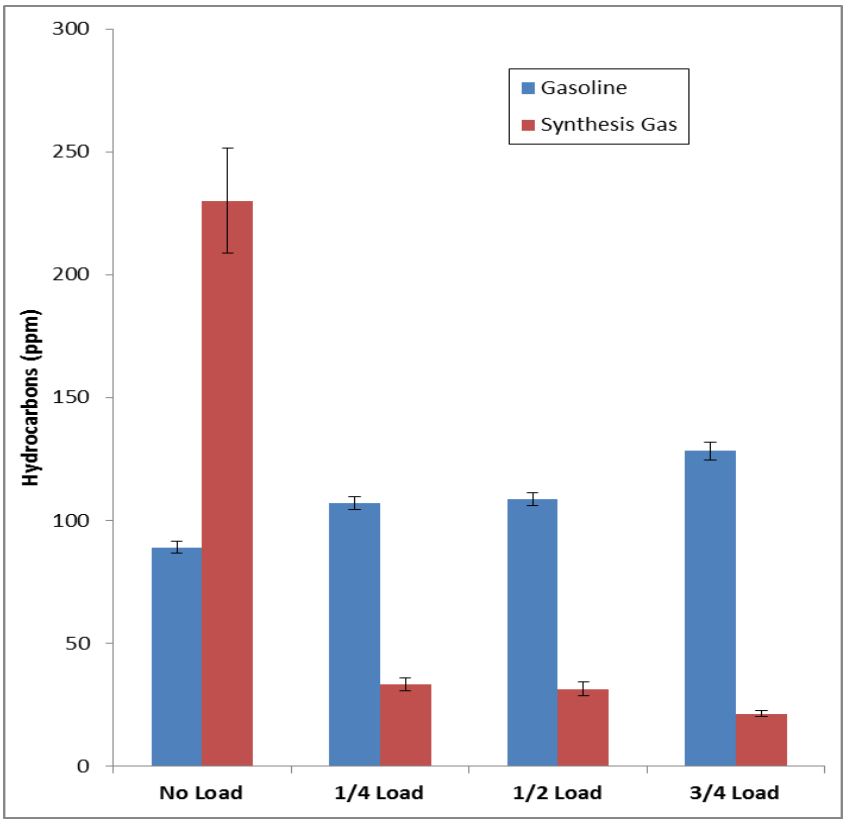

Figure 31. Exhaust emissions of hydrocarbon concentrations.

electrical loads. The HC concentration for synthesis gas fuel was highest (230 ppm) at 0 power load and lowest (28.8 ppm) at the highest load. Hydrocarbons in the exhaust gas are the unburned fuel that has been left because of incomplete combustion. A rich mixture, lack of oxygen or excess fuel results in high amounts of HC. Another cause is an excessively weak mixture that does not support complete combustion within the combustion chamber. HCs are also formed when fuel vaporizes and escapes into the atmosphere from the fuel system (Hillier and Coombes, 2004).The high HC level would result in the reduction in combustion efficiency. A rich mixture could be the reason why HCs are high in gasoline operation since the engine is at wide open throttle. Low HCs on synthesis gas operation at higher loads were directly related with the higher overall efficiency.

Carbon monoxide (CO) is formed during partial combustion of fuel. The combination of a carbon atom from hydrocarbon fuel with an oxygen atom from the inducted air forms CO. It is produced under rich condition or poor mixing of fuel and air resulting in pockets (Hillier and Coombes, 2004). CO emission was significantly lower for synthesis gas operation compared to gasoline operation, perhaps because of the lower carbon content in syngas when compared to gasoline. For gasoline operation, the higher CO emission could be due to the rich mixture as gasoline generators are usually designed and operated under rich conditions (Heywood, 1988). The substantial decrease in CO emission with the use of syngas as engine fuel reinforces its importance as low concentrations of CO would decrease the risk of suffocation caused by the strong adherence of CO to hemoglobin (Abdel-Rahman, 1998).

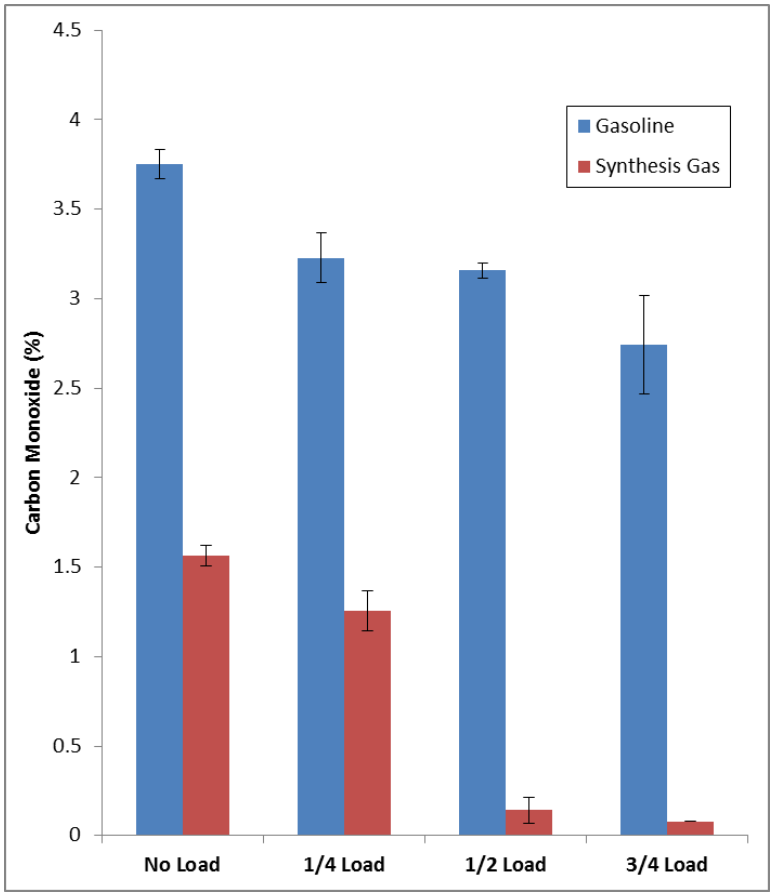

Figure 32. Exhaust emissions of carbon monoxide concentrations.

Carbon dioxide CO_2 emissions in the synthesis gas operation were significantly higher compared to that of gasoline operation. Carbon dioxide is a product of complete combustion. The more efficient the combustion is the higher the CO_2 content in the exhaust gas. The higher CO_2 emissions in the synthesis gas were due to the CO_2 component present in the synthesis gas used. Both fuels exhibited an increasing trend in CO_2 emissions as electrical power load increased. This is expected since the engine uses more fuel as the power load increases. The trends of the results for the different

emissions obtained in this study were similar to those obtained from previous studies conducted (Sobyanin et al., 2005) (Mustafi et al., 2006).

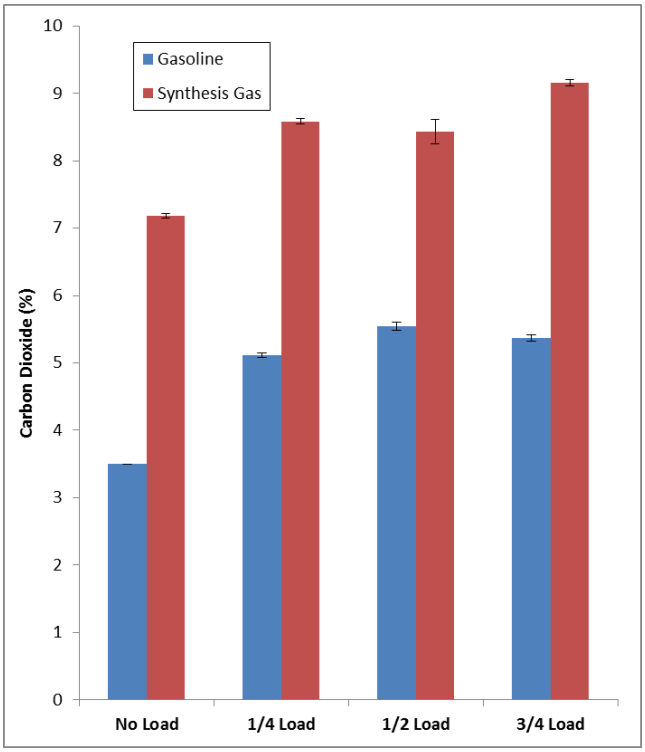

Figure 33. Exhaust emissions of carbon dioxide concentrations.

Table 17. Engine exhaust emissions

Exhaust Emissions		*Gasoline*				*Synthesis Gas*			
		No Load	*1/4 Load*	*1/2 Load*	*3/4 Load*	*No Load*	*1/4 Load*	*1/2 Load*	*3/4 Load*
Stack Temperature[s-f,l]	°C	216.43	278.81	331.82	373.56	365.22	397.20	451.54	446.70
Carbon Monoxide[s-f]	%	3.75	3.23	3.16	2.74	1.56	1.26	0.14	0.08
Carbon Dioxide[s-f]	%	3.50	5.11	5.54	5.37	7.19	8.58	8.43	9.16
Hydrocarbons[s-l]	ppm	89.03	107.20	108.63	128.37	230.13	33.36	31.52	21.45
NO_x[s-f,l]	ppm	21.01	57.61	179.28	237.13	63.42	61.44	70.39	104.62

[s-f,l] Engine fuel and Electrical load are significant terms. Significant term has p-value < 0.05
[s-f] Engine fuel is a significant term.
[s-l] Electrical load is a significant term.

Engine Visual Inspection

The formation of tar is a major nuisance in biomass gasification and presents a problem in the utilization of gasification technologies. Tar is a complex mixture of condensable hydrocarbons including oxygen with a molecular weight higher than benzene (Knoef, 2005). Tar causes problems in the process equipment and the engines and turbines used in the application of the producer gas (Devi, et.al. 2005). Tar is known to condense and cause subsequent plugging of downstream equipment. Tar formation was observed on the downstream engine generator. Thin layer of tar were seen in the venturi adapter and carburetor (Figure 34). However, this did not result in

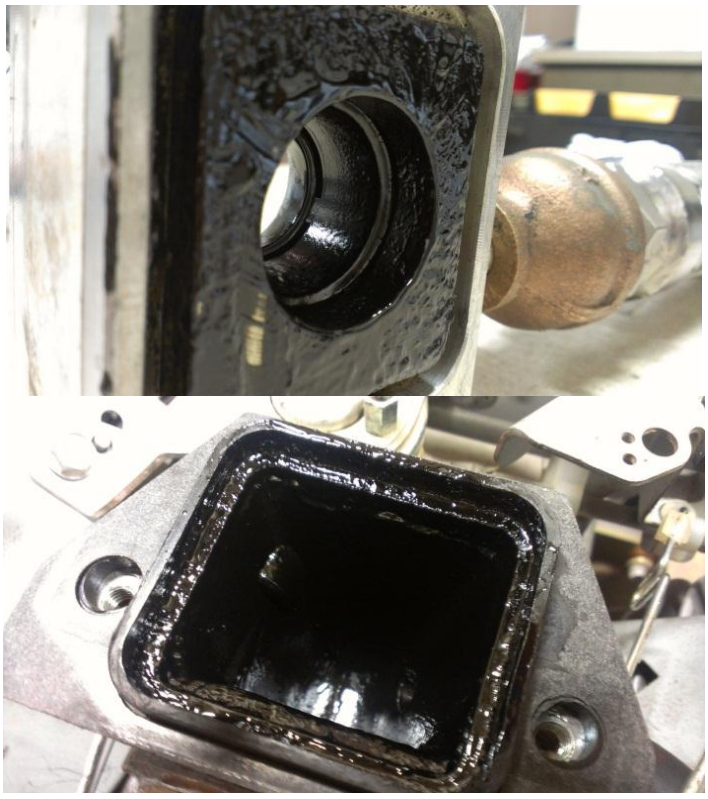

Figure 34. Tar formation on venturi adapter and carburetor

clogging even with a 3 mm opening of the holes in the venturi during the 2 h test. The tar did not harm the combustion chamber as tars are combustible with a heating value of 36 MJ kg^{-1} and carbon content of 83.2%. Tar deposits were also observed on the walls of the carburetor during its cleaning after switching the engine into gasoline operation but this would not pose much of a problem because solvents, like gasoline, would dissolve the tar on the carburetor and allow it to combust inside the engine chamber.

The spark plugs were inspected to assess their condition after the 2 h test. It was observed to have a regular carbon build-up (Figure 35). With these observations, it is suggested that clogging may be prevented by efficient solid particle removal from the synthesis gas and routine cleaning of the downstream connection. The intermittent use of

Figure 35. Spark plug condition after synthesis gas–fueled engine operation.

gasoline while using synthesis gas in the engine would clean out any tar build up. The set-up used in this study limited the connection from the gasification system to the engine with standard pipes. Thus, additional instrumentation going downstream to the engine would be required to have cleaner gas and reduced tar formation.

Synthesis Gas Upgrade

The PSA System

Figure 36 shows the schematic diagram of how the developed PSA system works. The raw gas mixture enters the bottom of the reactor with its flow being controlled by the mass flow controller. The solenoid valves divert the raw gas mixture into the proper active vessel. The active vessel (Vessel 1) is pressurized to the set pressure and when reached, the solenoid valve is activated to allow the flow of the product gas. The pressure inside is maintained at the desired value by controlling the flow rate of the product gas. The valves are then switched after the adsorption cycle is finished to allow equalization of pressure in the two adsorbent vessels. This step allows recycling some of the raw gas mixture to pressurize the inactive vessel (Vessel 2). As this is pressurized, the other reactor regenerates as the pressure decreases to atmospheric pressure through a vent or by directing it to a vacuum pump. Adsorption in the Vessel 2 completes the cycle and this process repeats to have a nearly continuous gas production.

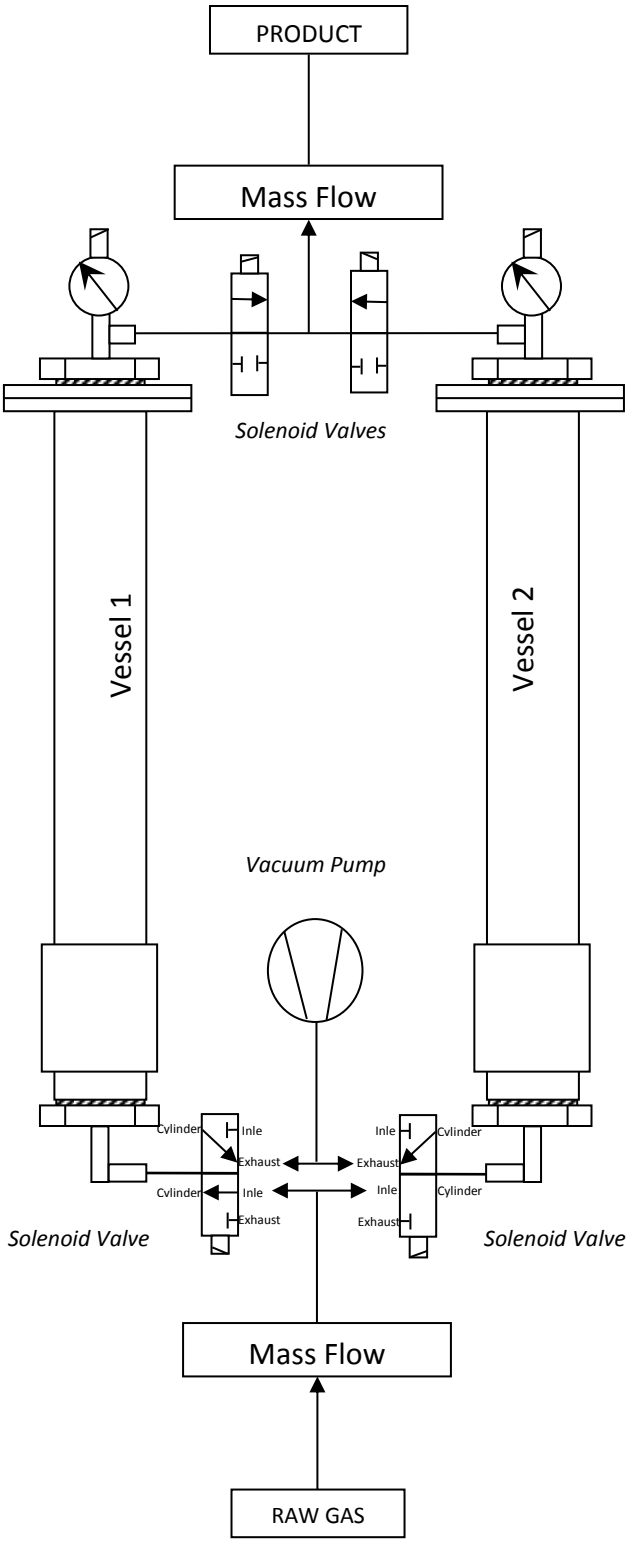

Figure 36. Schematic diagram of the PSA system.

Development of the PSA Control System

The control program developed for using the PSA is shown in Figure 37. The program included an option for manual control of the valves and flow rate and a fully automated control of the PSA system by setting the pressure setpoint, adsorbtion cycle time and input flowrate. The specifications of the system are shown in Table 18.

The development of the PSA control system happened at different stages as illustrated in Figure 38. The different stages were the same for both vessels but differed in its execution timing. The adsorbent vessel 1 was first pressurized to the desired pressure by having valve 2 open and all the other valves closed. The desired gas was produced during the adsorption stage of vessel 1 by opening valve 1

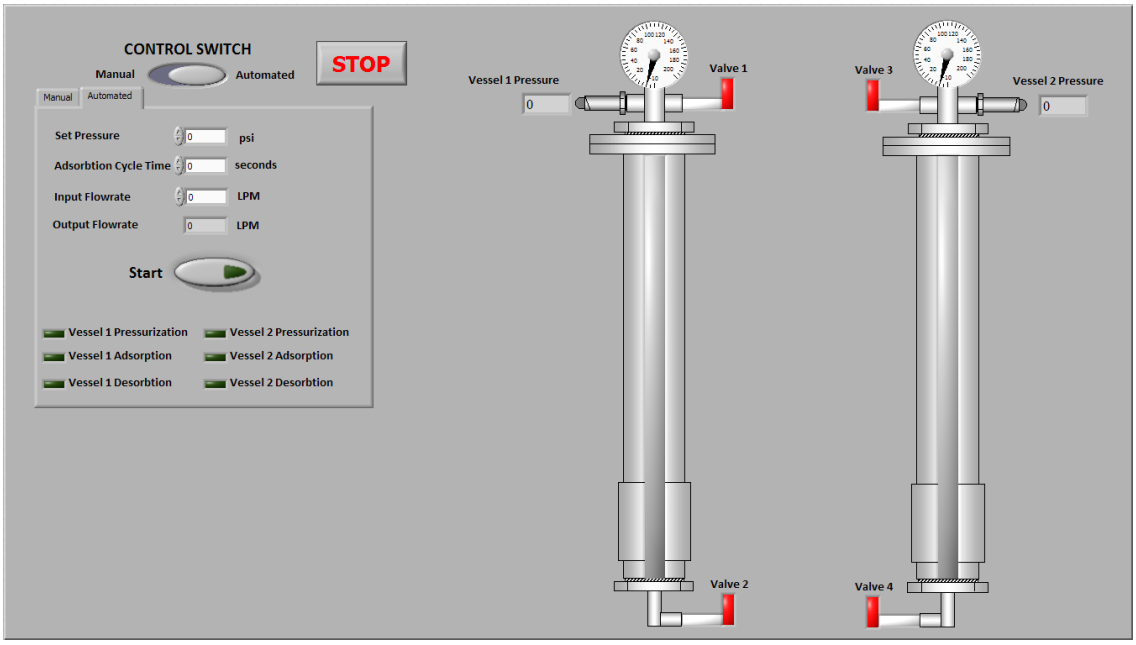

Figure 37. PSA control system, automated mode

Table 18. Pressure swing adsorption detailed specifications

PSA Component	Specifications
Adsorbent Vessel	316 Stainless Steel threaded components Maximum Operating Pressure: 150 psi @ 72°F (max of SS Cast Flange)
Instrumentation	
Mass Flow Controller	Operating Flow Rate: 0 – 15 L/min Max Pressure: 500 psi/3400 kPa Power Requirements: 12 VDC
2-Way Direct Acting Solenoid Valve	Pipe Size: ¼ inch Max Pressure: 275 psi/1900 kPa Cv Factor: 0.18 Operating Voltage: 120 VAC
3-Way Direct Acting Solenoid Valve	Pipe Size: ¼ inch Max Pressure: 250 psi/1720 kPa Cv Factor: 0.06 Operating Voltage: 120 VAC
Pressure Transmitter	Operating Pressure : 30 inHg – 0 – 100 psi Max Pressure: 200 psi Over Pressure: 300 psi Power Requirements: 13 to 30 VDC Output Signal: 4 to 20 mA
Solid State Relays	Control Voltage: 4 to 28 VDC Amp Rating: 3 A @ 12 to 280 VAC
AC to DC Transformers	DC Output: 5 VDC @ 0.6 Amps 12 VDC @ 2.5 Amps
Control Unit	
Multifunction DAQ	Analog Input: 8 (12 bit/10kS/s) Analog Output: 2 (12 bit, 150 S/s) Digital IO: 12 (TTL) Form Factor: USB
Programming Software	LabVIEW 8.6

and controlling the output flow rate. The cycle depends on the capacity of adsorbent used. When the adsorbent was in its full capacity, valve 1 closes and valve 4 opens such that pressure equalization of the two vessels was achieved. The other stage was the

pressurization of vessel 2 by having valve 1 open and valve 2 closed. Valve 2 is a three way valve which is vented to the atmosphere when it is deenergized.

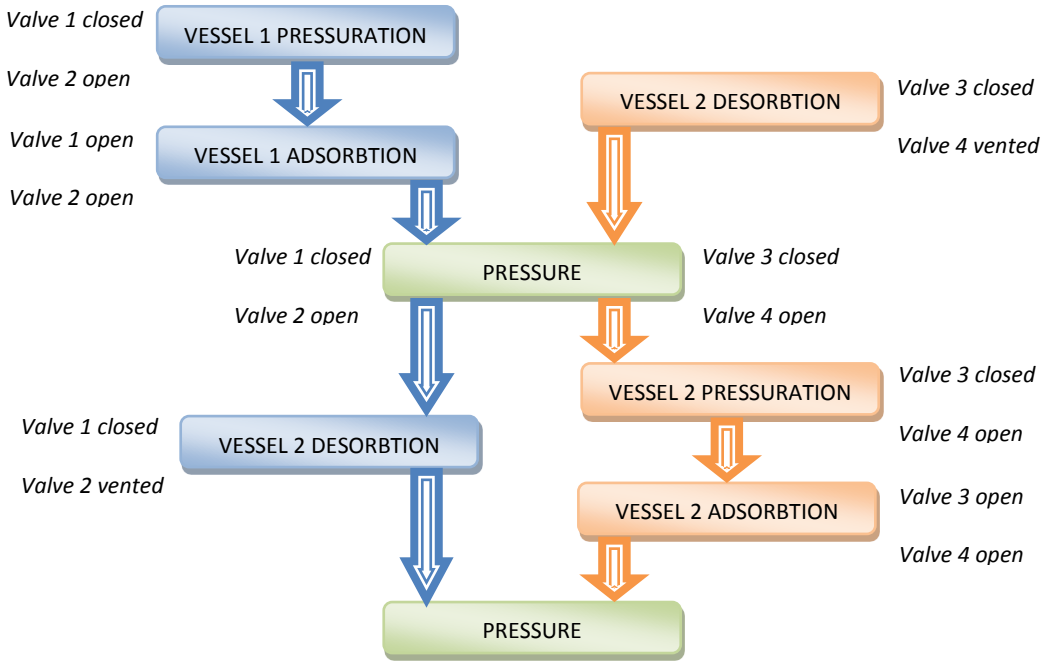

Figure 38. PSA system cycle.

This would reduce the pressure of the gas to atmospheric pressure through a vent or directed to a vacuum pump going to another stage, the desorbtion of Vessel 1. Vessel 2 would then undergo undergo the adsorption stage and the cycle continues. The program interface during operation and its code are shown in the Appendix H.

PSA Experiments

The results of the PSA experiments using the synthesis gas from MSW showed an average increase of 38% in the gas net heating value compared with certified gas standard (Table 19). The amount of hydrogen and methane was also significantly higher although the amount of the other hydrocarbons remained comparatively the same. The amount of carbon monoxide was significantly lower and no traces of carbon dioxide was observed in the PSA product gas indicating that that carbon dioxide had been completely adsorbed by the system.

Table 19. Product gas and certified gas standard chromatograph results

Components	*Certified Gas Standard (mol %)*	*PSA Product Gas (mol %)*
Hydrogen	5	*14.31*
Nitrogen	57.5	*59.91*
Carbon Monoxide	12	*4.89*
Methane	5	*10.83*
Carbon Dioxide	12	*0*
Acetylene	0.5	*0*
Ethylene	5	*5.28*
Ethane	0.5	*1.45*
Propylene	2	*2.5*
Propane	0.5	*0.83*
Net calorific value	245.45	*332.49*
% Increase		*38%*

During the pressurization stage, the raw gas inlet flow rate started at 9 LPM and ended at around 1 LPM until the vessel was desorbed and switched onto the other one (Figure 39a). The performance of the PSA system based on the product gas composition during the adsorption and desorption cycles is shown in Figure 39b. The desired concentration of the product gas was achieved in a short span of 1 minute during adsorption. Each adsorption cycle increases the hydrogen and THC concentration to an average of 14% and 19%, respectively and decreases the amount of carbon monoxide and carbon dioxide to 6% and 1%, respectively. A longer stable gas concentration may be achieved by using more adsorbent. As the adsorbent became saturated early, using a larger scale PSA system could address the problem. Having two additional PSA vessels would eliminate the product gas concentration cycle and produce a constant desired product gas concentration. With these limitations, however, the use of the PSA system presents a feasible application to producing a cleaner synthesis gas and reducing the problems in downstream operations.

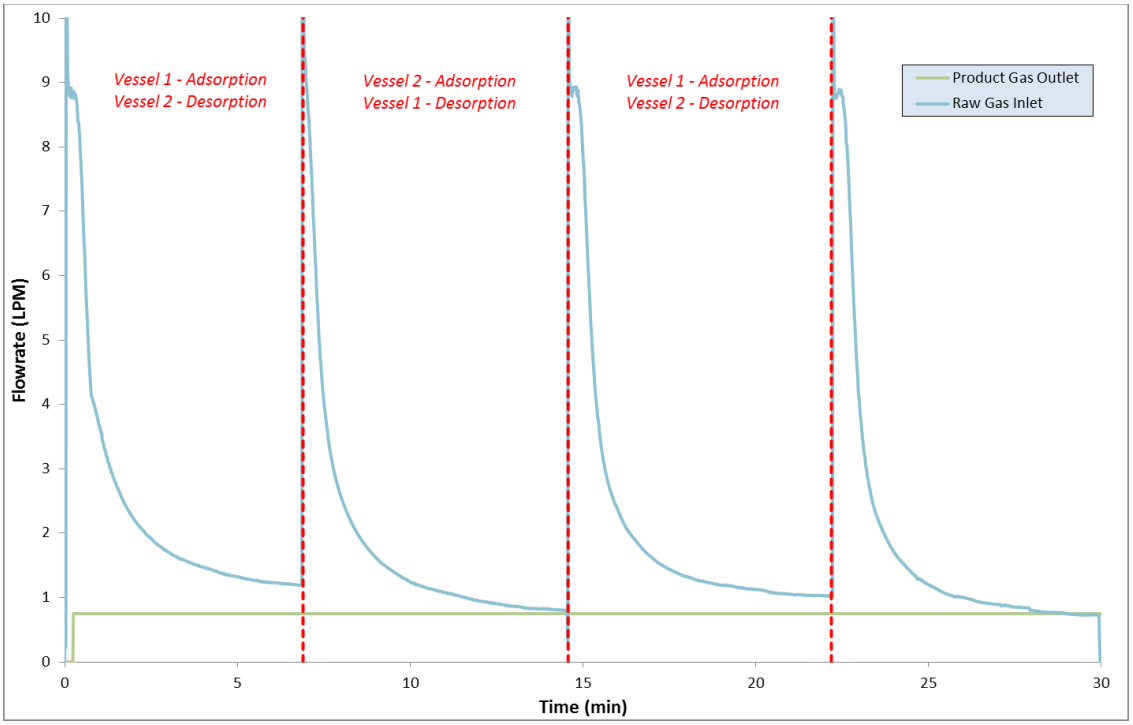

(a)

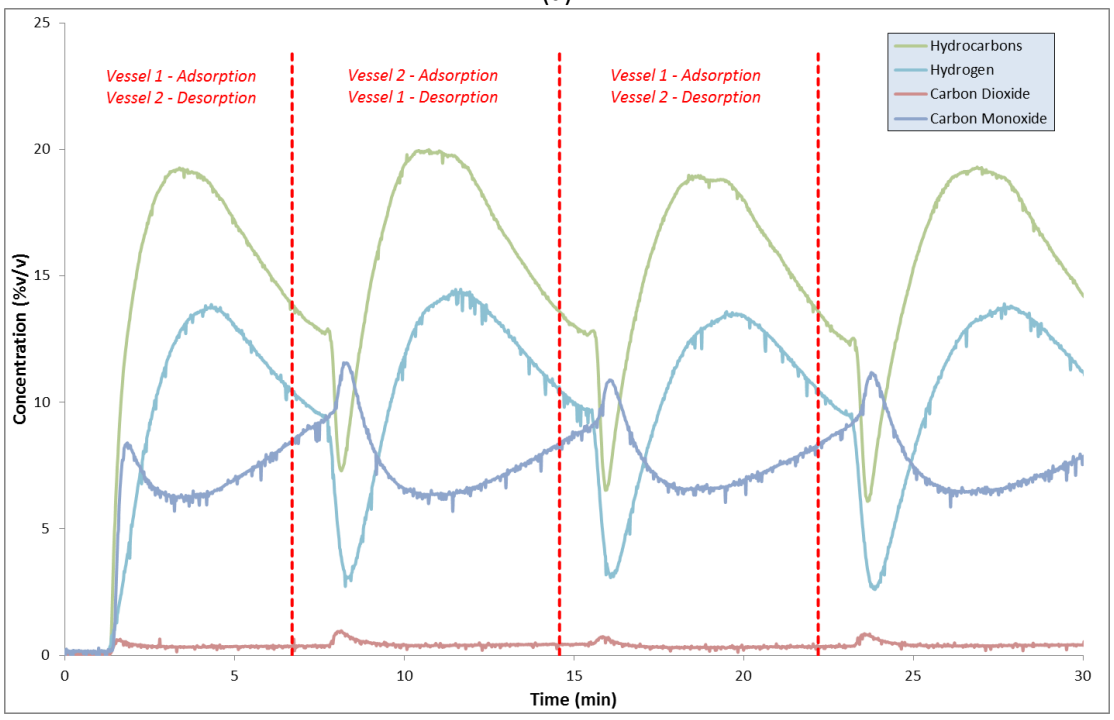

(b)

Figure 39. (a) Raw gas and product gas flow rate (b) product gas composition vs time

CONCLUSION

The overall performance of a spark ignition engine generator using synthesis gas from pelletized segregated municipal solid waste (MSW) gasification was evaluated based on its efficiency and exhaust emissions compared to a standard gasoline engine. In addition, the feasibility of upgrading the synthesis gas using the pressure swing adsorption (PSA) system was assessed. Gasification tests were conducted at the optimum condition of 740°C reaction temperature, equivalence ratio of 0.25 and operating pressure of 1660 mm of water. A 10 kW generator run by a 20 HP 614 cc Honda GX620 motor was integrated with the gasification system and made capable to use gaseous fuel, including synthesis gas, in a standard gasoline engine. A randomized complete block experimental design was used to determine the effects of the type of fuel and electrical power loads on the generator on the overall engine-generator efficiency, exhaust temperature and emissions.

The consumption of synthesis gas was observed to be the same for all power loads, but gasoline consumption increased with increasing power loads giving an average of 636 g $kW^{-1}h^{-1}$ which is twice the rated value of 313 g $kW^{-1}h^{-1}$ for a GX620 Honda engine. Using the measured lower heating value of the standard gasoline as 40 MJ kg^{-1} and 7.64 MJ Nm^{-3} (205 Btu scf^{-1}) for the synthesis gas, the overall engine-generator efficiency at 7.5 kW electrical power load was calculated to be 19.81% and 35.27% for gasoline and synthesis gas, respectively. The synthesis gas fueled engine also showed higher efficiency at all electrical power loads ranging from 12.61% to 35.27% compared to only 9.95% to 19.81% for gasoline.

The results of the PSA experiments showed an average increase of 38% in the net heating value of the synthesis gas over that of certified gas standard. The amount of hydrogen and methane was also significantly higher although the amount of the other hydrocarbons remained comparatively the same. The amount of carbon monoxide was significantly lower and no traces of carbon dioxide was observed in the PSA product gas indicating that carbon dioxide had been completely adsorbed by the system.

The raw gas inlet flow rate started at 9 LPM and ended at around 1 LPM until the vessel was desorbed and switched onto the other one. Based on the product gas composition during the adsorption and desorption cycles, the desired concentration of the product gas was achieved in a short span of 1 minute during adsorption. Each adsorption cycle increases the hydrogen and THC concentration to an average of 14% and 19%, respectively and decreases the amount of carbon monoxide and carbon dioxide to 6% and 1%, respectively. A longer stable gas concentration may be achieved by using more adsorbent. As the adsorbent became saturated early, using a larger scale PSA system could address the problem. Having two additional PSA vessels would eliminate the product gas concentration cycle and produce a constant desired product gas concentration. With these limitations, however, the use of the PSA system presents a feasible application to producing a cleaner synthesis gas and reducing the problems in downstream activities.

CHAPTER V

FOULING AND SLAGGING BEHAVIOR OF SEGREGATED MUNICIPAL SOLID WASTES (MSW) DURING THERMAL CONVERSION

INTRODUCTION

Formation of deposits on heat transfer surfaces, referred to as slagging and fouling, is one of the biggest problems for all solid fuel fired boilers, especially in biomass combustion (Tortosia-Masia et al., 2005). Slagging occurs in the boiler sections that are directly exposed to flame irradiation. Formation of slag involves stickiness, ash melting and sintering. Fouling deposits, on the other hand, form in the convective parts of the boiler mainly due to condensation of volatile species that have been vaporized in the other boiler sections and are loosely bonded. Slagging and sintering properties of different fuel ashes vary widely. Formation of deposits depends mainly on fuel quality, boiler design, and boiler operation. Although all biomass fuels exhibit fouling behavior, rates of fouling differ depending on the content and composition of the ash. For instance, woods tend not to foul at as high a rate as straws because at the same fuel firing rate, woods have a more favorable ash composition and less ash entering the combustor. Ash can also cause a variety of problems in gasification systems. For example, slagging can lead to excessive tar formation and/or complete blocking of the reactor (Stassen and Swaaij, 1982). Van der Drift et al. (2004) reported feeding issues when high ash content biomass was used in entrained flow gasification systems (Van der Drift et al., 2004).

There are numerous wood-based power installations worldwide (Ahtikoski et al., 2008). Low-ash-content wood materials do not exhibit slagging and fouling problems even in the combustion mode (Hustad et al., 1995). The most common application of biomass for large scale power production has been co-firing with coal. Biomass co-firing has been successfully demonstrated in over 150 installations worldwide for most combinations of fuel and boiler type in the range of 50-700 MW_e (i.e., electrical output in MW) (Al-Mansour and Zuwala, 2010). The primary reason for co-firing of biomass with coal is the minimal slagging and corrosion problems observed when only a small percentage of biomass is used (Pronobis, 2005). Detailed laboratory experiments are normally conducted for each biomass type to gain knowledge of the fundamental combustion phenomena for that material. Removal of troublesome elements in the biomass by leaching some elements with water has been recommended by Jenkins et al. (1998) to help reduce slagging and fouling in furnaces and other thermal conversion systems (Jenkins et al., 1998). A better understanding of the ash properties of biomass before it is used would be desirable to avoid problems in the gasification operation (Skrifvars et al., 1992; Zevenhoven-Onderwater et al., 2001). Avoiding or reducing slagging and fouling would consequently reduce investment and operational costs and increase performance efficiency of gasifiers or any thermal conversion equipment. While a number of indices relating composition to fouling and slagging behavior have been developed for coal and other fuels, these have proven to be of limited value for biomass (Jenkins et al., 1998). Nevertheless, these empirical indices have been widely used to predict ash behavior and deposition tendencies for biomass fuels.

To evaluate the slagging and fouling potential of various biomass residues, Vamvuka and Zografos (2004) used the alkali index (AI), the base-to-acid ratio ($R_{b/a}$) and the bed agglomeration index (BAI) (Vamvuka and Zografos, 2004). They found that the removal of troublesome elements by leaching the biomass with water reduced slagging and fouling in furnaces. Leaching with water resulted in significant reductions in ash (up to 40%) and in the problematic elements K (up to 93%), Na (up to 96%), P (up to 85%) and Cl (up to 97%) and in the heavy metals Co, U, Mo, Pb and As. A lower combustion temperature or water leaching substantially reduced the fouling potential due to the presence of alkali compounds. The term "alkali" is used to describe the sum of potassium and sodium compounds, generically expressed as the oxides K_2O and Na_2O (Miles et al., 1995). The alkali index (AI) expresses the quantity of alkali oxide in the fuel per unit of fuel energy (kg alkali GJ^{-1}). It is computed using Equation [17]:

$$AI = \frac{kg(K_2O + Na_2O)}{GJ} \quad [17]$$

When the AI values are within the range of 0.17-0.34 kg/GJ, fouling or slagging may or may not occur but would surely happen when the values are above this range (Vamvuka and Zografos, 2004).

The $R_{b/a}$ in the ash is obtained as shown in Equation [18]:

$$R_{b/a} = \frac{\%(Fe_2O_3 + CaO + MgO + K_2O + Na_2O)}{\%(SiO_2 + TiO_2 + Al_2O_3)} \quad [18]$$

where the label for each compound makes reference to its weight concentration in the ash. As $R_{b/a}$ increases, the fouling tendency of a fuel ash increases.

The BAI relates ash composition to agglomeration in fluidized-bed reactors (Skrifvars et al., 1992). It is calculated using Equation [19]:

$$\mathrm{BAI}=\frac{\%(\mathrm{Fe_2O_3})}{\%(\mathrm{K_2O}+\mathrm{Na_2O})} \quad [19]$$

Bed agglomeration occurs when BAI values are lower than 0.15 (Vamvuka and Zografos, 2004).

Two slagging and fouling indices are used for coal, namely, the slagging factor, R_s and the fouling factor, R_f (ASME, 1974). R_s is defined as the ratio of the total base to the total acid constituents multiplied by the sulfur content (Equation [20]) and R_f is the ratio of the total base to the total acid constituents multiplied by the Na_2O concentration (Equation [21]). The basic constituents are Fe_2O_3, CaO, MgO, Na_2O and K_2O while the acid constituents are SiO_2 ,Al_2O_3 and TiO_2

$$R_s=\frac{\mathrm{Base}}{\mathrm{Acid}}\times S \quad [20]$$

$$R_s=\frac{\mathrm{Base}}{\mathrm{Acid}}\times \mathrm{Na_2O} \quad [21]$$

When coal samples are to be used in combustion systems, R_f and R_s factors are always calculated. The degree of slagging and fouling are found by referring to the slagging and fouling index values found in Table 20. The slagging and fouling types are classified as low, medium, high or severe (ASME, 1974).

Table 20. Slagging and fouling index for coals.

Slagging/Fouling Type	R_s	R_f
Low	<0.6	<0.2
Medium	0.6 – 2.0	0.2 – 0.5
High	2.0 – 2.6	0.5 – 1.0
Severe	>2.6	>1.0

Ash pellet compressive strength measurements have likewise been used in the prediction of ash agglomeration during pulverized coal combustion (Skrifvars et al., 1994). More recently, modeling techniques have also been applied to visualize slagging and fouling tendencies using mass and energy balances (Tortosia-Masia et al., 2005). On-line monitoring systems which model heat transfer between the flue gas and the water/steam cycle and deposit formation on heat exchanger surfaces have been developed. Van der Drift et al. (2004) studied the slagging/melting tendencies of selected fuels using a thermodynamic equilibrium model (FACTSAGE), minimizing Gibbs free energy and applying it to a hypothetical (pressurized) entrained-flow gasification system (Van der Drift et al., 2004). The results showed that only 10-25% of the ash forming components of beech were liquid at typical operating temperatures of 1300-1500°C which was explained by the dominance of CaO, which melts at temperatures higher than 1700°C. The behavior of the slag was minimally affected at the high temperature region of 1300-2000°C.

The goal of this study was to evaluate the slagging and fouling behavior of the ash from segregated municipal waste (MSW) and compare it with earlier results for cotton gin trash (CGT) and dairy manure (DM). The specific objectives were to: (a)

determine various slagging and fouling indices of the ash from MSW based on its inorganic composition, (b) determine the compressive strengths of MSW ash pellets exposed at different temperatures and correlate these with structural observations from scanning electron micrograph (SEM) photos and Energy Dispersive X-ray Spectroscopy (EDS) elemental analysis, and (c) evaluate the suitability of various slagging and fouling indices for MSW biomass feedstock.

METHODOLOGY

Composition and Characteristics of the Biomass and Ash

Ten grams of MSW biomass and 10 grams of the MSW ash samples were sent to the Huffman Laboratories Inc., Denver, Colorado, for ultimate analysis (for carbon (C), hydrogen (H), oxygen (O), nitrogen (N) and sulfur (S) contents) and complete inorganic ash analysis using ASTM Standard Methods (ASTM, 2009). The procedures followed at Huffman Lab were as follows: (1) samples were ground to nominally -200 mesh size particles using a Wiley Mill prior to all analyses; (2) moisture content was determined by oven drying a sample overnight in air at 105°C (ASTM E871, Standard Method for Moisture Analysis of Particulate Wood Fuels); (3) the amounts of carbon, hydrogen and nitrogen were determined using ASTM D 5373 (Standard Test Methods for Instrumental Determination of Carbon, Hydrogen and Nitrogen in Laboratory Samples of Coal); (4) sulfur analysis was performed using ASTM D 4239 (Standard Test Methods for Sulfur in the Analysis Sample of Coal and Coke Using High Temperature Tube Furnace Combustion methods); (5) the ash content was determined by heating a sample at 750°C

in air for 8 hours (ASTM E830, Standard Test methods for Ash in the Analysis Sample of Refuse-Derived Fuel) and (6) the percentage of oxygen was determined by difference between the original weight of dry sample and the weight total of the carbon, hydrogen, nitrogen, sulfur and ash assuming no halogens were present. Ash metal oxides were analyzed using Inductive Coupled Plasma – Atomic Emission Spectrometry (ASTM D6349, Standard Test Method for Determination of Major and Minor Elements in Coal, Coke and Solid Residues from Combustion of Coal and Coke by Inductive Coupled Plasma – Atomic Emission Spectrometry). All values were expressed as percentages of the total and reported as averages of 2 replicates.

Slagging and Fouling Indices Calculations

The results of the complete biomass inorganic ash analyses were used to calculate the empirical indices (AI, $R_{b/a}$, BAI, R_f, R_s) discussed earlier (Equations 17-21). The resulting values were used to evaluate the slagging and fouling potential of MSW.

Compressive Strength of the Ash Pellets

Pellets measuring 2.54 cm in diameter and 1.65 cm in height were prepared using five (5) grams of ash samples from MSW. Uniformity of the size and density of the pellets was obtained by using a fabricated pellet mold of the exact size as the required measurements. The samples were compressed by applying uniform load on an MTS Model 810 Material Stress Test System (Gray Machinery Company, Prospect Heights,

Chicago, IL).The pellets were then heated in air at 550, 600, 700, 800 and 900°C for 4 h. The compressive strength of the pellets was determined in three replicate samples at each temperature using the same MTS Model 810 Material Stress Test System. The relationship between compressive strength of the pellets and the heating temperature was plotted to determine the temperature at which the ash in the sample melts. This would indirectly indicate the slagging and fouling tendencies of the ash samples. When a mixture of material (in this case ash components) melts (called its eutectic point), the components crystallize exhibiting a brittle plastic range with weak compressive strength (Stanzl-Tschegg, 2009). This behavior was used to determine the melting point of the inorganic ash components in the biomass.

Scanning Electron Microscopy (SEM) and EDS Elemental Analysis of the Biomass Ash Samples

One pellet for each operating temperature mentioned earlier was analyzed at the Microscopy and Imaging Center at Texas A&M University, College Station, Texas for SEM evaluation. SEM specimens were prepared by spreading particles of each sample on carbon double stick tabs and subsequently coating it with PtPd (80/20) ~ 10 nm thickness. The carbon tape and film were used for fixation of particles and removal of accumulated charges. Micrographs were taken using a FEI Quanta 600 FE-SEM (Field Emission) scanning electron microscope equipped with a tungsten electron gun. It was operated at a 5 kV acceleration voltage with a 10 mm working distance and spot size of 3. In addition, elemental analysis of the samples was conducted using Energy Dispersive

X-ray Spectroscopy (EDS) operated at a 10 kV acceleration voltage, spot size of 4 and 5 sec live time. These images and results of elemental analysis were interpreted to show how bonding occurs at the different exposure temperatures and see changes in granular or fused states of the ash as exposure temperature was increased.

RESULTS AND DISCUSSION

Composition of MSW, DM and CGT Biomass and Ash

The ultimate analyses of MSW biomass by weight are shown in Table 21 together with the data for CGT, DM, lignite, Wyoming coal and redwood (LePori and Soltes, 1985; Maglinao and Capareda, 2010b). Except for the ash content of the redwood biomass (0.2%), MSW contained the lowest amount of ash (2.6%) compared with the ash content of CGT (18.62%), DM (11.86%), lignite (10.4%) and Wyoming coal (4.2%). The carbon content of the MSW ash was higher than its content in DM and

Table 21. Utimate analysis of different biomass

Ultimate Analysis (weight %)	MSW	CGT[a]	DM[a]	Lignite[b]	Wyoming Coal[b]	Redwood[b]
Moisture	1.66	9.17	13.26	-	-	-
Carbon	60.79	39.30	35.40	64.0	71.5	53.5
Hydrogen	9.75	5.42	5.04	4.2	5.3	5.9
Nitrogen	0.12	1.44	1.78	0.9	1.2	0.1
Oxygen	25.01	41.65	38.76	19.2	16.9	40.3
Sulfur	0.08	0.34	0.4	1.3	0.9	0
Ash	2.6	11.86	18.62	10.4	4.2	0.2

[a] Source: (LePori and Soltes, 1985)
[b] Source: (Maglinao and Capareda, 2010b)

CGT ash and comparable with those from lignite, coal and redwood. Hydrogen was highest in MSW (9.75%) while the amounts of nitrogen (0.12%) and sulfur (0.08%) were relatively the lowest.

Rajvanshi (1986) stated that severe slagging can be expected for fuels having ash content of 12% and above. In general, no slagging had been observed with fuels that have ash content below 5-6%. For fuels with ash content between 6 and 12%, the slagging behavior depends to a large extent on the ash melting temperature, which is influenced by the presence of trace elements giving rise to the formation of low melting point eutectic mixtures (Rajvanshi, 1986). With the relatively low ash content of MSW, melting of inorganic components could be expected not to occur at the various exposure temperatures used. Melting could be expected to be more severe for DM and CGT ash.

The inorganic composition of MSW ash is shown in Table 22. The values for CGT and DM ashes were included for comparison. The MSW ash contained higher amounts of Al_2O_3, CaO, Na_2O and TiO_2 compared with the ash from CGT and DM but it showed the lowest amounts of MgO, MnO, P_2O_5, SiO_2, SO_3, and K_2O. A striking difference is in the K_2O content; the K_2O content was more than 800 times and about 17 times that of the MSW ash of the CGT and DM ash, respectively.

Miles et al. (1995) reported that potassium is an important contributor to ash fusion or deposition through vaporization and condensation. Potassium is transformed during combustion and combines with other elements such as sulfur, chlorine and silica. Silica in combination with alkali and alkaline earth metals, especially with the readily

Table 22. Analysis of the ash from MSW, DM and CGT biomass

Components(%)	MSW Ash	CGT Ash	DM Ash
Al_2O_3	7.02	3.46	3.12
CaO	35.32	23.30	27.41
Fe_2O_3	1.6	1.11	1.84
MgO	1.86	5.69	10.90
MnO	0.02	0.06	0.14
P_2O_5	0.36	2.25	4.98
K_2O	0.31	24.62	5.28
SiO_2	12.91	21.70	32.46
Na_2O	10.36	0.76	1.82
SO_3	1.46	7.40	6.12
TiO_2	24.28	0.25	0.22
Total	95.50	90.60	94.29

volatilized form of potassium present in biomass, can lead to the formation of low melting point compounds which readily slag and foul at normal biomass boiler furnace temperatures of 800-900^{0}C. The alkali earths, MgO and CaO are also important in slagging and deposit formation because their very high fusion temperatures tend to inhibit the eutectic effects of alkalis, especially in fluidized beds.

Indices of Slagging and Fouling

The calculated AI, $R_{b/a}$ ratio, R_f, R_s, and BAI of the MSW ash are shown in Table 23. Again, the values for CGT and DM ash are also presented. Vamvuka and Zografos (2004) suggested that an alkali index of more than 0.34 kg GJ^{-1} would indicate certainty of fouling. As the base-to-acid ratio increases, the slagging tendency also increases. The high values of alkali index and the base-to acid ratio for both CGT and DM ashes indicate that fouling and slagging would surely occur during combustion. These values

of indices of slagging and fouling favor the suitability of MSW biomass during thermal conversion over CGT and DM. The relatively favorable inorganic composition of MSW ash indicates less or no problem of slagging and fouling during combustion. The melting temperature of ash tends to be parabolic with respect to $R_{b/a}$, reaching a minimum at intermediate values. For coal, a minimum is frequently located in the vicinity of $R_{b/a}$ = 0.75, but for biomass the minimum tends to appear at lower values (Jenkins et al., 1998). This information suggests that CGT and DM would not be a good fuel for combustion.

Table 23. Calculated slagging and fouling indices of the ash from MSW, DM and CGT

Slagging and Fouling Index	MSW Ash	CGT Ash	DM Ash	Slagging and Fouling Potential/Degree
Alkali Index	0.09	1.96	0.95	*> 0.34 certain to occur*
Base to Acid Ratio	1.12	2.18	1.32	> 1 fouling tendency would increase
R_f (Fouling Factor)	0.15	0.02	0.02	*< 0.2 Low fouling potential*
R_s (SlaggingFactor)	0.12	0.16	0.08	*< 0.6 Low slagging potential*
Bed Agglomeration Index	0.02	0.04	0.26	*Bed agglomeration occurs when index < 0.15*

Obviously, the calculated values of the alkali index and the base-to-acid ratio indicate that ash deposition tendencies are certain to occur for both CGT and DM but not for MSW. However, the low BAI values for MSW and CGT indicate their higher fouling tendency.

The slagging (R_s) and fouling (R_f) factors (Table 23) suggest that the MSW, CGT and DM biomass should have very low fouling and slagging potential. All have R_s values of less than 0.6 and R_f values of 0.02 or less. However, this is contradictory to the high potential for fouling and slagging indicated by the other indices. This observation could be explained by the fact that these parameters are not normally used for lignitic type ash which is similar to ash from agricultural biomass residues. R_f is known to give incorrect results for lignite (ASME, 1974).

Compressive Strength of the Ash Pellets

The compressive strengths of the treated MSW, DM and CGT ash pellets are shown in Figure 40. For the segregated MSW pellets, there was a small increase in the pellet strength from 550°C until about 600°C then it decreased to a low point at 700°C after which there was sharp increase up to about 850°C. The compressive strength of CGT ash was lowest at the lowest temperature of 550°C but continued to increase sharply until about 800°C after which its compressive strength rapidly decreased. On the other hand, DM ash pellets exhibited the highest compressive strength at a temperature of only 600°C. The difference in the behavior of the compressive strength plots between MSW and CGT and DM pellets could be attributed to the heterogeneous nature of the municipal waste used which is normally composed of items that cannot be traditionally recycled such as food packaging wastes, waxed cardboard and software wastes. It is also possible that MSW ash contains some trace elements with low melting point. The

analysis of variance indicates significant differences in the compressive strengths of MSW, CGT and DM ash pellets (p-value < 0.001) subjected to different temperatures.

The temperature at which the compressive strength is highest before any decrease with increasing temperature is suggested to be the maximum combustion temperature at which slagging and fouling of ash could be avoided. Based on these results, care must be observed when DM and CGT are thermally converted especially at operating temperatures above 600°C for DM and above 800°C for CGT. These are the melting

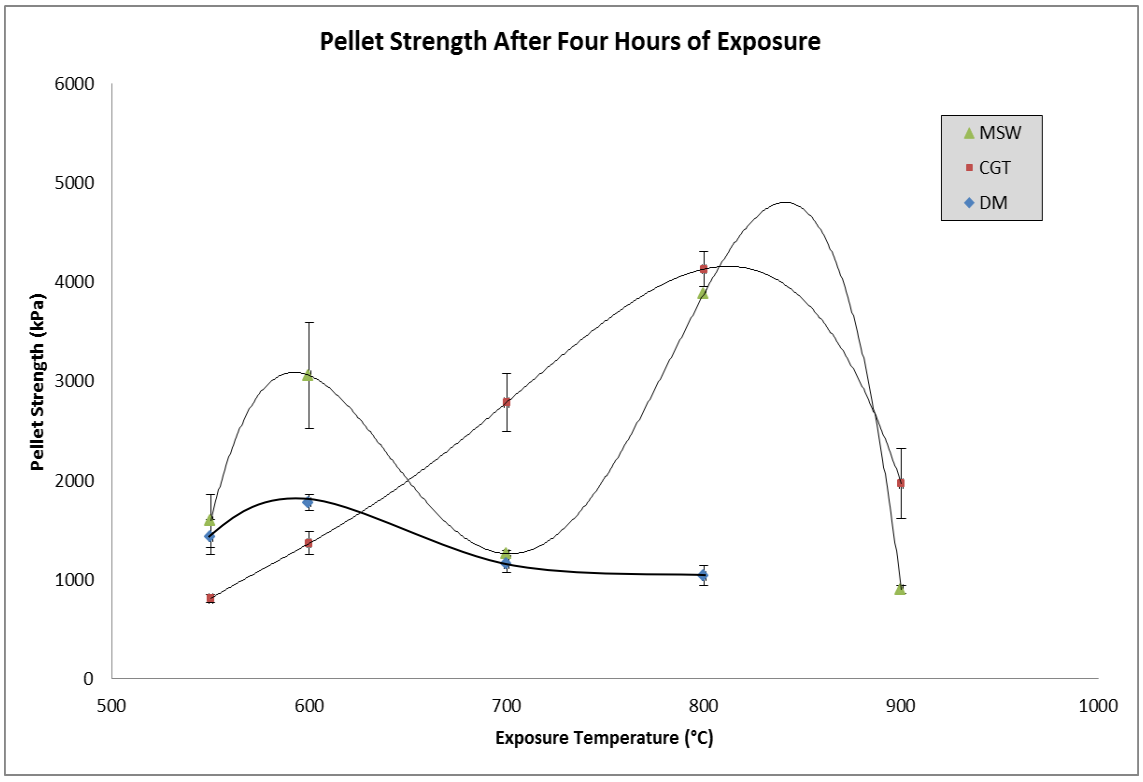

Figure 40. Compressive strength of MSW, DM and CGT ash pellets subjected to different temperatures

temperatures of the ash at which brittleness of the pellets was observed. In the case of MSW, brittleness of the pellets occurred above 600°C but later on gained compressive strength after 700°C indicating that thermal conversion can still be continued to a high temperature of about 850°C without slagging and fouling. The loss in strength after 600°C could indicate a temporary meltdown of some trace elements which might have been compensated by the strength of the other major components of the ash. Another possibility is the resolidification of the melted component of the ash material contributing to the gain in strength observed.

The operating temperature for the gasification system used at Texas A&M University was approximately 760°C (Maglinao et al., 2008). Thus, MSW and CGT may be gasified conveniently at this operating temperature with minimal slagging. DM, however, would be difficult to gasify at 760°C because significant slagging would likely occur. Conventional atmospheric fluidized bed combustion temperatures are normally within the range from 800-900°C, thus only MSW could be considered suitable for atmospheric combustion because of this higher operating temperature requirement (Levy et al., 1981).

Fernandez Llorente and Carrasco Garcia (2005) noted that the compressive strength measurement method described earlier does not adequately predict the ash sintering behavior of woody fuels and other biomass with lower contents of alkaline elements (Fernández Llorente and Carrasco García, 2005). However, they reported that the method seems to offer consistent results for biomass with high alkaline oxide contents when compared with the disintegrating and fusibility methods. The samples

used in this study have relatively high alkaline oxide contents (1.1:1 for MSW, 2.2:1 for CGT and 1.3:1 for DM) and thus the compressive strength method would seem to be valid.

Scanning Electron Microscopy (SEM) of the Biomass Ash Samples

Scanning electron micrographs of the segregated MSW ash samples subjected to different temperatures are shown in Figure 36. These electron microscopy images indicate the bonding behavior and granular structure of the ash samples at various furnace exposure temperatures. As seen in Figure 41, ash particles showed its surface to be primarily covered by areas of smooth material at 700°C and 900°C. The fused material at those temperatures could be related to the lower compressive strengths of the ash pellets.

EDS analysis of the MSW indicated the presence of metals ash samples (Figure 42). Ca and other metals such as K, Mg, Si, Ti, and Al were found in the ash. It was observed that Ca was relatively higher at temperatures of 550°C, 700°C, and 900°C where compressive strengths were lower. The glassy appearance of the bonded particles also showed the highly viscous melt formed on the surface and remained in its glassy phase at temperatures below its solidus value (Fryda et al., 2008). Such bonds were observed by Arvelakis et al. (2002), where a sticky layer containing potassium led to agglomeration (Arvelakis et al., 2002). The main elements of the bridges and coatings of agglomerates were identified as Si, K and Ca (Zevenhoven-Onderwater et al., 2001).

Compared with the SEM for the DM ash samples, areas of bonding or fused state was at the lowest exposure temperature of 550°C (Maglinao and Capareda, 2010b). As exposure temperature increased, more agglomeration of the particles was observed. On the other hand, the CGT images showed granular structure at 550°C and 600°C with agglomeration starting at around 700°C. A large area of fused material was exhibited at a temperature of 800°C indicating that CGT requires much higher temperature than DM for the same type of bonding to occur. This observation was consistent with the small variation in the compressive strengths of the DM ash pellets and the wider range of compressive strengths of the CGT ash pellets over the range of temperatures studied.

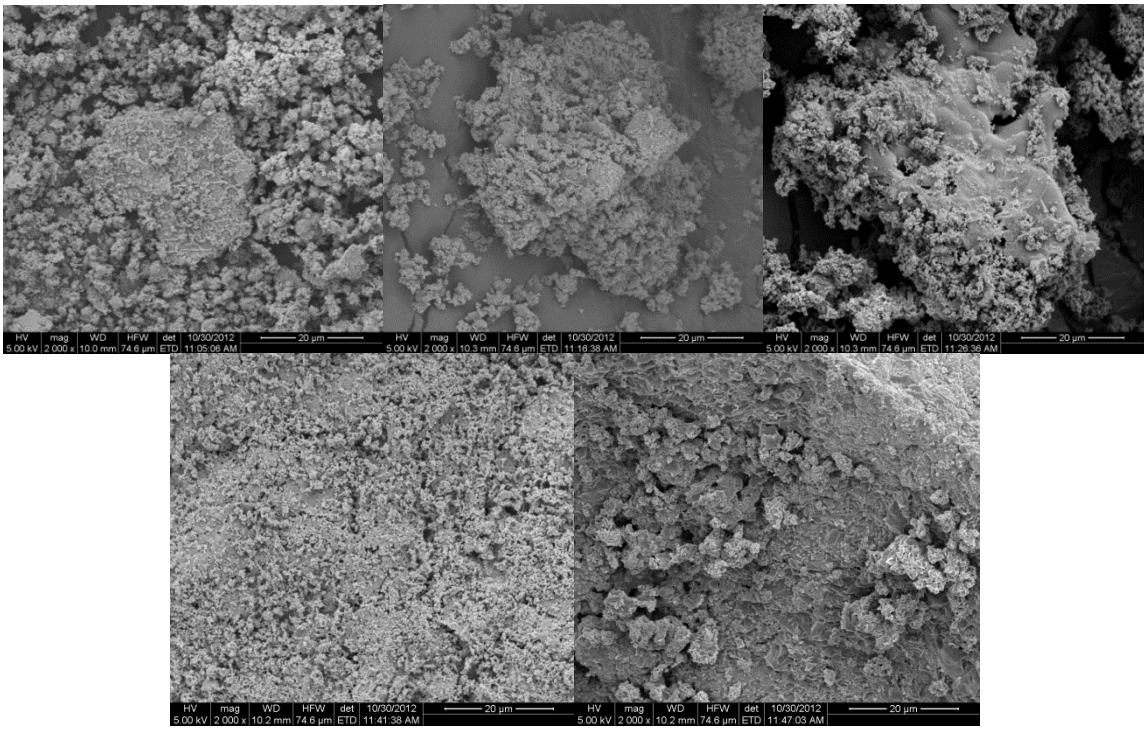

Figure 41. SEM pictures of MSW biomass ash samples exposed at different temperatures (2000x)

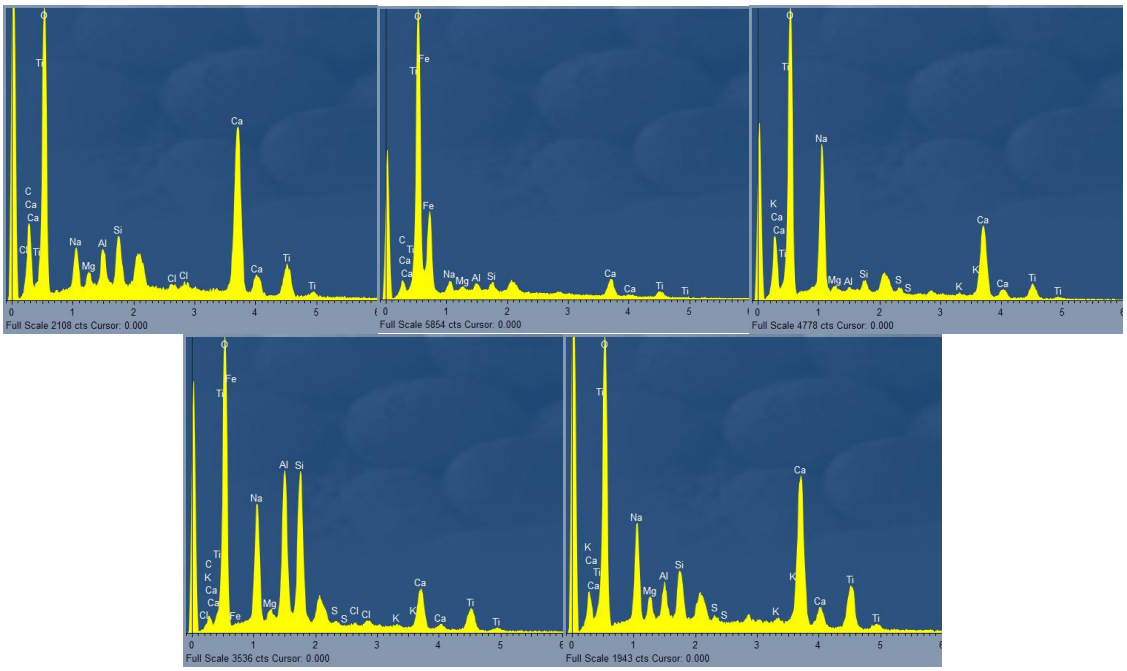

Figure 42. EDS analysis of the MSW biomass ash samples exposed at different temperatures

CONCLUSIONS

In this study, the AI, $R_{b/a}$ ratio and BAI of MSW ash were calculated and compared with the earlier values observed by Maglinao and Capareda (2010) for DM and CGT. These were used to evaluate its slagging and fouling behavior during thermal conversion. The indices R_f and R_s, typically used in the evaluation of slagging and fouling of coal materials, were also examined in this study.

Fouling and slagging was predicted to occur in both CGT and DM during combustion as shown by the high values of the AI and the $R_{b/a}$ ratio. MSW ash had lower values of these indices indicating no or low fouling and slagging tendencies. The calculated values indicate that there would be a higher ash deposition tendency with

CGT than DM. The low bed agglomeration index of CGT ash further supports the higher fouling tendency expected with the CGT feedstock. The prediction based on the three indices of slagging are in agreement with the inference made based on the high K_2O content of the CGT ash. However, the slagging and fouling indices used for coal are apparently inapplicable to agricultural residues and wastes. The R_s and R_f factors for CGT and DM suggest low slagging and fouling potential, contrary to the above predictions. The R_s and R_f factors are normally not recommended for lignites, which have similar characteristics to most types of agricultural biomass.

The compressive strength of the ash was used to estimate the temperature at which the ash material melted. The observed compressive strengths of CGT ash and DM ash were highest at 800°C and 600°C, respectively. For MSW, the brittleness of the pellets indicating the lowest compressive strength occurred at 700°C and 900°C. It is worth noting that it later gained in compressive strength after 700°C indicating that thermal conversion can still be continued to a high temperature of about 850°C without slagging and fouling. The temperature at which the compressive strength was observed to peak can be considered as the maximum combustion temperature at which slagging and fouling of the ash could be avoided.

The SEM images of the MSW ash showed agglomeration or fusion at 700°C and 900°C which showed correspondence with the peaks of the EDS elemental analysis. The SEM images of the DM ash particles showed that they started to bond at 550°C, with increasing agglomeration observed at higher exposure temperatures. For the CGT ash, a granular structure was observed at 550°C with fusion clearly shown from 700°C to

900°C exposure temperature. These observations were consistent with the small variation in the compressive strengths of the DM ash pellets and the wider range of compressive strengths of the CGT ash.

CHAPTER VI

CONCLUSIONS AND RECOMMENDATIONS

The ever increasing generation of waste materials from different sources poses a big challenge to develop applicable and economical waste management programs and strategies that will produce value added products and at same time enhance environmental quality. Wastes, especially coming from different industries, can be used as fuel for waste-to-energy facilities. Waste-to-energy plants can convert waste streams into biofuels or steam using direct combustion, anaerobic digestion, or gasification technologies.

Gasification is regarded an effective technology for the thermochemical conversion of biomass to energy or synthesis gas and different uses of gas shows its flexibility be integrated with several industrial processes, including power generation systems. Gasification technologies are expected to play a key role in the future of solid waste management since the conversion of municipal and industrial solid wastes to a gaseous fuel significantly increases its value.

This research study developed a municipal solid waste gasification system for electrical power generation using segregated municipal solid waste (MSW). Gasification experiments were conducted using a fluidized bed gasifier. The feasibility of making use of devices and control system to facilitate the management and operation of the gasification processes was evaluated based on the sample characteristics and the different parameters and the optimum conditions for the gasification processes to

proceed. The synthesis gas produced was used as a fuel to run a spark ignition engine generator and its performance evaluated based on engine efficiency and exhaust gas emissions.

In about 55 min reaction time, the automated control system had full control of the operation of the gasifier with the desired gasification reaction temperature of 700°C maintained for about 1 h during the test. The control system was also able to check the fluidization conditions and kept the fluidizing air velocity at an average of 48 cm s^{-1}. This was 30% higher than the minimum fluidization velocity indicating good fluidization of the bed inside the reactor. The appropriate equivalence ratio was controlled and continuous adjustment in the fuel feed was experienced to compensate for the decrease in fuel in the bin that caused the change of the flow in the screw conveyor. The gasification temperature profile showed that the reaction temperature was well maintained at the desired value of 700°C. Near isothermal condition within the reactor was observed and the stable pressure profile showed good fluidization. Analysis of the gas produced indicated a heating value (HV) of 7.94 MJ Nm^{-3}. The gasification system operated at 94% carbon conversion efficiency and 59% cold gasification efficiency. Gas production went at a rate of 4.00 kg/min and a yield of 2.78 m^3 kg^{-1} of fuel.

Analysis of the samples showed a heating value of about 30 MJ kg^{-1}, ash content of 2.6% and volatile matter of 93%. The heating value was found to be 82% higher and the ash content 80% lower than that cotton gin trash. The ultimate analysis indicated that MSW is mainly composed of carbon, hydrogen and oxygen and only traces of nitrogen and sulfur. With low sulfur content, SO_2 emissions would not pose a problem

in the utilization of MSW in energy conversion. Based on its elemental composition and stoichiometric combustion properties, it would require only about 1.8 kg to 3.7 kg of air per kg of MSW to achieve good operation of the gasification system with an equivalence ratio in the range of 0.2 to 0.4.

Within the set limits of the tests, the highest production of synthesis gas and the net heating value of 8.97 MJ Nm^{-3} resulted from gasification at 725°C and ER of 0.25. This is very close to the predicted value of 7.47 MJ Nm^{-3} based on the response surface plot which also indicated it was not affected by gasification temperature but significantly affected by the equivalence ratio. The ANOVA at 95% confidence level and the coded coefficients of the proposed quadratic models indicated that the gasification temperature and equivalence ratio had no significant effect on the hydrogen concentration of the synthesis gas. The equivalence ratio affected carbon monoxide and ethylene concentration while propylene and methane concentration was affected by both the gasification temperature and equivalence ratio. Significant effects of temperature on the production of hydrogen gas might have been observed had the experiments been conducted at a higher temperature because of the endothermic reactions in gasification. Gasification at lower equivalence ratio is predicted to produce higher net heating value of synthesis gas. However, gasification at a lower equivalence ratio is predicted to produce less synthesis gas (by volume) per unit of feedstock used.

The consumption of synthesis gas was observed to be the same for all power loads, but gasoline consumption increased with increasing power loads giving an average of 636 g $kW^{-1}h^{-1}$ which is twice the rated value of 313 g kW^{-1} h^{-1} for a GX620

Honda engine. Using the measured lower heating value of the standard gasoline as 40 MJ kg^{-1} and 7.64 MJ Nm^{-3} (205 Btu scf^{-1}) for the synthesis gas, the overall engine-generator efficiency at 7.5 kW electrical power load was calculated to be 19.81% and 35.27% for gasoline and synthesis gas, respectively. The synthesis gas fueled engine also showed higher efficiency at all electrical power loads ranging from 12.61% to 35.27% compared to only 9.95% to 19.81% for gasoline.

The use of the PSA system presents a feasible application to producing cleaner synthesis gas and reducing the problems in downstream activities. It increased the net heating value of the gas by an average of 38% gas over that of certified gas standard. The amount of hydrogen and methane was also significantly higher although the amount of the other hydrocarbons remained comparatively the same. The amount of carbon monoxide was significantly lower and no traces of carbon dioxide were observed in the PSA product gas indicating that carbon dioxide had been completely adsorbed by the system.

Based on the product gas composition during the adsorption and desorption cycles of the PSA system, the desired concentration of the product gas was achieved in a short span of 1 minute during adsorption. Each adsorption cycle increases the hydrogen and THC concentration to an average of 14% and 19%, respectively and decreases the amount of carbon monoxide and carbon dioxide to 6% and 1%, respectively. A longer stable gas concentration may be achieved by using more adsorbent which could be addressed by using a larger scale PSA system. Having two additional PSA vessels

would eliminate the product gas concentration cycle and produce a constant desired product gas concentration.

MSW showed relatively lower fouling and slagging tendencies than cotton gin trash (CGT) and dairy manure (DM). The compressive strength of the ash of CGT ash and DM ash were highest at 800°C and 600°C, respectively. For MSW, the brittleness of the pellets indicating the lowest compressive strength occurred at 700°C and 900°C. The high compressive strength of MSW after 700°C indicates that thermal conversion can still be continued to as high as 850°C without slagging and fouling. The SEM images and EDS elemental analysis of MSW ash further confirmed this observation.

Further research is recommended to provide added information, specifically conducting extensive research on the engine exhaust emissions. Halogens and HCl emissions can be analyzed since the process is dealing with municipal solid wastes. In addition, increasing the gasification efficiency can also be studied. Since gasification is an exothermic process, utilization of the heat produced, such as steam reforming or autothermal reforming, are some processes to increase the process efficiency. Ethylene is another viable product of the process that can be studied further.

REFERENCES

Abdel-Rahman, A. A. 1998. On the emissions from internal-combustion engines: A review. *International Journal of Energy Research* 22(6):483-513.

Ahmed, I. I., and A. K. Gupta. 2010. Pyrolysis and gasification of food waste: Syngas characteristics and char gasification kinetics. *Applied Energy* 87(1):101-108.

Ahtikoski, A., J. Heikkila, V. Alenius, and M. Siren. 2008. Economic viability of utilizing biomass energy from young stands: The case of Finland. *Biomass and Bioenergy* 32(11):988-996.

Al-Mansour, F., and J. Zuwala. 2010. An evaluation of biomass co-firing in Europe. *Biomass and Bioenergy* 34(5):620-629.

Anderson, N. 1997. *Instrumentation for Process Measurement and Control*. 3rd ed. CRC Press, New York.

Annadurai, G., and R. Sheeja. 1998. Use of Box-Behnken design of experiments for the adsorption of verofix red using biopolymer. *Bioprocess and Biosystems Engineering* 18(6):463-466.

Arena, U. 2011. Gasification: An alternative solution for waste treatment with energy recovery. *Waste Management* 31(3):405-406.

Arena, U., and M. L. Mastellone. 2006. Fluidized bed pyrolysis of plastic wastes. In *Feedstock Recycling and Pyrolysis of Waste Plastics: Converting Waste Plastics into Diesel and Other Fuels* 435-474. J. Scheirs, and W. Kaminsky, eds. Chichester, UK: John Wiley & Sons, Ltd.

Arena, U., L. Zaccariello, and M. L. Mastellone. 2010. Fluidized bed gasification of waste-derived fuels. *Waste Management* 30(7):1212-1219.

Arvelakis, S., H. Gehrmann, M. Beckmann, and E. G. Koukios. 2002. Effect of leaching on the ash behavior of olive residue during fluidized bed gasification. *Biomass and Bioenergy* 22:55-69.

ASME. 1974. *Coal Fouling and Slagging Parameters*. American Society of Mechanical Engineers, Research Committee on Corrosion and Deposits from Combustion Gases, New York, N.Y.

Basu, P. 2006. *Combustion and Gasification in Fluidized Beds*. CRC Press, New York.

Bridgwater, A. 1995. The technical and economic feasibility of biomass gasification for power generation. *Fuel* 74(5):631-653.

Bridgwater, A., and K. Maniatis. 2004. The production of biofuels by the thermochemical processing of biomass. In *Molecular to Global Photosynthesis*, 521-612. M. D. Archer, and J. Barber, eds. London UK: IC Press.

Bridgwater, T. 2006. Biomass for energy. *Journal of the Science of Food and Agriculture* 86(12):1755-1768.

Bui, T., R. Loof, and S. Bhattacharya. 1994. Multi-stage reactor for thermal gasification of wood. *Energy Conversion and Management* 19(4):397-404.

Bullock, D. B., S. Weingarden, and L. Lami. 2008. *Combined Heat and Power Potential using Texas Agricultural Wastes*. Gulf Coast CHP Regional Application Center, Woodlands,TX.

Cao, Y., Y. Wang, J. Rileya, and W. Pan. 2005. A novel biomass air gasification process for producing tar-free higher heating value fuel gas. *Fuel Processing Technology* 87(4):343-353.

Carson, J. 2008. Hopper/Bin design. In *Bulk Solids Handling: Equipment Selection and Operation*, 68-98. D. McGlinchey, ed. Oxford, UK Blackwell Publishing Ltd.

Chiang, K.-T. C., C-C, and N.-M. Liu. 2009. Application of response surface methodology in describing the thermal performances of a pin-fin heat sink. *International Journal of Thermal Sciences* 48(6):1196-1205.

Chiemchaisri, C., B. Charnnok, and C. Visvanathan. 2010. Recovery of plastic wastes from dumpsite as refuse-derived fuel and its utilization in small gasification system. *Bioresource Technology* 101(5):1522-1527.

Consonni, S., and F. Viganò. 2012. Waste gasification vs. conventional Waste-To-Energy: A comparative evaluation of two commercial technologies. *Waste Management* 32(4):653-666.

Cormos, C.-C. 2012. Hydrogen and power co-generation based on coal and biomass/solid wastes co-gasification with carbon capture and storage. *International Journal of Hydrogen Energy* 37(7):5637-5648.

Dasappa, S., G. Sridhar, H. V. Sridhar, N. K. S. Rajan, P. J. Paul, and A. Upasini. 2005. Producer gas engines — proponent of clean energy technology. In *Proceedings of 15th European biomass conference & exhibition – from research to market deployment – biomass for energy, industry and climate protection*. Germany.

Dasappa, S., D. N. Subbukrishna, K. C. Suresh, P. J. Paul, and G. S. Prabhu. 2011. Operational experience on a grid connected 100 kWe biomass gasification power plant in Karnataka, India. *Energy for Sustainable Development* 15(3):231-239.

De Swaan Arons, J., H. Van der Kooi, and K. Sankaranarayanan. 2004. Biomass production and conversion. In *Efficiency and Sustainability in the Energy and Chemical Industries*. New York, NY: Marcel Dekker, Inc.

Devi, L., M. Craje, P. Thüne, K. J. Ptasinski, and F. J. J. G. Janssen. 2005. Olivine as tar removal catalyst for biomass gasifiers: Catalyst characterization. *Applied Catalysis A: General* 294(1):68-79.

Elbaba, I. F., C. Wu, and P. T. Williams. 2011. Hydrogen production from the pyrolysis–gasification of waste tyres with a nickel/cerium catalyst. *International Journal of Hydrogen Energy* 36(11):6628-6637.

EPA. 2010. Municipal Solid Waste Generation, Recycling, and Disposal in the United States: Facts and Figures for 2010. Washington, DC.

Fernández Llorente, M. J., and J. E. Carrasco García. 2005. Comparing methods for predicting the sintering of biomass ash in combustion. *Fuel* 84(14–15):1893-1900.

Fryda, L. E., K. D. Panopoulos, and E. Kakaras. 2008. Agglomeration in fluidised bed gasification of biomass. *Power Technology* 81:307-320.

Fu, Y., and D. Liu. 2007. Novel experimental phenomena of fine-particle fluidized beds. *Experimental Thermal and Fluid Science* 32:341-344.

Gopal, G., P. Srinivasa Rao, K. V. Gopalakrishnan, and B. S. Murthy. 1982. Use of hydrogen in dual-fuel engines. *International Journal of Hydrogen Energy* 7(3):267-272.

Goswami, Y., and F. Kreith. 2008. *Energy Conversion*. Mechanical and Aerospace Engineering Series. CRC Press, Boca Raton, FL.

Greene, N., F. E. Celik, B. Dale, and M. Jackson. 2004. Growing Energy: How Biofuels can Help End America's Oil Dependence. New York: Natural Resources Defense Council. Available at: http://www.nrdc.org/air/energy/biofuels/contents.asp.

Hao, X., H. Yang, and G. Zhang. 2008. Trigeneration: A new way for landfill gas utilization and its feasibility in Hong Kong. *Energy Policy* 36(10):3662-3673.

Heermann, C., F. J. Schwager, and K. J. Whiting. 2001. *Pyrolysis & Gasification of Waste*. Second ed. Juniper Consultancy Services Ltd, Gloucestershire, England.

Heywood, J. B. 1988. *Internal Combustion Engine Fundamentals*. McGraw-Hill, New York.

Hillier, V. A. W., and P. Coombes. 2004. *Fundamentals of Motor Vehicle Technology*. Fifth ed. Nelson Thornes Ltd, Gloucestershire, England.

Hustad, J. E., O. Skkeiberg, and O. K. Sonju. 1995. Biomass combustion research and utilization in EIA countries. *Biomass and Bioenergy* 9(15):235-255.

Jenike, A. 1964. *Storage and Flow of Solids*. No. Bulletin No. 123. University of Utah Engineering Experiment Station, Utah.

Jenkins, B. M., L. L. Baxter, T. R. Miles Jr, and T. R. Miles. 1998. Combustion properties of biomass. *Fuel Processing Technology* 54(1–3):17-46.

Jeong, G.-T., H.-S. Yang, and D.-H. Park. 2009. Optimization of transesterification of animal fat ester using response surface methodology. *Bioresour Technol* 100:25-30.

Johansson, T., K. McCormick, L. Nei, and W. Turkenburg. 2006. The Potentials of Renewable Energy. In *Renewable Energy: A Global Review of Technologies Policies and Markets*. D. Assmann, U. Laumanns, and D. Uh, eds. Trowbridge, UK.: Cromwell Press.

Jorapur, R., and A. Rajvanshi. 1997. Sugarcane leaf-bagasse gasifiers for industrial heating applications. *Biomass and Bioenergy* 13(3):141-146.

Karim, G. A. 2003. Hydrogen as a spark ignition engine fuel. *International Journal of Hydrogen Energy* 28(5):569-577.

Klein, A., K. Whiting, E. Archer, and R. J. Schwage. 2004. Gasification and pyrolysis: what is the current situation for waste management? *Waste Management World* 71:75.

Knoef, H. 2005. Practical Aspects of Biomass Gasification. In *Handbook Biomass Gasification*. H. Knoef, ed. Enschede, Netherlands: BTG Biomass Technology Group.

Kunii, D., and O. Levenspiel. 1969. *Fluidization Engineering*. Robert E. Krieger Publishing Co. Inc., New York.

Lai, W.-H., M.-P. Lai, and R.-F. Horng. 2012. Study on hydrogen-rich syngas production by dry autothermal reforming from biomass derived gas. *International Journal of Hydrogen Energy* 37(12):9619-9629.

LePori, W. A., and E. J. Soltes. 1985. Thermochemical Conversion for Energy and Fuel. In *Biomass Energy: A Monograph*, 10-49. E. A. Hiler, and B. A. Stout, eds. College Station: Texas A&M University System: Texas A&M University Press.

Leva, M. 1959. *Fluidization*. McGraw-Hill Book Company, New York.

Levy, A., R. E. Barret, R. D. Giammar, and H. R. Hazard. 1981. Coal combustion. In *Coal Handbook*. R. A. Meyers, ed. New York, N.Y.: Marcel Dekker.

Maglinao, A. 2009. Instrumentation and Evaluation of a Pilot Scale Fluidized Bed Biomass Gasification System. Texas A&M University, Biological and Agricultural Engineering, College Station, Texas

Maglinao, A., and S. Capareda. 2010a. Development of computer control system for the pilot scale fluidized bed biomass gasification system. In *ASABE International Conference*. Pittsburgh, Pennsylvania: ASABE.

Maglinao, A., and S. Capareda. 2010b. Predicting fouling and slagging behaviour of dairy manure (DM) and cotton gin trash (CGT) during thermal conversion. *Transactions of the ASABE* 53(3):903-909.

Maglinao, A., S. Capareda, C. B. Parnell, and D. Carney. 2008. Demonstration and simulation of a fluidized bed gasification system for power generation. In *ASABE International Conference*. Rhode Island: ASABE.

Malkow, T. 2004. Novel and innovative pyrolysis and gasification technologies for energy efficient and environmentally sound MSW disposal. *Waste Management* 24(1):53-79.

Martínez, J. D., K. Mahkamov, R. V. Andrade, and E. E. Silva Lora. 2012. Syngas production in downdraft biomass gasifiers and its application using internal combustion engines. *Renewable Energy* 38(1):1-9.

Mastellone, M. L., and U. Arena. 2008. Olivine as a tar removal catalyst during fluidized bed gasification of plastic waste. *AIChE Journal* 54(6):1656-1667.

Mathieu, P., and R. Dubuisson. 2002. Performance analysis of a biomass gasifier. *Energy Conversion and Management* 43(9–12):1291-1299.

McKendry, P. 2002. Energy production from biomass (part 1): overview of biomass. *Bioresource Technology* 83:37-46.

McMillian, M. H., and S. A. Lawson. 2006. Experimental and modeling study of hydrogen/syngas production and particulate emissions from a natural gas-fueled partial oxidation engine. . *International Journal of Hydrogen Energy* 31(7):847-860.

Miles, T. R., T. R. M. Jr., L. L. Baxter, R. W. Bryers, B. M. Jenkins, and L. L. Oden. 1995. *Alkali deposits found in biomass power plants: A preliminary investigation of their extent and nature*. National Renewable Energy Laboratory, Golden, Colorado.

Mohon Roy, M., E. Tomita, N. Kawahara, Y. Harada, and A. Sakane. 2009. Performance and emission comparison of a supercharged dual-fuel engine fueled by producer gases with varying hydrogen content. *International Journal of Hydrogen Energy* 34(18):7811-7822.

Murphy, J. D., and E. McKeogh. 2004. Technical, economic and environmental analysis of energy production from municipal solid waste. *Renewable Energy* 29(7):1043-1057.

Mustafi, N. N., Y. C. Miraglia, R. R. Raine, P. K. Bansal, and S. T. Elder. 2006. Spark-ignition engine performance with 'Powergas' fuel (mixture of CO/H2): A comparison with gasoline and natural gas. *Fuel* 85(12–13):1605-1612.

Narvaez, I., A. Orio, M. Aznar, and J. Corella. 1996. Biomass Gasification with Air in an Atmospheric Bubbling Fluidized Bed. Effect of Six Operational Variables on the Quality of the Produced Raw Gas. *Ind. Eng. Chem. Res.* 35(7):2110-2120.

Nhuchhen, D., and P. Abdul Salam. 2012. Estimation of higher heating value of biomass from proximate analysis: A new approach. *Fuel* 99:55-63.

Nise, N. 2000. *Control Systems Engineering*. 3rd ed. John Wiley & Sons, Inc, New York.

Paolucci, M., P. D. Filippis, and C. Borgianni. 2010. Pyrolysis and Gasification of Municipal and Industrial wastes blends. *Thermal Science* 14(3):739-746.

Pinto, F., C. Franco, R. N. André, M. Miranda, I. Gulyurtlu, and I. Cabrita. 2002. Co-gasification study of biomass mixed with plastic wastes. *Fuel* 81(3):291-297.

Pronobis, M. 2005. Evaluation of the influence of biomass co-combustion on boiler furnace slagging by means of fusibility correlations. *Biomass and Bioenergy* 28(4):375-383.

Rajput, R. K. 2005. *Internal Combustion Engines*. Laxmi Publications, New Delhi, India.

Rajvanshi, A. 1986. Biomass Gasification. In *Alternative Energy in Agriculture*, 83-102. D. Y. Goswami, ed. New York: Taylor and Francis.

Rapagnà, S., K. Gallucci, M. Di Marcello, M. Matt, M. Nacken, S. Heidenreich, and P. U. Foscolo. 2010. Gas cleaning, gas conditioning and tar abatement by means of a catalytic filter candle in a biomass fluidized-bed gasifier. *Bioresource Technology* 101(18):7123-7130.

Roos, C. 2009. *Clean heat and power using biomass gasification for industrial and agricultural projects*. Northwest CHP Application Center, Olympia, WA.

Sagues, C., P. Garcia-Bacaicoa, and S. Serrano. 2007. Automatic control of biomass gasifiers using fuzzy inference systems. *Bioresource Technology* 98(4):845-855.

Sakai, S., S. E. Sawell, A. J. Chandler, T. T. Eighmy, D. S. Kosson, J. Vehlow, H. A. van der Sloot, J. Hartlén, and O. Hjelmar. 1996. World terends in municipal solid waste management. *Waste Management* 16(5–6):341-350.

Shah, A., R. Srinivasan, S. D. Filip To, and E. P. Columbus. 2010. Performance and emissions of a spark-ignited engine driven generator on biomass based syngas. *Bioresource Technology* 101(12):4656-4661.

Shashikantha, W. Klose, and P. P. Parikh. 1994. Development of a 15 kWe spark ignition producer gas engine and some investigations of its in-cylinder processes. *Renewable Energy* 5(5–8):835-837.

Shirai, T. 1958. *Fluidized Beds (In Japanese)*. Tokyo Institute of Technology, Japan.

Shudo, T., T. Nagano, and M. Kobayashi. 2003. Combustion characteristics of waste pyrolysis gases in an internal combustion engine. *International Journal of Automotive Technology* 4(1):1-8.

Sipila, K. 1995. Research into Thermochemical Conversion of Biomass into Fuels, Chemicals and Fibers. In *Biomass for Energy, Environment, Agriculture and Industry, Proceedings of the 8th EC Conference*. Vienna, Pergamon.

Skrifvars, B. J., M. Hupa, R. Backman, and M. Hiltunen. 1994. Sintering mechanisms of FBC ashes. *Fuel* 73(2):171-176.

Skrifvars, B. J., M. Hupa, and M. Hiltunen. 1992. Sintering of ash during fluidized bed combustion. *Industrial & Engineering Chemistry Research* 31(4):1026-1030.

Sobyanin, V., V. Sadykov, V. Kirillov, V. Kuzmin, N. Kuzin, Z. Vostrikov, A. Khristolyubov, V. Luksho, and A. Afanasiev. 2005. Syngas as a Fuel for IC and Diesel Engines: Efficiency and Harmful Emissions Cut-off. In *International Hydrogen Energy Congress and Exhibition*. Istanbul, Turkey.

Sridhar, G., S. Dasappa, H. V. Sridhar, P. J. Paul, N. K. S. Rajan, and V. S. P. Kummar. 2005. Green electricity—a case study of a grid linked independent power producer. In *Proceedings of 15th European biomass conference & exhibition – from research to market deployment – biomass for energy, industry and climate protection*. Germany.

Sridhar, G., P. J. Paul, and H. S. Mukunda. 2001. Biomass derived producer gas as a reciprocating engine fuel—an experimental analysis. *Biomass and Bioenergy* 21(1):61-72.

Stanley-Wood, N. 2008. Bulk powder properties: Instrumentation and techniques. In *Bulk Solids Handling: Equipment Selection and Operation*, 1-67. D. McGlinchey, ed. Oxford,UK: Blackwell Publishing Ltd.

Stanzl-Tschegg, S. E. 2009. Fracture Properties of Wood and Wood Composites. *Advanced Engineering Materials* 11(7):600-606.

Stassen, H. E. M., and W. P. M. v. Swaaij. 1982. Application of biomass gasification in developing countries. In *Proceedings in International Conference on Biomass: Energy from Biomass*, 705-714. A. Strub, P. Chartier, and G. Schleser, eds. London UK: Applied Science Publishers.

Svrcek, W., D. Mahoney, and B. Young. 2000. *A Real-time Approach to Process Control*. Prentice- Hall, England, UK.

Swanson, R. M., J. A. Satrio, R. C. Brown, A. Platon, and D. D. Hsu. 2010. *Techno-economic analysis of biofuels production based on gasification*. National Renewable Energy Laboratory, Golden CO.

Tortosia-Masia, A., F. Ahnert, H. Spliethofff, J. Loux, and K. Hein. 2005. Slagging and fouling in biomass co-combustion. *Thermal Sci* 9(3):85-98.

Turner, J. 2009. *Automotive Sensors*. Momentum Press, New Jersey.

Vamvuka, D., and D. Zografos. 2004. Predicting the behaviour of ash from agricultural wastes during combustion. *Fuel* 83(14–15):2051-2057.

Van der Drift, A., H. Boerrigter, B. Coda, M. K. Cieplik, and K. Hemmes. 2004. Entrained flow gasification of biomass: Ash behavior, feeding issues, and system analyses. Dutch Agency for Research in Sustainable Energy (SDE).

Wang, J., G. Cheng, Y. You, B. Xiao, S. Liu, P. He, D. Guo, X. Guo, and G. Zhang. 2012. Hydrogen-rich gas production by steam gasification of municipal solid waste (MSW) using NiO supported on modified dolomite. *International Journal of Hydrogen Energy* 37(8):6503-6510.

Warnecke, R. 2000. Gasification of biomass: comparison of fixed bed and fluidized bed gasifier. *Biomass and Bioenergy* 18(6):489-497.

Woodcock, C., and J. Mason. 1987. *Bulk Solids Handling: An Introduction to the Practice and Technology*. 1st ed. Chapman and Hall, New York.

Xiao, X., X. Meng, D. D. Le, and T. Takarada. 2011. Two-stage steam gasification of waste biomass in fluidized bed at low temperature: Parametric investigations and performance optimization. *Bioresource Technology* 102(2):1975-1981.

Zevenhoven-Onderwater, M., R. Backman, B.-J. Skrifvars, and M. Hupa. 2001. The ash chemistry in fluidised bed gasification of biomass fuels. Part I: predicting the chemistry of melting ashes and ash–bed material interaction. *Fuel* 80(10):1489-1502.

Zhao, Z., N. Lakshminarayanan, J. N. Kuhn, A. Senefeld-Naber, L. G. Felix, R. B. Slimane, C. W. Choi, and U. S. Ozkan. 2009. Optimization of thermally impregnated Ni–olivine catalysts for tar removal. *Applied Catalysis A: General* 363(1–2):64-72.

APPENDIX

Appendix A. NI LabVIEW Cold Fluidization Experiments

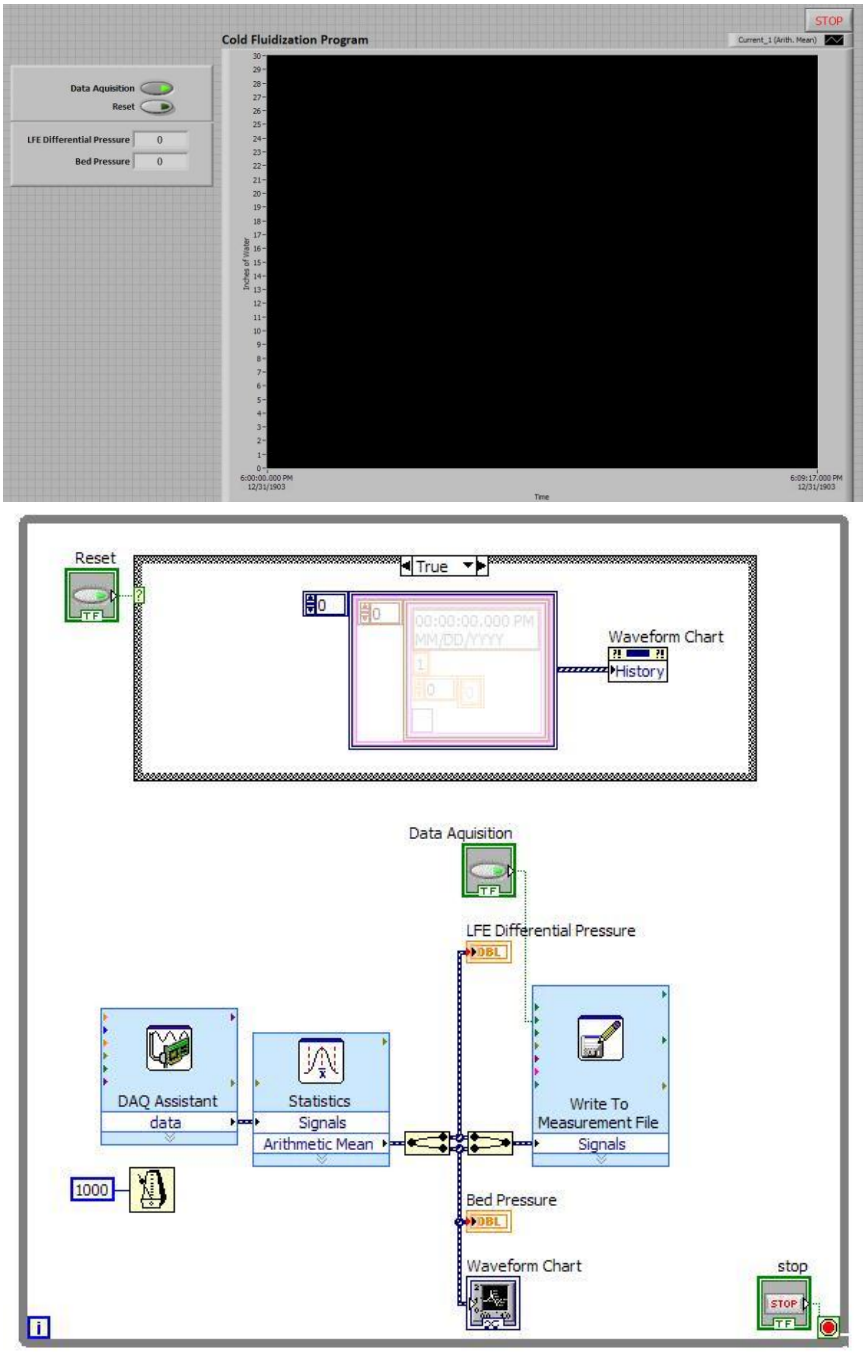

Appendix B. Different gasification control system graphical user interface

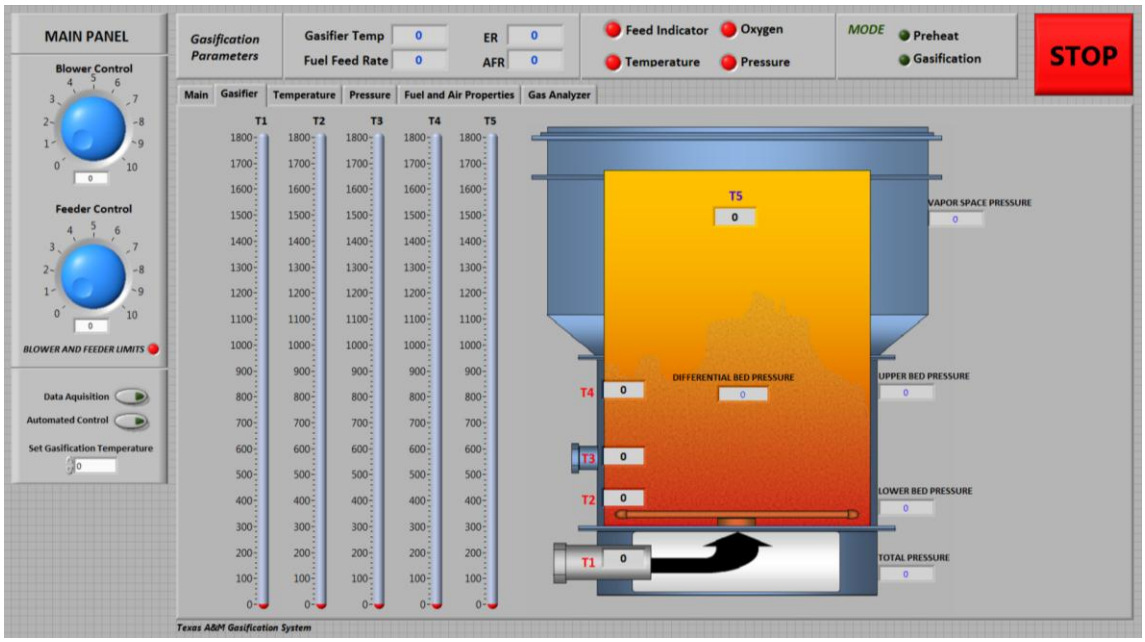

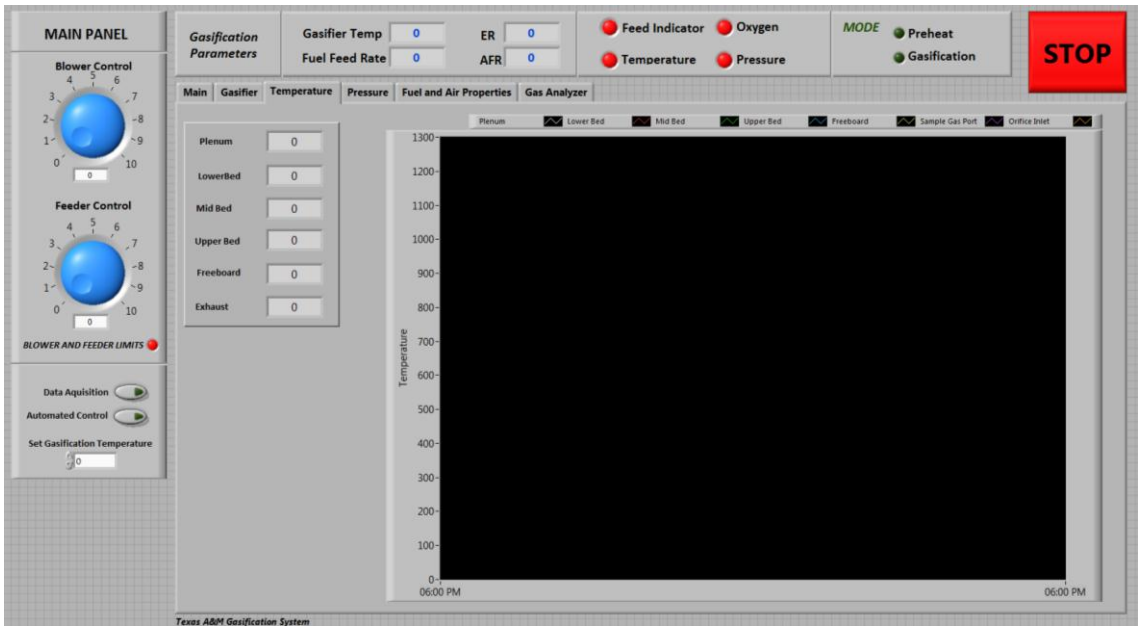

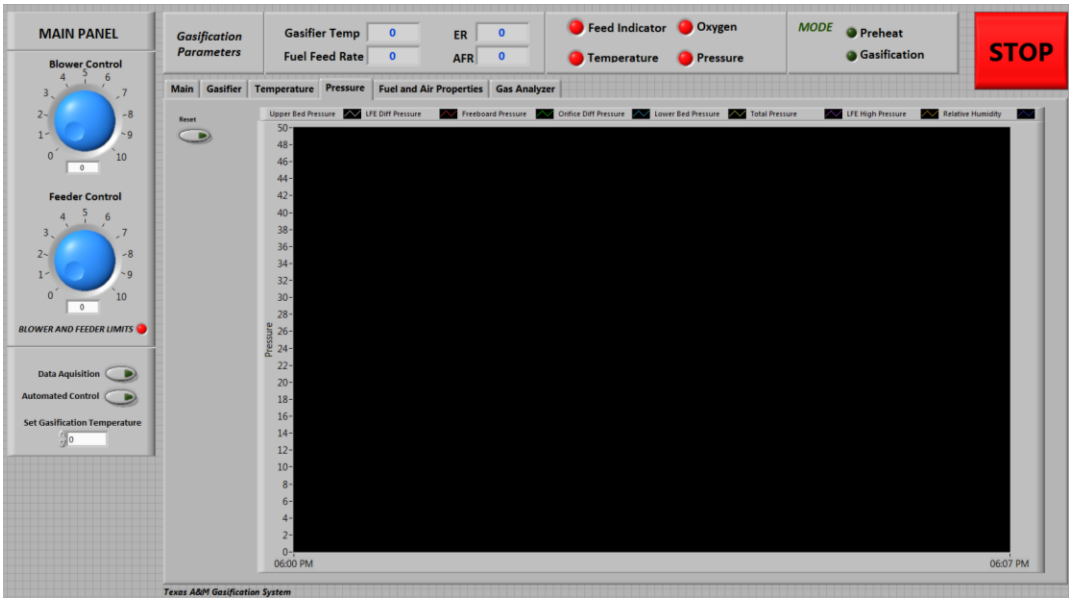
MAIN PANEL
Blower Control
Feeder Control
BLOWER AND FEEDER LIMITS
Data Aquisition
Automated Control
Set Gasification Temperature
Gasification Parameters
Gasifier Temp
Fuel Feed Rate
ER
AFR
Feed Indicator
Oxygen
Temperature
Pressure
MODE
Preheat
Gasification
STOP
Main
Gasifier
Temperature
Pressure
Fuel and Air Properties
Gas Analyzer
Reset
Upper Bed Pressure
LFE Diff Pressure
Freeboard Pressure
Orifice Diff Pressure
Lower Bed Pressure
Total Pressure
LFE High Pressure
Relative Humidity
Pressure
06:00 PM
06:07 PM
Texas A&M Gasification System

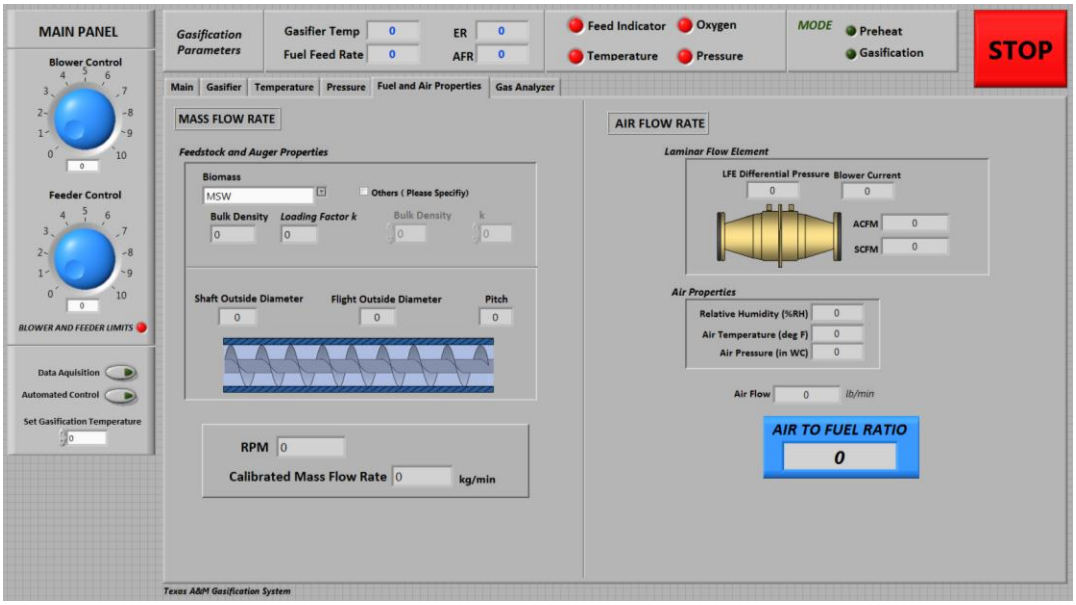
MAIN PANEL
Blower Control
Feeder Control
BLOWER AND FEEDER LIMITS
Data Aquisition
Automated Control
Set Gasification Temperature
Gasification Parameters
Gasifier Temp
Fuel Feed Rate
ER
AFR
Feed Indicator
Oxygen
Temperature
Pressure
MODE
Preheat
Gasification
STOP
Main
Gasifier
Temperature
Pressure
Fuel and Air Properties
Gas Analyzer
MASS FLOW RATE
Feedstock and Auger Properties
Biomass
MSW
Others (Please Specify)
Bulk Density
Loading Factor k
Shaft Outside Diameter
Flight Outside Diameter
Pitch
RPM
Calibrated Mass Flow Rate
kg/min
AIR FLOW RATE
Laminar Flow Element
LFE Differential Pressure
Blower Current
ACFM
SCFM
Air Properties
Relative Humidity (%RH)
Air Temperature (deg F)
Air Pressure (in WC)
Air Flow
lb/min
AIR TO FUEL RATIO
Texas A&M Gasification System


MAIN PANEL
Blower Control
Feeder Control
BLOWER AND FEEDER LIMITS
Data Aquisition
Automated Control
Set Gasification Temperature
Gasification Parameters
Gasifier Temp
Fuel Feed Rate
ER
AFR
Feed Indicator
Oxygen
Temperature
Pressure
MODE
Preheat
Gasification
STOP
Main
Gasifier
Temperature
Pressure
Fuel and Air Properties
Gas Analyzer
HORIBA GAS ANALYZER
HYDROGEN
CARBON MONOXIDE
TOTAL HYDROCARBONS
OXYGEN
CARBON DIOXIDE
Texas A&M Gasification System

Appendix C. Screw Conveyor Calibration

Fuel Type: MSW Pellets
Reduction Ratio: 129

Motor Speed (Magnetic pickup) *RPM*	Auger Speed *RPM*	Fuel Feed Rate *lbs/min*
1946	11.35	4.75
1947	11.36	4.85
1900	11.08	4.85
1903	11.10	4.85
1660	9.68	4.20
1660	9.68	4.20
1146	6.68	2.95
1146	6.68	2.98
645	3.76	1.70
640	3.73	1.68
397	2.32	0.90

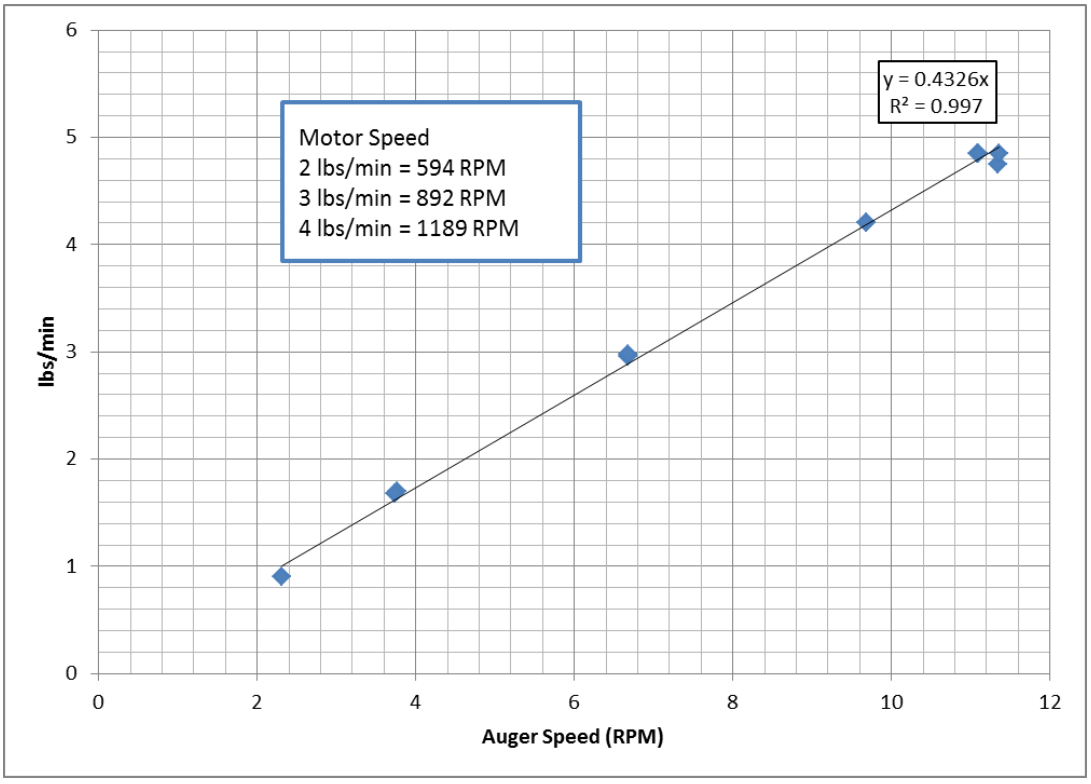

Appendix D. Laminar flow element constants and correction factor

$$SCFM = (B \times DP + C \times DP^2)\left(\frac{\mu_{std}}{\mu_f}\right)\left(\frac{P_f}{P_{std}}\right)\left(\frac{T_{std}}{T_f}\right)\left(\frac{\rho_{wet}}{\rho_{dry}}\right)$$

B = 53.601

C = -0.1033

Humidity Correction Factor

Table A-35600 (NBSIR 83-2652)
Humidity correction factor for air = ρ_{wet} / ρ_{dry}

	% Relative Humidity				
°F	20%	40%	60%	80%	100%
40	.9993	.9987	.9981	.9975	.9969
50	.9990	.9981	.9973	.9964	.9955
60	.9986	.9973	.9960	.9948	.9934
70	.9981	.9962	.9944	.9925	.9907
80	.9974	.9948	.9922	.9895	.9870
90	.9964	.9928	.9892	.9855	.9818
100	.9951	.9902	.9854	.9805	.9756

Appendix E. SRI GC Settings

Columns ShinCarbon ST, 100/120 mesh, 2m, 1/16in. OD, 1.0 mm ID
Molecular sieve 13x 2m, 1/16in. OD, 1.0 mm ID

Sample Gasification synthesis gas –Permanent gases- C1-C3 hydrocarbons

Injection Injection volume: 100 µL
Injection Temp: 100°C

Oven 65°C (hold for 9.5 min.) to 250°C at 16°C/min (hold 15 min.)

Carrier Gas He, constant flow at 10 mL/min (39 psi)

Detectors HID at 150°C
TCD at 150°C

10 Port Gas Sampling Valves

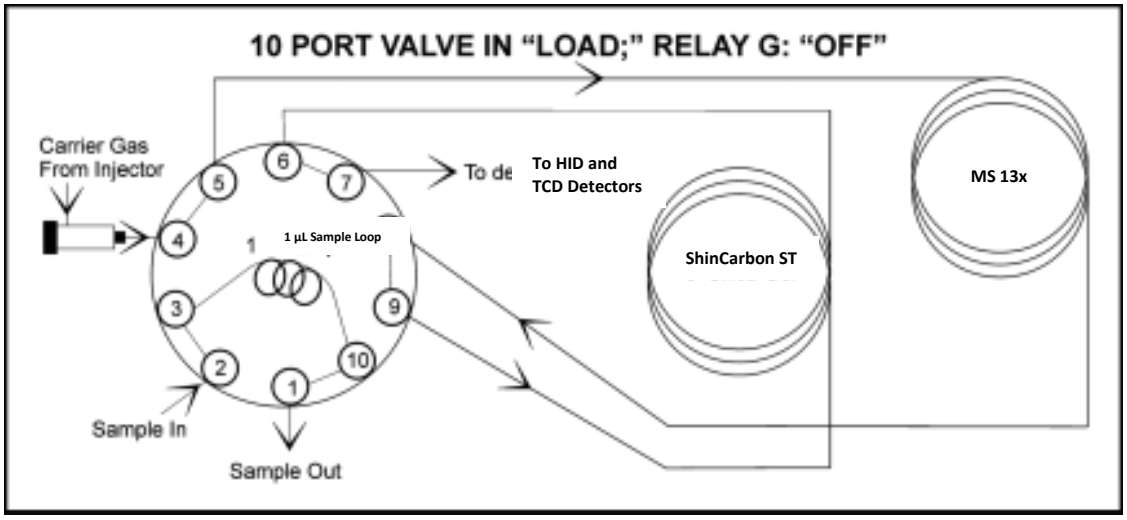

Valves Event Program Zero at 0 min
Valve A (sample IN) ON at 0 min
Valve G (inject) ON at 0.5 min
Valve A (sample IN) OFF at 0.5 min
INTEGRATE at 1.5 min
Valve G (Load) OFF at 9.5 min

Appendix F. Response Surface

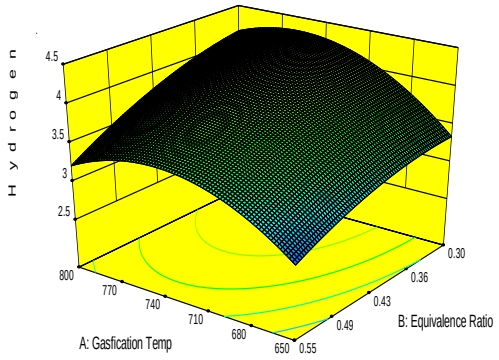

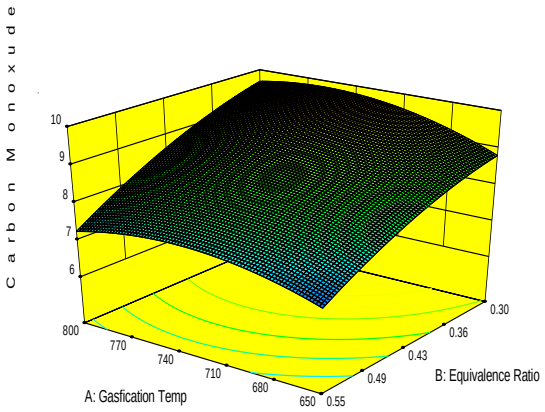

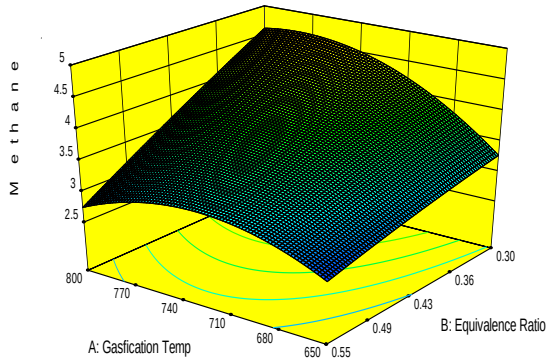

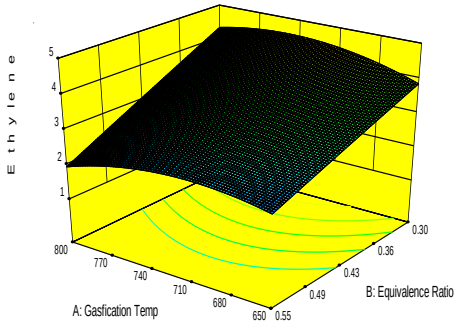

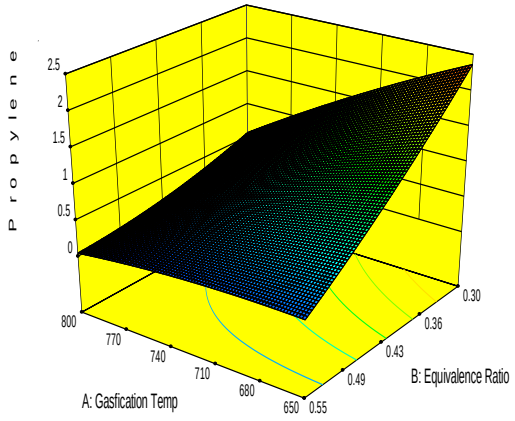

Appendix G. Technical specifications of GX620 Honda Engine

GX620-QDF Type

Length × Width × Height	15.2 × 18.0 × 17.8 in (386 × 456 × 452 mm)
Dry weight	90.4 lb (41.0 kg)
Engine type	4-stroke, overhead valve, 2 cylinders (90° V-Twin)
Displacement [Bore × Stroke]	37.5 cu-in (614 cm^3) [3.03 × 2.60 in (77 × 66 mm)]
Max. output	20 bhp (14.9 kW, 20.3 PS) at 3,600 rpm
Max. torque	32.5 ft-lb (44.13 N•m, 4.50 kg-m) at 2,500 rpm
Fuel consumption	0.51 lb/hph (313 g/kWh, 230 g/PSh)
Cooling system	Forced air
Ignition system	Transistorized magneto
PTO shaft rotation	Counterclockwise

APPENDIX H. PSA

PSA Cycle process

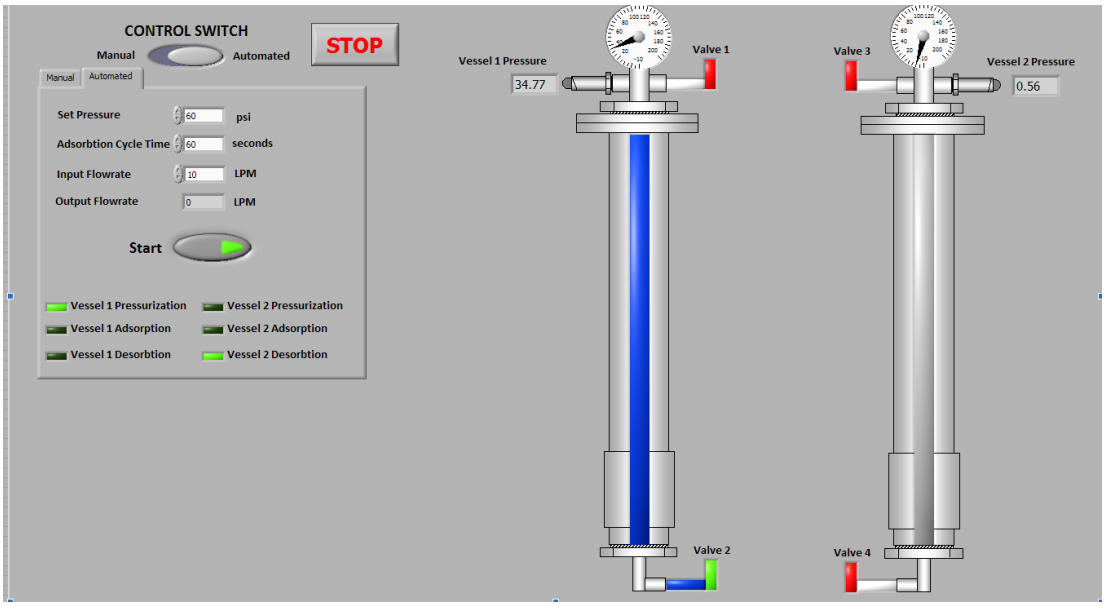

Vessel 1 Adsorption – Vessel 2 Desorbtion

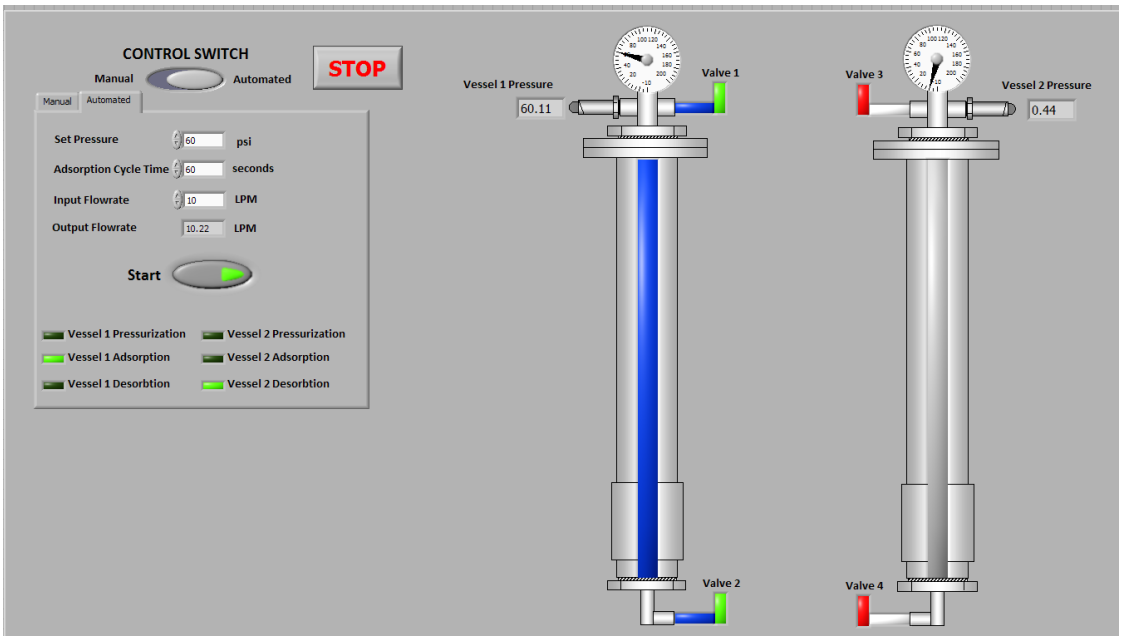

Vessel 1 Adsorption – Vessel 2 Desorbtion

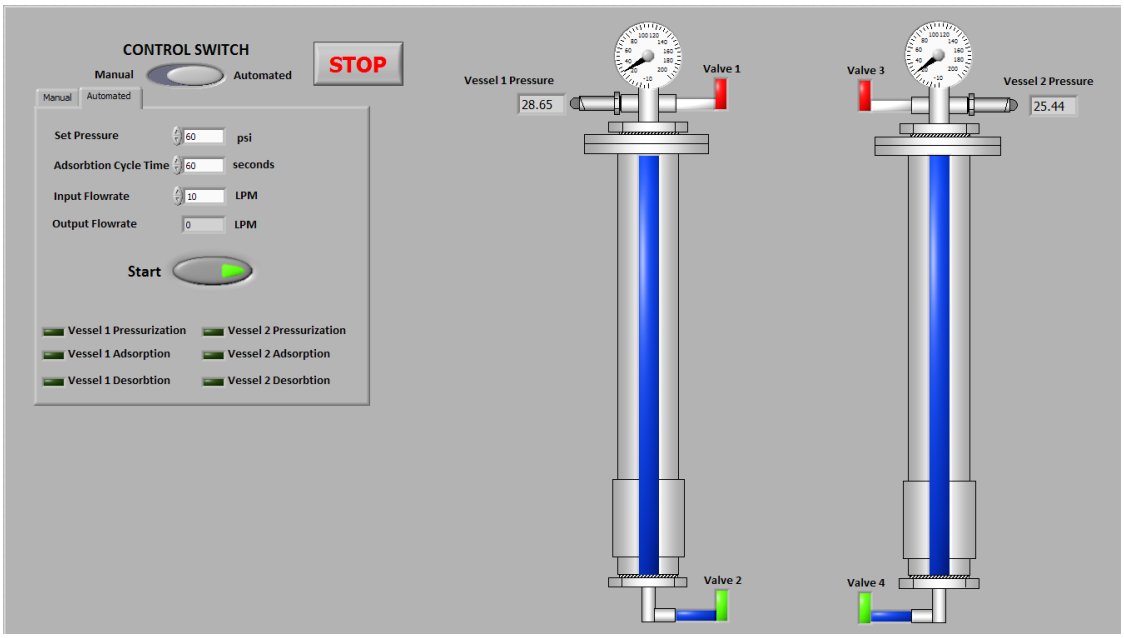

Vessel Pressure Equalization

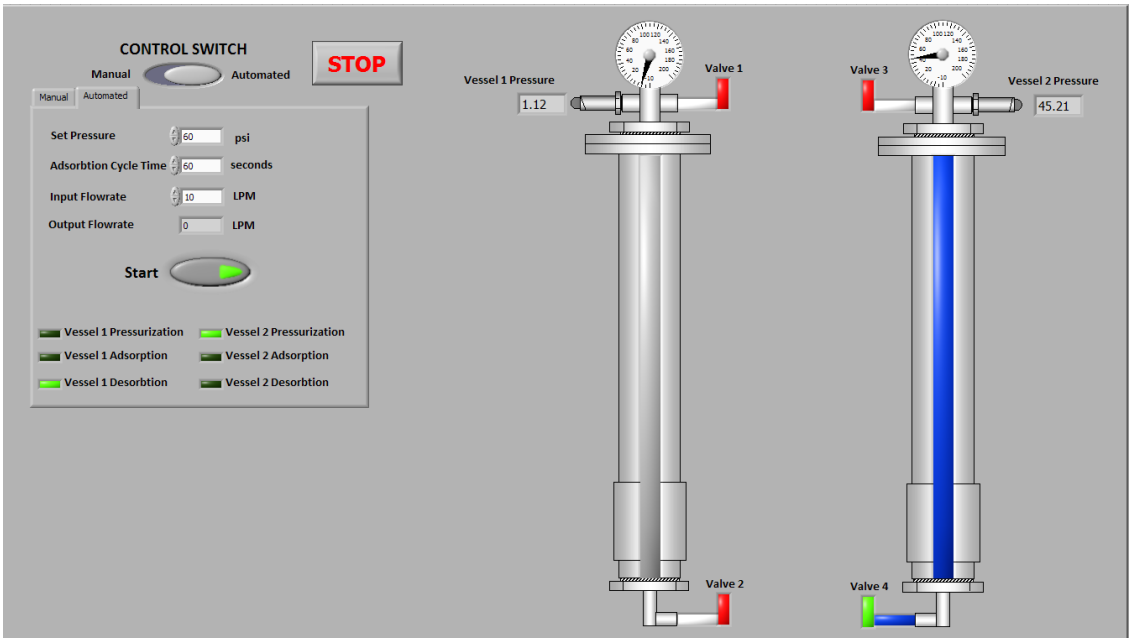

Vessel 2 Pressurization – Vessel 1 Desorbtion

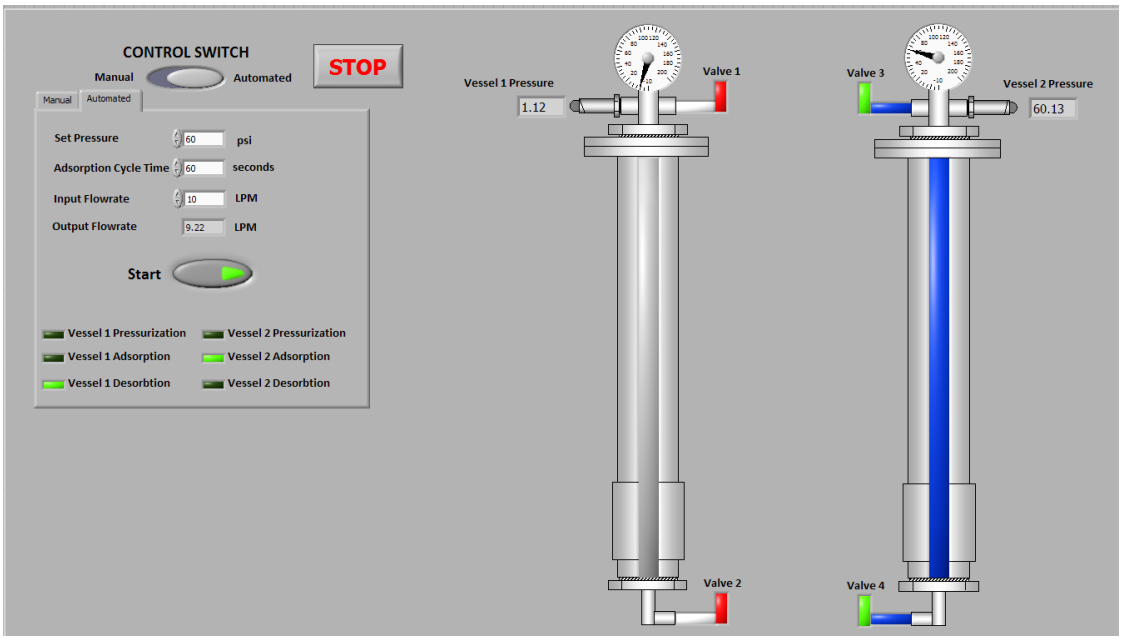

Vessel 2 Adsorption – Vessel 1 Desorption

LabVIEW Code

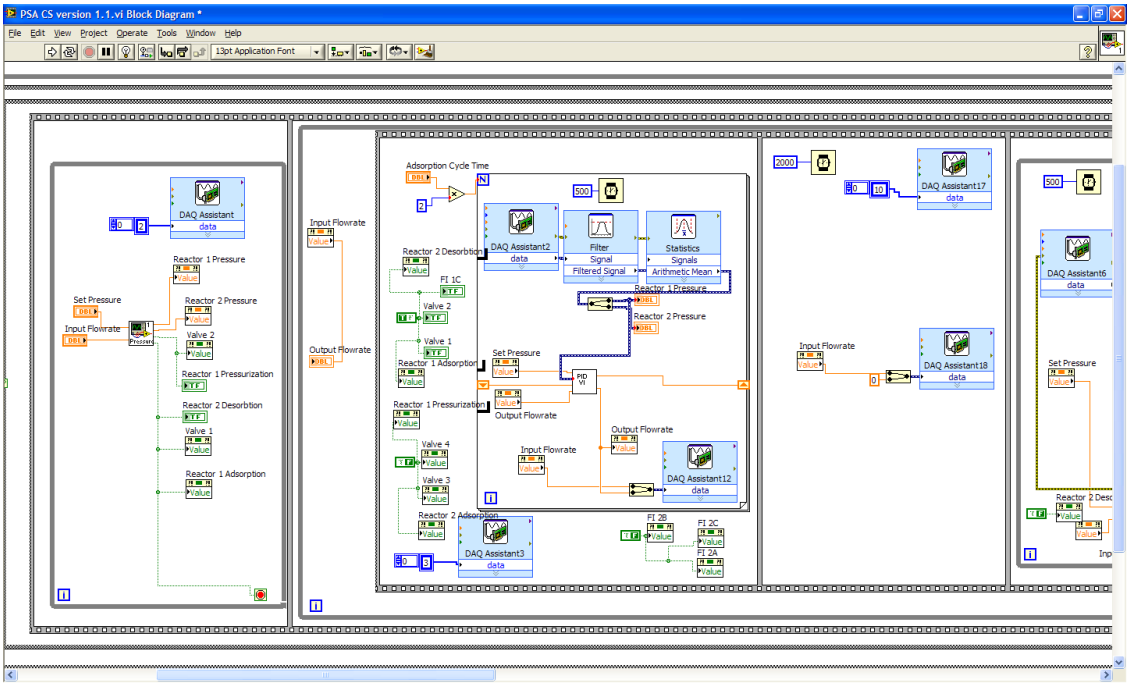

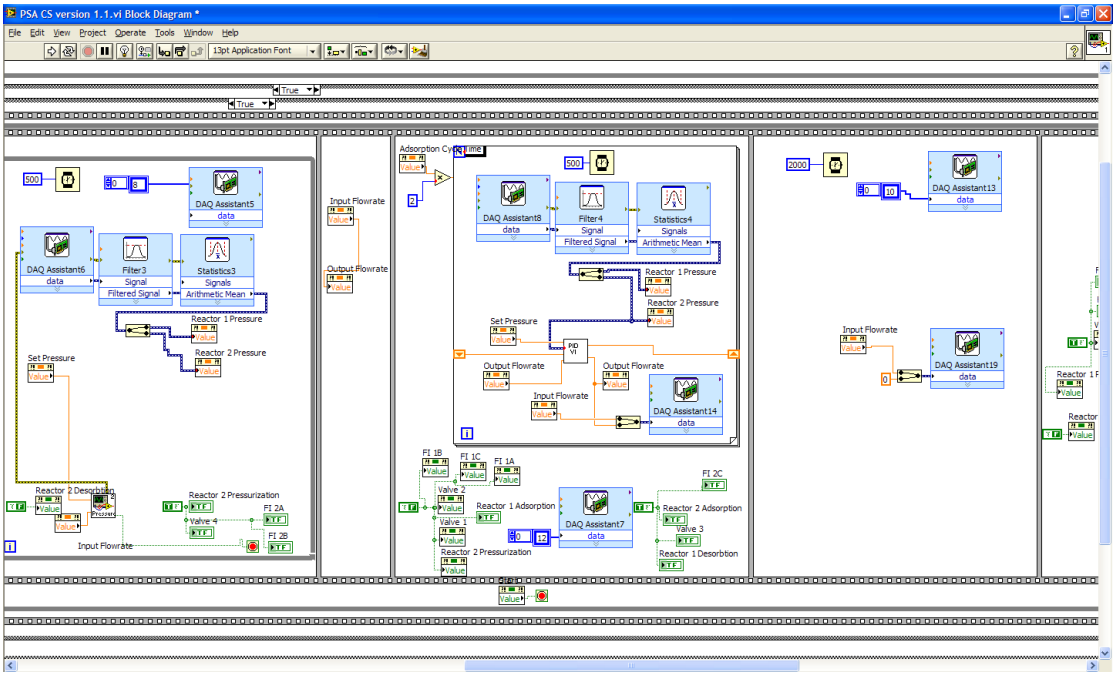
PSA CS version 1.1.vi Block Diagram *
File Edit View Project Operate Tools Window Help
13pt Application Font
DAQ Assistant5
data
DAQ Assistant6
Filter3
Signal
Filtered Signal
Statistics3
Signals
Arithmetic Mean
Reactor 1 Pressure
Reactor 2 Pressure
Set Pressure
Input Flowrate
Output Flowrate
Reactor 2 Desorption
Reactor 2 Pressurization
FI 2A
FI 2B
Adsorption Cycle Time
DAQ Assistant8
Filter4
Statistics4
PID VI
DAQ Assistant14
FI 1B
FI 1C
FI 1A
Valve 2
Valve 1
Reactor 1 Adsorption
DAQ Assistant7
FI 2C
Reactor 2 Adsorption
Valve 3
Reactor 1 Desorbtion
DAQ Assistant13
DAQ Assistant19